Nigerian Journal of Polymer Science and Technology

Volume 16, 2021

ISSN: 1119-4111

A PUBLICATION OF THE POLYMER INSTITUTE OF NIGERIA

Nigerian Journal of Polymer Science and Technology
ISSN: 1119-4111 Volume 16, 2021

EDITORIAL BOARD

NATIONAL OFFICERS AND COUNCIL MEMBERS OF THE POLYMER INSTITUTE OF NIGERIA (PIN)

Engr. (Dr.) Innocent Akuvue, FPIN	Chairman, Board of Directors
Chief Alexis N. Ajuebon, FPIN	Immediate Past Board Chairman
Prof. P. A.P Mamza, FPIN, FICCON, FCSN	President
Dr. J. E Imanah, FPIN, FCSN	Immediate Past President
Prof B. T Nwufo, FPIN, FICCON	Secretary to the Board
Prof. (Mrs) C. D Igwebike-Ossi	Vice President (Operations)
Dr. F. O Biotidara, FPIN	Vice President (Finance)
Engr. (Dr.) F. P Momoh, FPIN	General Secretary
Engr. (Dr.) N. C Iheaturu	Assistant Secretary General
Prof. P. M Ejikeme, FCSN	Treasurer
Mr. Ishaya G. Kure	Ag. Publicity Secretary
Engr. (Dr.) G. O Ihekweme	Membership Secretary
Chief A. S. Ogunkoya	Lagos District
Prof. Onyewuchi Akaranta, FPIN	Port Harcourt District
Mr. Inegbedion Festus	Auchi District
Dr. Owen Egharevba	Benin District
Prof Emmanuel Osabohien	Warri District
Prof. Isaac Igwe, FPIN	Owerri District
Prof. Clement Gonah	Zaria District
Prof. (Mrs.) Clementina Igwebike-Ossi	Anambra/Enugu/Ebonyi District
Dr. Adeyanju Olusola	Jos District
Mr. Noble Alu	Abuja District
Dr. Abdullahi Usman Garin Gabas	Kano/Jigawa District
Dr. (Mrs) Doris Boryo	Adamawa/Bauchi/Gombe Chapter
Dr. (Mrs) C. Obele	Anambra Chapter

Prof. Victor Adeola Popoola, FPIN	Ondo/Ekiti Chapter
Mr. Godfrey Okorie	Oyo/Ogun Chapter
Prof. D.S Oguniyyi	Ilorin Chapter
Prof. S. Achi (Acting)	Kaduna Chapter
Prof. Olumuyiwa Turoti	Osun Chapter
Dr. Misbahu M. Ladan (Acting)	Sokoto/Kebbi/Zamfara Chapter
Dr. Micheal Eneji	Kogi/Niger Chapter

PAST & PRESENT PRESIDENT(S) OF THE

POLYMER INSTITUTE OF NIGERIA

1. Chief Engr. K. Ogunade, FPIN	1989 – 1995
2. Ms. May Ikokwu, FPIN	1995 – 1998
3. Dr. T. O Odozi, FPIN	1998 – 2001
4. Dr. P. C. O Nzelu, FPIN	2001 – 2005
5. Dr. E. J Asore, FPIN	Oct., 2005 – Dec., 2005
6. Prof. B. T Nwufo, FPIN, FICCON	Dec., 2005 – Oct., 2011
7. Dr. J. E Imanah, FPIN, FCSN	2011 – 2015
8. Prof. P. A. P Mamza, FPIN, FICCON, FCSN	2015 – till date

CORRESPONDENCE

Editor-in-Chief
Prof. S. M Gumel, FCSN, FPIN, FCAI
(smgumel.chm@buk.edu.ng)

Published by:
POLYMER INSTITUTE OF NIGERIA

Nigerian Journal of polymer Science and Technology

Information to Authors

Scope of the Journal

The Journal is devoted to publishing original research and short communications in all aspects of Polymer Science and Technology (Engineering). Articles in the related discipline of Materials Science Technology will also be considered for publication.

Preparation of Manuscript

Manuscript should be written in the third person in an objective, formal and impersonal style. The SI system should be used for all scientific and laboratory data. The full stop should not be included in abbreviations, example m (not m.) ppm not (p.p.m.). All mathematical expressions should be included in the manuscript. Care should be taken to distinguish between capital and lowercase letters, between zero (0) and letter (O), between the numeral (1) and letter (I), etc. Mathematical expressions should fit into a single column when set in type. Fractional powers are preferred to root signs and should always be used in more elaborate formulas. The solids (/) should be used instead of the horizontal lines for fractions whenever possible. Numbers that identify mathematical expressions should be enclosed in parentheses. Refer to equations in the text as "Eq. (1)", etc., or "Equation (1)", etc., at the beginning of a sentence.

Content

All pages must be numbered consecutively. A manuscript would normally include a title, abstract, keywords, introduction, materials and methods, results and discussion, conclusions and references.

i. **Title page**: A short title which should be concise but informative must be provided. This should be followed by the names and full addresses of all authors. E-mail addresses of the corresponding authors must be included.
ii. **Abstract**: The abstract should not be more 220 words. It should give concise factual information about objectives of the work, the methods used, the results obtained and the conclusions reached.
iii. **Keywords**: The authors should list below the abstract keywords for information retrieval purposes. The keywords should identify with main point in the paper.
iv. **Abbreviations and Notations**: Nomenclature must be listed at the

beginning of the paper and should conform to the system of standard SI units. Acronyms and abbreviations should be spelt out in full at their first appearance in the text.

v. **Text**: Papers should be typed single column, with double line spacing on one side of the paper only with ample margins on all sides. The text should be divided into sections each with a separate heading, numbered consecutively. The section heading be typed on a separate line and should be bold.

vi. **Conclusionsand Recommendations**: The conclusions should summarise the findings, clearly stating the contributions and their relevance. Recommendations for implementation or for areas of further work on the subject matter should be made.

vii. **Acknowledgements**: These should be brief and relevant. The names of funding organizations should be written in full. Dedications are not permitted.

viii. **References**: References to publish work should be indicated at the appropriate place in the text, according to the Harvard system (i.e. using author(s)' name(s) and date), with a reference list in alphabetical order, at the end of the manuscript. All references in this list should be indicated at some point in the text and vice versa. Papers by more than two authors but with same first author should be listed by year sequence and alphabetically within each year.

Examples of layout of reference are given below:

Book

Onyeyili, I.O. (2003) Analysis of statistically Determine Structures. El' DemakPublishers, Enugu.

Thesis

Ihueze, C.C. (2005) Optimum Buckling Response Model of GRP Composites. Ph.D. Thesis, University of Nigeria, Nsukka.

Journal

Umerie, S.C., Ogbuagu, A.S., Ogbuagu, J.O. (2004) Stabilisation of palm oils by using Ficusexasprata leaves in local processing methods. *Bioresources Technology*, 94: 307-310.

Conference

Menkiti, M.C., Ugodulunwa, F.X.O., Onukwuli, O.D. (2007) studies on the coagulation and flocculation of coal washery effluent. *Proceedings of the 37th annual conference of the Nigerian Society of Chemical Engineers*, Enugu, 22-24 November, pp169-184.

ix. **Illustrations**: All figures whether line drawings, graphs or photographs should be given a figure number be Arabic numeral in ascending order as reference is first made to them in the text (e.g. Fig. 1). Tables are to be similarly numbered. Captions of figures should be below the respective figures while captions of table should be above the respective tables. The measured quantity with the units, usually in brackets, and the numerical scale should be given alongside the ordinate and abscissa of every graph. All illustrations including chemical structures should be placed in the appropriate places within the text.

x. **Submission of Manuscript**: Manuscript should be submitted to the Editor-in-Chief via pineditor2017@gmail.com.

xi. Manuscripts are considered for acceptance on the understanding that the work described is original and have not been published or submitted for consideration elsewhere and that the author has obtained necessary authorization for publication of the material submitted. Submission of a multi-authored manuscript implies the consent of all the participating authors. A processing fee of N3, 000.00 (Three thousand naira only) is charged per manuscript. Make payment to PIN National Account, Polymer Institute of Nigeria account number **0006664735** at Union Bank Plc. A publication fee for accepted manuscript of **NGN10, 000.00** (Ten Thousand Naira) is charged and should be remitted to Polymer Institute of Nigerian Account number **0006664735** at Union Bank Plc.

xii. **Copyright**: By submitting a manuscript, the authors agree that the copyright for the article is transferred to the Polymer Institute of Nigeria, if and when the article is accepted for publication.

xiii. **Disposal of Material**: Once published, all copies of the manuscript and correspondence will be held for three months before disposal. Authors must contact the Technical secretary if they wish to have any material returned

LIST OF APPROVED DISTRICTS/CHAPTERS OF THE INSTITUTE AND CONTACT INFORMATION ON THEIR CHAIRMEN

CHAPTER	NAME OF CHAIRMAN	PHONE NO.	EMAIL ADDRESS
ABUJA	Mr Noble Alu	08060038607	greengreenpower@yahoo.com
AUCHI	Mr Inegbedion Festus	07038274039	festusinegbedion@yahoo.com
BAUCHI/GOMBE/ ADAMAWA	Dr (Mrs) Doris Boryo E.A.	08037243593	deaboryo@yahoo.com
BENIN	Dr Owen Egharevba	07036858714	eowen@yahoo.com
ENUGU/EBONYI	Prof. (Mrs) Clementina Igwebike-Ossi	08037952401	clemdossi@yahoo.com
ILORIN	Prof. Ogunniyi D.S.	08035828764	dsogunniyi@yahoo.com dsogunniyi@hotmail.com
JOS	Gerald Kure	07032881237	geraldtel@yahoo.com geraldlarry82@gmail.com
KANO/JIGAWA	Dr. Abdullahi Usman Garin Gabas	08065610456	aasalisu@yahoo.com aasalisu.chm@buk.edu.ng
KOGI/NIGER	Dr Michael Eneji	07036552658	michaeleneji@yahoo.com
LAGOS	Chief A.S. Ogunkoya		ogunkoyaabiodun@yahoo.com
ONDO	Prof Babatope Babaniyi	08034718487	niyibabatope@gmail.com bbabatope@oauife.edu.ng
OWERRI	Prof. Isaac Igwe	08066355637	Zik3gh@gmail.com
PORT HARCOURT	Prof. Onyewuchi Akaranta	08033845642	onyewuchi.akaranta@uniport.edu.ng
WARRI	Prof. Emmanuel Osabohien	08036761310	eosabohien@delsu.edu.ng
ZARIA	Prof. Clement Gonah		
OSUN	Prof. Olumuyiwa Turoti	08033766099	muyiwaturotl@yahoo.co.uk
ANAMBRA	Dr. (Mrs.) C. Obele		angelobele1@yahoo.co.uk

TABLE OF CONTENT

Contents

Nigerian Journal of Polymer Science and Technology, 2021, Vol. 16, pp1-22
Received: 23/02/2021 Accepted: 23/06/2021

SYNTHESIS OF CELLULOSE (MAIZECOB)-GRAFT-POLY(ACRYLAMIDE) COPOLYMER FOR THE AD SORPTION OF INDIGO BLUE

S. M. Gumel, S.A. Isah* and M. Ladan

Department of Pure and Industrial Chemistry, Bayero University Kano, Nigeria
*Corresponding author: safiyaabubakarisah@gmail.com

ABSTRACT
In this study, hydrogel was synthesized by graft copolymerization of acrylamide into a maize cob cellulose backbone using N'N-Methylene Bis Acrylamide (MBA) as crosslinker and potassium persulphate (KPS) as an initiator. The hydrogel swelling properties in-terms of monomer concentration, cross-linker concentration and pH were investigated. The structure, thermal stability and surface morphology were characterized by FTIR, DSC and SEM, respectively. Phase evolution, before and after grafting, was investigated using X-ray Diffraction (XRD).Energy Dispersion Spectroscopy (EDS) was used to determine the elemental compositions of the raw maize cob, the bleached maize cob and the hydrogel before and after adsorption. The developed hydrogel showed good characteristics, the best result obtained was a percentage removal,74.46% of indigo blue at 40-minute contact time, 45^{0}C temperature and 0.5g hydrogel dose. The result obtained in this work shows that hydrogel has promising applications in adsorption of dye.

Keywords: Cellulose, Maize cobs, Acrylamide, Hydrogel

1. Introduction

Maize cobs are by products of maize crops with high fiber content whose main chemical components contain abundant cellulose, hemicellulose and lignin (Ma *et al*., 2017). So far the utilization of waste maize cobs is not high, except for a limited comprehensive utilization as feed, fertilizer, industrial raw materials, fuel, and so forth (Xu *et al*., 2016). Maize cobs consist of about 40% cellulose contents which belongs to a linear and extended polysaccharide that stands out as one of the most significant natural polymers (Winarti *et al*., 2018; Morgan *et al.,* 2012).Cellulose is a major constituent of plants and they are abundant in nature. Cellulose possesses a high crystallinity due to the numerous intra- and inter-molecular hydrogen bonds among its chains, restricting its solubility in water and most common organic solvents, thereby hampering many potential applications (Kang *et al.,* 2016; Suhas *et al*., 2016; Mondal and Harque, 2019). Cellulose possesses certain advantages such as; non-toxic, biodegradability, biocompatibility and availability. Cellulose and its derivatives are excellent building blocks for fabrication of gels. Chemical and/or physical crosslinking can be introduced during the preparation of cellulose-based gels (Suhas *et al*., 2016). In the fabrication of cellulose-based gels, cellulose graft copolymers are major building block and they find wide application in different fields depending on the properties required (Song *et al*., 2019; Mondal and Harque, 2019). Cellulose based hydrogels are normally utilized as adsorbents because of their ease of fabrication, low cost material requirements, ability to uphold water for

an extended time period and high efficiency (Karadag *et al,* 2015; Muhammad *et al*, 2016; Zhong *et al*.; 2019).

Some works have been done within this realm with focus on preparation of hydrogels based on cellulose, lignin, melanin and petroleum based polymers such as poly acrylic acid (PAA) and poly acryl amide (PAAM). Dai *et al*., (2019) reported on the enhanced adsorption performance of hydrogel based on pineapple peel carboxymethyl grafted with poly (acrylic acid-co-acrylamide)/graphene oxide. The swelling dynamic mechanism of the hydrogel also agreed well with Fickian diffusion and Schott's pseudo-second-order models. Winarti *et al*., (2018), reported on the effect of different concentration of epichlorohydrin and cellulose on the characteristics of nanohydrogels. The cellulose was extracted from corncob based and was crosslinked with epichlorohydrin. The outcome of the study revealed that the concentration of the crosslinker, the higher the swelling ratio. Sami *et al*., (2017) reported on the removal of anionic dyes from wastewater using chitosan-starch based nanocomposite hydrogel. It was discovered from the study that the electrostatic and hydrophobic interaction between the starch and the chitosan provide better dye removal when compared to chitosan alone. Nurfadila *et al*., (2019), reported on the characteristics of nano-hydrogel by gamma irradiation. The hydrogel was synthesized using corncob and the result showed that hydrogel with gamma irradiation swells more than hydrogel without gamma irradiation.

However, there is less report about wastewater treatment using maize cobs. In our study, we selected the maize cob as an ingredient with grafted acrylamide monomer to ascertain removal of indigo blue dye component from industrial effluent.

The new material, a potential candidate as eco-friendly adsorbent, can rapidly remove indigo blue dye from industrial effluent of dyeing pits. What's more, the comprehensive utilization of waste maize cob was enriched. This action can not only prevent atmospheric contamination from abandoned maize cob, but water pollution deriving from organic dyes discharged into water as well. The effect of the dosage of absorbent, contact time, and temperature on the adsorption capacity of the hydrogel, using a batch adsorption technique was investigated. The physio-chemical parameters of the indigo dye effluent before and after adsorption were also investigated.

2. Materials and Methods

2.1. Materials and Reagents

Acrylamide monomer (99% Xilong Chemicals),Potassium Persulphate (98%, Kermel), N'Nmethylenebisacrylamide (MBA) (97%, BDH Chemicals), Ethanol (98%, Qualikem) and Sodium Hydroxide (98%, LOBA). All other reagents were of analytical grade and used as obtained without further purification.

2.2. Pretreatment of Maize Cob (MC)

The maize was de-kernelled to obtain the cobs while the moisture content was determined using thermogravimetric method. The MC was sliced into smaller fragments and then sun dried for 35 days and the resulting fragments were then pulverized to obtain finer particles. The

resulting particles were then sieved with a 300 μm sieve size while the moisture content was also determined to ensure adequate dryness. As discussed in Ibrahim *et al.,* (2010), delignification of the resulting powder was achieved using acid-alkali pulping methodology. During the process, 100g of MC particles was weighed in a digital weighing balance and subjected to acid pulping using pulping conditions of 5% H_2SO_4, with a liquor to fiber ratio of 10:1. The solution were cooked in a pressure cooker for 2 hours at a temperature of 170^{o}C. The pressure was released and the pulped resulting solution was washed with water to obtain a neutral solution, then the percentage recovery was determined. This process was followed with alkaline pulping using 10% sodium hydroxide (NaOH) and a liquor to fiber ratio of 10:1. The solutions were also cooked in a pressure cooker at a temperature of 170^{o}C for 2 h and after then, the pressure was released and the solution was washed with water till neutrality and then dried. The resulting cellulose fibers were bleached with hydrogen peroxide of 10:1 liquor to fiber ratio for 1 hour 30 minutes in a water bath at 80^{o}C. To achieve total bleaching of the fiber, the fiber was re-bleached for 1 hour with hydrogen peroxide of 10:1 liquor to fiber ratio, it was then washed till neutrality and air dried in accordance with a report (Abdul Razak *et al.*, 2014).

2.3. Preparation of Cellulose (MC)-g-Poly (AAm) Hydrogels

The synthesis of cellulose (MC)-g-poly (AAm) hydrogels involved a free radical graft copolymerization of maize cob with acrylamide in the presence of the initiator ($K_2S_2O_8$) and MBA as crosslinker. In the process, 0.5 g of maize cob pulp was added to a 15 ml of distilled water in a three necked flask fitted with magnetic stirrer, a reflux condenser and a nitrogen line at 40^{o}C for bubbling oxygen free nitrogen for 10 min before starting the reaction. Thereafter, 0.6 g of acrylamide was dissolves in 7 ml of distilled water and added to the initial pulp mixture. The whole mixture was stirred for 10 minutes under the nitrogen gas atmosphere. 0.1 g of $K_2S_2O_8$ and 0.1g MBA were added into the mixture, the reaction was then allowed to proceed for 2 hours between 60 to 70^{o}C to form a gel. The hydrogel produced was poured into a beaker, wash with ethanol and distilled water so as to remove the unreacted monomer and impurities while the resulting mixtures was oven dried. The monomer concentration was varied between 0.6 and 1.4 with constant concentration of 0.1g MBA. This was to enable determine the effect of monomer concentration on the swelling property of hydrogels. Using the monomer concentration which give the best swelling property, effect of crosslinker concentration was studied.

2.4. Characterizations

2.4.1 XRD (X-Ray Diffraction) Analysis

A Panalytical Emperean X-Ray diffractometer with a Cu-Ka radiation source (λ = 0.15418nm) with a continuous sweep in the direction of angle 2θ and range 3^o to 50^o was employed in determining the crystalline phase of the raw maize cob, the maize cob cellulose and the cellulose (maize cob)-g-polyacrylamide hydrogel.

2.4.2*Fourier Transform Infrared Spectroscopy (FTIR)*

Fourier Transform Infrared (FTIR) spectrometer (Cary 630 Agilent, United States) at a resolution of 8 cm^{-1} and a wavelength range of 650 to 400 cm^{-1} was

used in recording the FTIR spectra of the samples.

2.4.3 Scanning Electron Microscope (SEM)

The morphology of the synthesized hydrogel, the raw maize cob and the bleached maize cob were recorded using Scanning Electron Microscope (SEM) Phenom ProX model.

2.4.4 Differential Scanning Calorimetry (DSC)

Differential Scanning Calorimetry (DSC) was carried out using POLYMER DSC 180 System-Mettler Toledo. In this test, the samples were placed on an aluminium crucible pressed and sealed followed by heating and cooling while the wide temperature scan in heat and cool cycles generated up to 120 thermocouples arranged in several layers.

2.5. Evaluation of Swelling Ratio, Yield and pH Response of the Hydrogel

The swelling response test was carried out as detailed in Dai *et al*., (2019). The hydrogel was wholly immersed in distilled water at room temperature and left for 24 hours. The hydrogel was observed to ensure swell has occurred and then weighed immediately after removal of the excess water.

Eq. 1 was then applied to determine the swelling ratio.

$$swelling\ ration = \frac{w_t - w_t}{d} \quad (1)$$

Where W_t (g) depicts the weight of swollen hydrogels at time t (min), and W_d (g) represents the weight of dried hydrogels. Yield measurement was done using Eq. 2

$$Yield = wd/w \times 100\% \quad (2)$$

W is the total weight of the cellulose, monomer, initiator and crosslinker (Huang *et al.,* 2019). Buffer solution at pH of 2, 4, 6, 8, 10 and 12 was also used to determine water absorbency of the hydrogels

2.6. Adsorption Studies

2.6.1 Collection of Dye Effluent and Physio-chemical Parameters Measurements

Dye effluents were collected from Kofar mata dyeing pits in Kano state in Nigeria. The dye liquor was then taken to the Central Laboratory Complex at Bayero University Kano in Nigeria for physio-chemical analysis. The analysis includes pH, Total Dissolved Solid (TDS), Dissolved Oxygen (DO), and conductivity using Jenway3320 pH meter, LT-15 labtronics auto digital TDS meter and DOH-SDI Omega DO meter respectively. The aim of the physio-chemical analysis was to ensure the dye effluent meets the recommended standard stipulated by the World Health Organization (WHO).

Since the hydrogel was to be tested for the remediation of indigo blue dye in the collected effluent and the concentration of indigo blue in the effluent is not known yet. The collected effluent was first scanned using PerkinElmer UV/Vis Spectrum Lambda 35 machine to ascertain the maximum wavelength and absorbance of the indigo blue present in the dye solution. In order to ascertain the concentration of the indigo blue present in the effluent solution, 1000ppm standard solution of indigo blue was prepared, lower concentration of 5ppm, 10ppm,15ppm, 20ppm, 25ppm, and higher concentration 20ppm 40ppm, 60ppm,80ppm and 100ppm using serial dilution method. Using the wavelength and absorbance of the indigo present in

the dye effluent as a reference, the prepared standard indigo solutions were then scanned in the PerkinElmer UV/Vis Spectrum Lambda 35 and calibration curves were plotted by the machine software. From the calibration curve of the synthetic indigo blue serial solutions, the concentration of the indigo blue present in the effluent was calculated from the slope of the serial curve using Eq. (3)

$$y = mx+c \quad (3)$$

Where $c = 0$, y = Absorbance, m = slope and x = the unknown concentration of the indigo present in the effluent.

2.6.2 Effect of Hydrogel Dosages on Removal Percentage of Indigo Blue

After ascertaining the initial concentration of the indigo blue present in the effluent, the effect of different quantities of the hydrogel on the adsorption of the effluent were determined. This was achieved by adding 0.1g to 0.5g of the hydrogel separately to 30 ml of the effluent in different beakers at a temperature 45 ^{o}C for 45 minutes at a constant speed of 200rpm till equilibrium was attained. The remaining concentration of dye in solution was obtained using Perkin UV/Vis Spectrum. The removal percentage (R%) of the prepared hydrogels was calculated based on the changes of the dye concentration before and after adsorption, according to Eq. (4).

$$Removal\ \% = \frac{Co-Ce}{Co} X\ 100\% \quad (4)$$

where C_0 (mg/L) and Ce (mg/L) are the concentrations of dye solutions at the initial time and equilibrium respectively (Dongzhuo *et al*., 2017)

2.6.3 Effect of Contact Time on Removal Percentage of Indigo Blue

The effect of contact time on the on the adsorption of the blue indigo dye at a temperature of 303 K, 0.1g fixed hydrogel and at a mixing speed of 200 rpm was studied at different time intervals of 40, 60, 80, 100 and 120 minutes using 30 ml of dye solution.

2.6.2 Effect of Temperature on Removal Percentage of Indigo Blue

The effect of temperature was also studied so as to help ascertain the efficiency of the adsorbent at different temperature levels. This was achieved by adding 0.1 g fixed quantity of dried hydrogel to a 30 ml of dye solution at a contact time of 40 min, a speed of 200 rpm and system temperatures of 30^{o}C, 35^{o}C, 45 ^{o}C, 55 ^{o}C and 60 ^{o}C.

3. Results and Discussion

3.1.Pretreatment of Maize Cob

Acid-alkaline pulping treatment was applied as a chemical pulping method for the maize cob. The acid treatment was to solubilize the hemicellulose and lignin while the alkaline treatment was to ensure delignification (Wang et al., 2017). Color changes was observed during the pulping and this could be as a result of the removal of cell wall component and lignin removal (Ibrahim et al., 2010).The percentage recovery of the acid pulp and alkaline pulp fiber were 57.7% and 48.5%, respectively. Similar percentage recovery had been reported by Ibrahim *et al*., (2010) which were 41.3%, 52. 5% and 43.6%, 48.5% for acid pulp and alkaline pulp of Rice and banana fibers respectively. Further bleaching was applied to remove residual lignin that might affect crosslinking during grafting.

Percentage recovery of the bleached cellulose was determined to be 56.7%.

3.2.Chemical compositions of synthesized hydrogel

Table 1 and 2 show the chemical compositions of the synthesized hydrogel.

Table 1: Monomer concentration in synthesized hydrogels with constant concentration of MBA (0.2)

Hydrogels	Cellulose(g)	AAm(g)	KPS(g)	MBA(g)
P_1	0.5	0.6	0.1	0.1
P_2	0.5	0.8	0.1	0.1
P_3	0.5	1	0.1	0.1
P_4	0.5	1.2	0.1	0.1
P_5	0.5	1.4	0.1	0.1

Table 2: MBA concentration in synthesized hydrogels with constant monomer concentration (1.4g).

Hydrogels	Cellulose(g)	AAm(g)	KPS(g)	MBA(g)
P_6	0.5	1.4	0.1	0.1
P_7	0.5	1.4	0.1	0.2
P_8	0.5	1.4	0.1	0.3
P_9	0.5	1.4	0.1	0.4
P_{10}	0.5	1.4	0.1	0.5

3.3.Characterizations

3.3.1 FTIR Analysis

Fig. 1 (a and b) depicts the FT-IR of the raw and bleached maize cob which has similar adsorption band peaks which is in accordance with the theoretical values of Kim *et al*., (2019) and Ibrahim and El-Zawawy (2013). It can be seen that the peak at 1722 cm^{-1} in fig 1a, which is assigned mainly to C=O stretching vibration of the carbonyl and acetyl groups in the xylan component of hemicellulose and also typical for structural features of lignin disappeared after bleaching with hydrogen peroxide in fig 1b. Further absorption band of lignin at 1514 cm^{-1}(aromatic ring stretch) disappeared in the bleached fiber as well. Moreover, the band near 1242 cm^{-1} corresponding to axial asymmetric strain of =C–O–C disappears in the bleached fiber, it is assigned to =C–O- resulting from ether-, ester-, and phenolic groups (Ibrahim and El-Zawawy; 2013). This disappearance is attributed with complete removal of lignin and hemicellulose by chemical treatment. The slight difference in the cellulose characteristics peaks of the raw maize cob and bleached cellulose can be associated with the total bleaching achieved leading to shifts in some of the characteristics peaks with intense transmittance of the bleached peaks (Kim *et al.;* 2019).

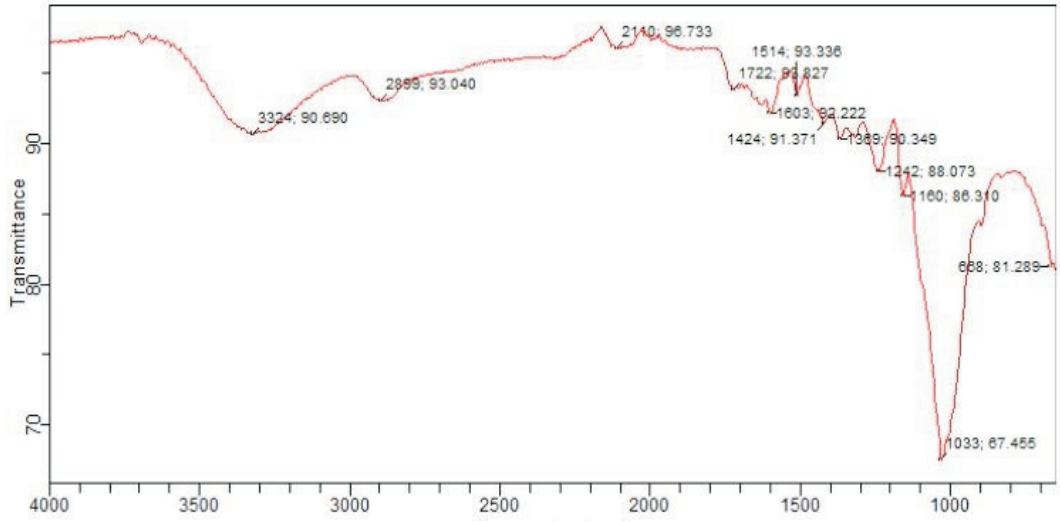

Fig. 1a. FTIR spectra of raw maize cob cellulose.

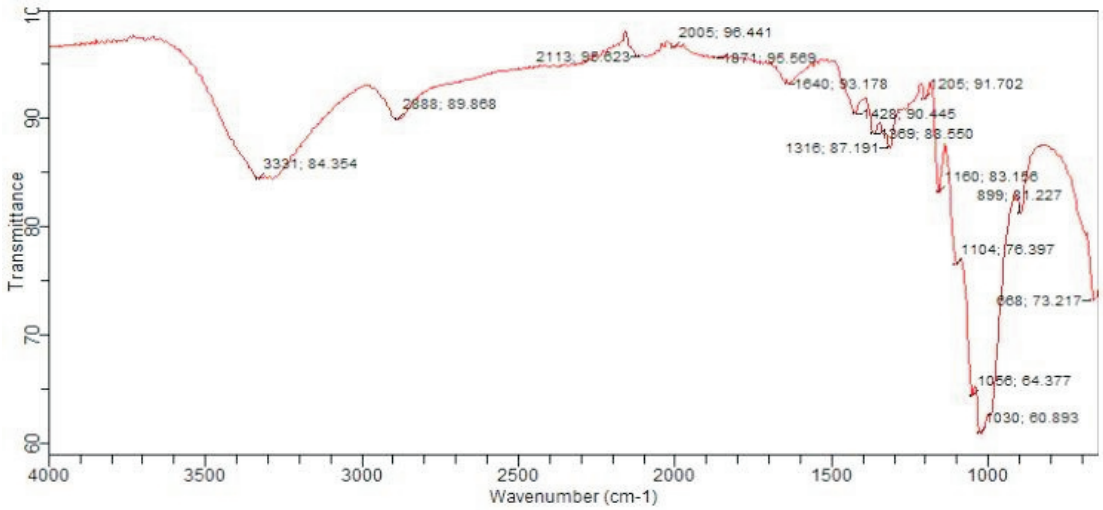

Figure 1b. FTIR spectra of bleached maize cob cellulose.

From the FT-IR spectral in figure 1c, Cellulose(MC)-g-AAm hydrogel shows the basic functional groups of acrylamide of – NH_2 stretch peak and – NH_2 bending vibration at 3328 cm^{-1} and 1603 cm^{-1}, respectively. Cellulose functional and characteristics groups in Fig. 1c as compared to Fig 1b have slight shift in their peaks which might be associated with the presence of AAm (Kim *et al.,* 2019). The absorption band observed at 1048 cm^{-1} in Fig 1c was attributed to the stretching vibration of C-O-C which indicate that the graft polymerization of acrylamide on the cellulose backbone was successful. This result indicate that cellulose was well interacted with AAm through the formation of intermolecular bonds between the acrylamide and hydroxyl group of cellulose. The C=O and N-H stretching at 1652 cm^{-1} and 1108 cm^{-1}, respectively is attributed to the cross linker present during the polymerization

which cross-linked the two growing cellulose chains.

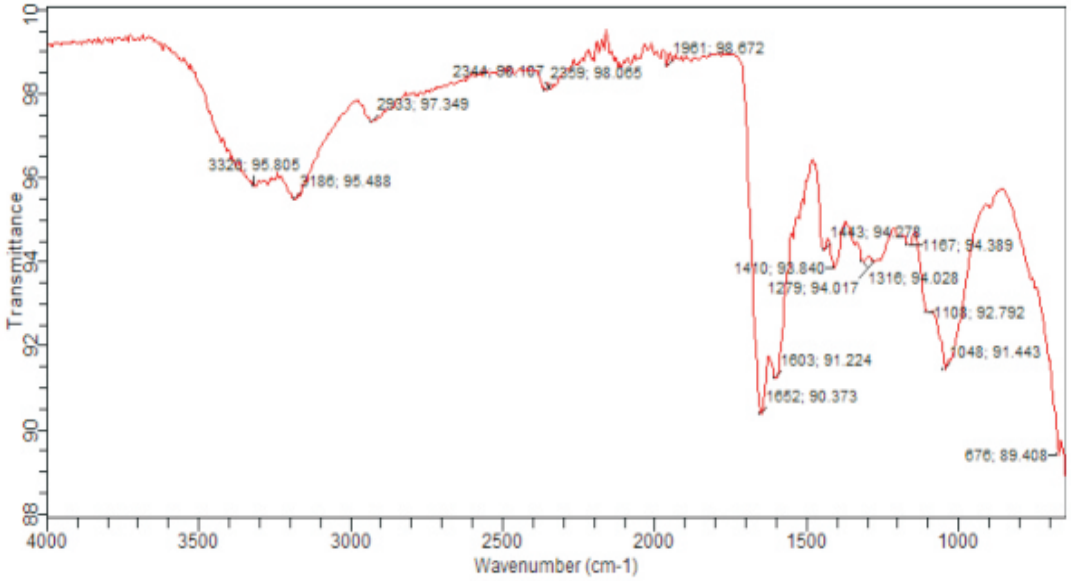

Fig. 1c. FTIR Spectrum of Cellulose-g-(AAm) Hydrogel

3.3.2 XRD Analysis

Fig. 2a, 2b and 2c represent the X-ray power diffraction of the raw maize cob, the bleached maize cobs and the final hydrogel. As shown in fig. 2a, the raw maize cob displayed a broad amorphous peak and two well defined peaks at $2\theta = 34.8^0$ and $2\theta = 57.6^0$

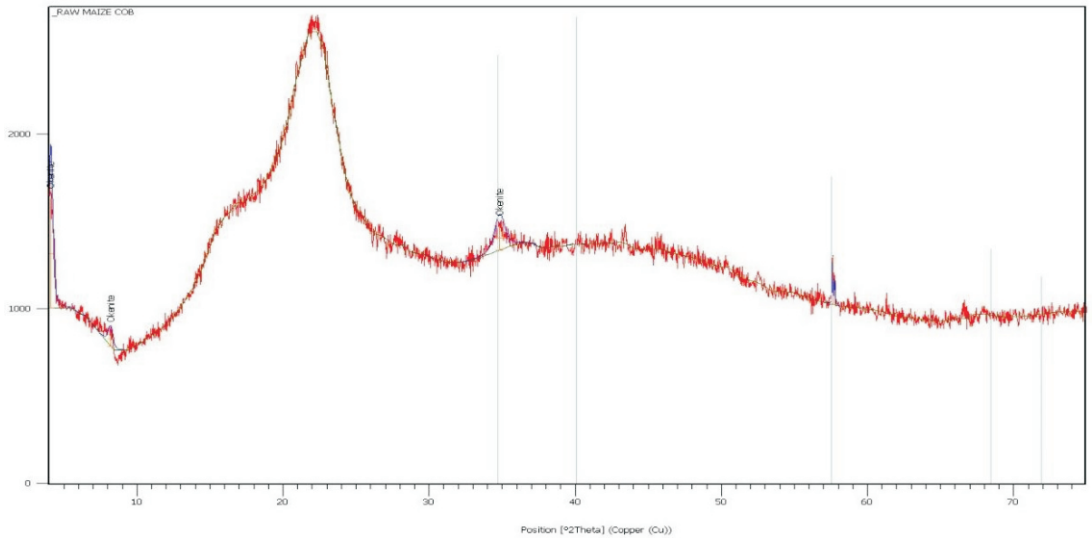

Figure 2a. XRD patterns of raw maize cob

From fig. 2b represent the bleached maize cob cellulose XRD pattern which displays three well-defined crystalline diffraction peaks at 2θ = 22.8°, 26.7°, 34.6° respectively which is in accordance with the pattern of CNC as investigated by Kim *et al*., (2019) displaying four well-defined crystalline diffraction peaks at 2θ

= 14.6°, 16.2°, 22.58°, and 34.4° respectively. The observed peaks showed the cellulose isolated from other fiber source while the broader patterns observed in the raw maize cob cellulose depicts the presence of non-crystalline hemicellulose and lignin as also reported by (Shogren et al., 2011, Abe & Yano, 2010). The result also showed that some portion of the hemicellulose and lignin were separated from the maize cob after bleaching.

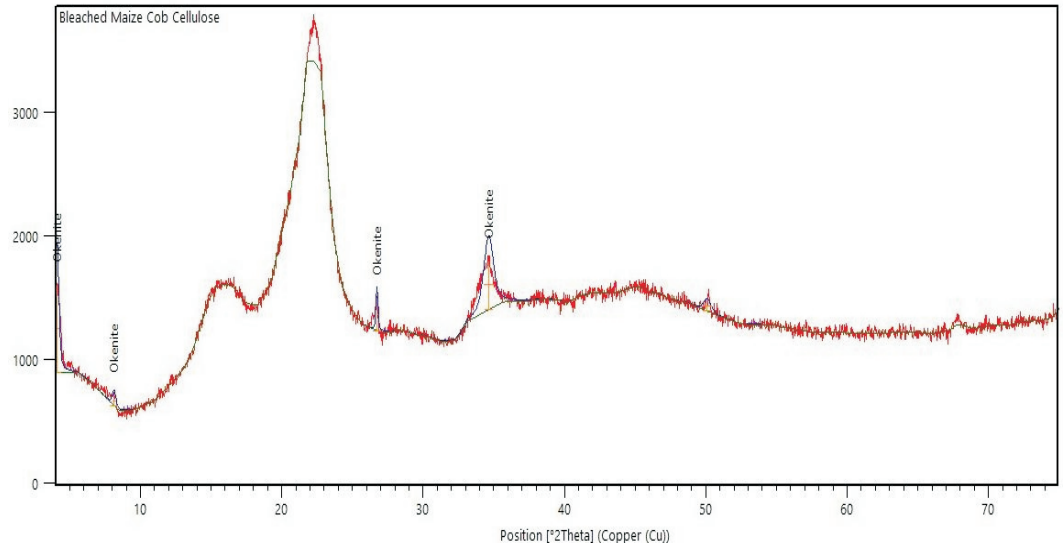

Figure 2b. XRD patterns of bleached raw maize cob

Fig. 2c shows the XRD patterns of the cellulose(MC)-g-PAAm hydrogel. It can be seen that the initial crystalline properties were almost lost such that the only noticeable peak was at $2\theta = 22.7^0$. The observed change maybe as a result of the successful grafting of the polyacrylamide into the cellulose backbone giving the final hydrogel an amorphous structure (Dong et al., 2018).

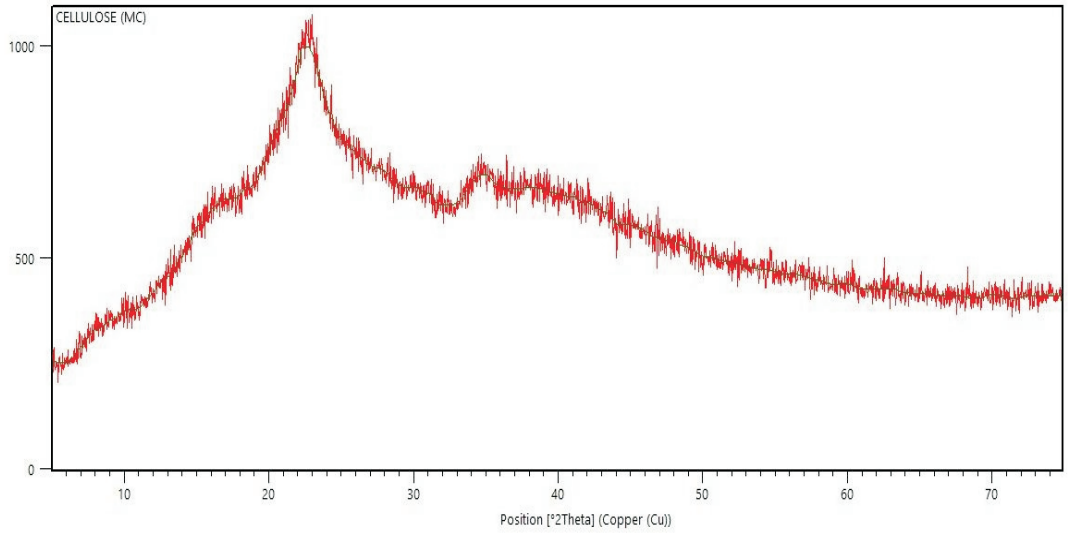

Figure 2c. XRD patterns of the cellulose(MC)-g-PAAm hydrogel

3.3.3 SEM analysis

The SEM images of the raw maize cob cellulose, the bleached maize cob cellulose and cellulose(MC)-g-PAAm hydrogel before adsorption are shown in fig. 3a, fig. 3b and fig. 3c.

From fig. 3a, at a magnification of 500 x, vascular bundles with visible fragmented cells structures can be seen in the cellulose of the raw maize cob indicating the presence of fibrous lignocellulose. This results depicts the typical microstructure of maize cob cellulose (Anukam et al., 2017). The microscale pores and their aligned channels was also visible from fig. 3a. In fig. 3b, the cell wall of the bleached maize cob appears more uniform compared to that of the raw maize cob. The SEM micrograph of the bleached maize cob cellulose also shows a reduction in the lignocellulose fibers that exhibit irregular shapes and sizes. Colour changes was also observed after the bleaching action. From fig. 3c, the cellulose (MC)-g-PAAm before adsorption is characterized by larger pore sizes and smooth surfaces indicating that the cell lumens were successfully filled with the polymer (PAAm) and the cross linking was successful. This result is consistent with a report by Wu et al., (2018).

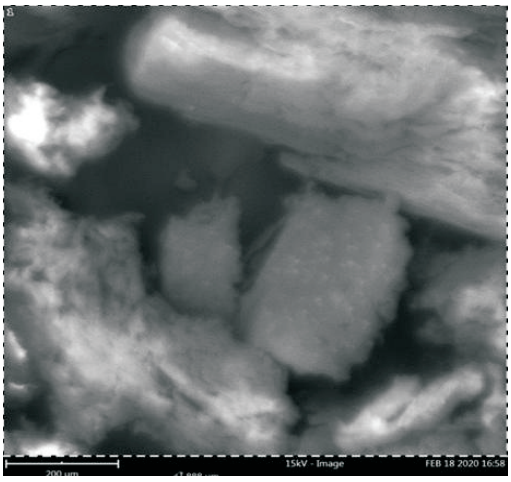

Figure 3a. SEM image of raw maize cob cellulose

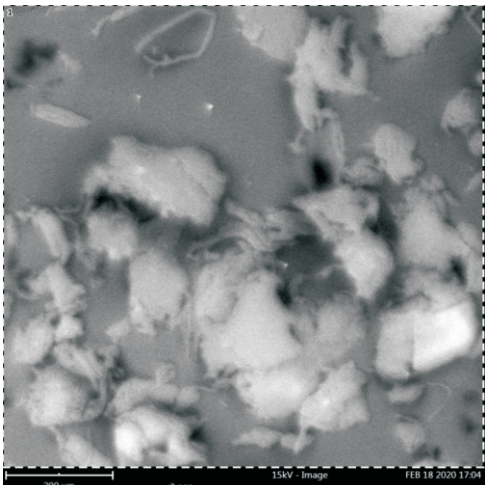

Figure 3b. SEM image of bleached maize cob cellulose

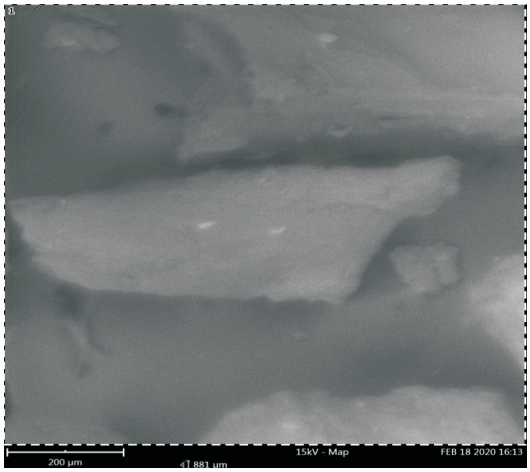

Figure 3c. SEM image hydrogel before adsorption

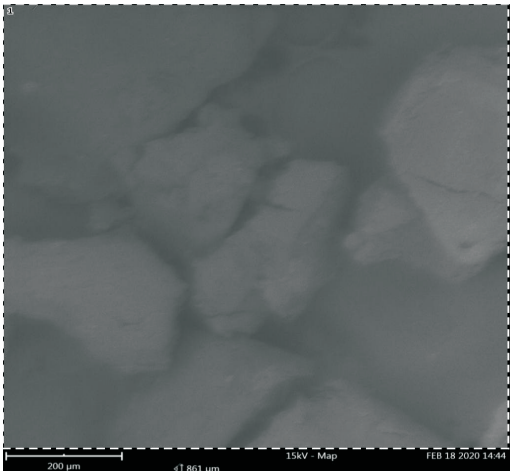

Figure 3d. SEM image hydrogel after adsorption

Fig. 3d represent the SEM micrograph of the hydrogel after adsorption. The surface morphology of the hydrogel before adsorption (fig. 3c) differs that of the hydrogel after adsorption in terms of pore size. The pore structures of the hydrogel before adsorption are characterized with large and smooth surfaces compared which becomes small and rough after adsorption. This signifies a successful absorption of the dye effluents solutions by the hydrogel.

3.3.4 Energy Dispersive X-ray Spectroscopy (EDS)

The EDS attached to the SEM was used for the elemental analysis of the raw maize cob, the bleached maize cob and the synthesized hydrogel. Fig. 4a, 4b and 4c shows the EDS peaks of carbon, oxygen and other elements. Carbon and oxygen was present in all the patterns with different atomic concentration. The atomic concentration of carbon increased from 48.09 (fig. 4a) for the raw maize cob cellulose to 67.25 (fig. 4b) of the bleached maize cob cellulose which indicates treatment has taken place. It can also be seen from the EDS spectrum of the bleached maize cob that potassium, nitrogen and oxygen with respective atomic concentration of 11.03, 0.87 and 1.87 respectively (fig. 4b) increased to 16.58, 2.01 and 3.81 (fig 4c) of the hydrogel. This can be attributed to the presence of KPS, PAAm and MBA in the final hydrogel. The atomic concentration of the C also reduced from 67.25 (fig. 4b) to 54.87 (fig. 4c) indicating successful grafting on the cellulose backbone (Lu et al., 2020).

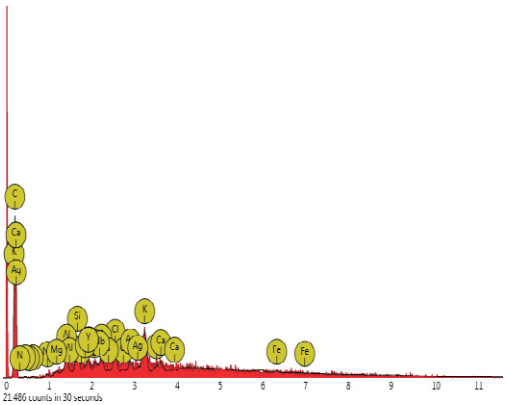

Figure 4a. EDS image of raw maize cob cellulose

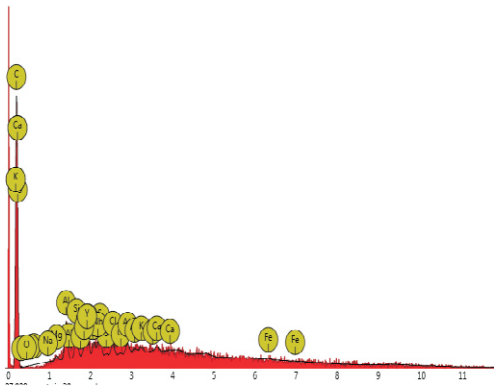

Figure 4b. EDS image of bleached maize cob cellulose

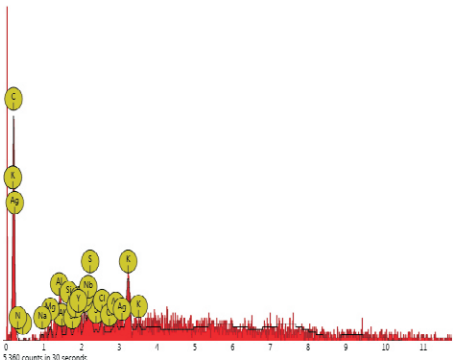

Figure 4c. EDS hydrogel before adsorption

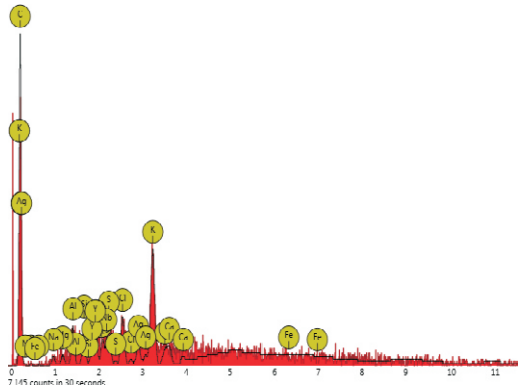

Figure 4d. EDS image of hydrogel after Adsorption

Fig. 4d is the EDS image of the hydrogel after adsorption. It can be seen that the atomic concentration of O, K and Cl increased to 3.89, 16.58 and 6.43 respectively and this can be attributed to the increased adsorption efficiency of the hydrogel.

3.3.5 Differential Scanning Calorimetry (DSC)

The DSC of the produced hydrogel is depicted in fig. 5. The DSC analysis depict that the endothermic process of the hydrogel from 30^0C to 93^0C are caused by evaporation of free water from the hydrogel. As the temperature continues to rise, the exothermic decomposition of the hydrogel prevails indicating that at higher temperature, the hydrogel undergoes thermal decomposition. This result signifies that the developed hydrogel is not viable for application in high temperature conditions.

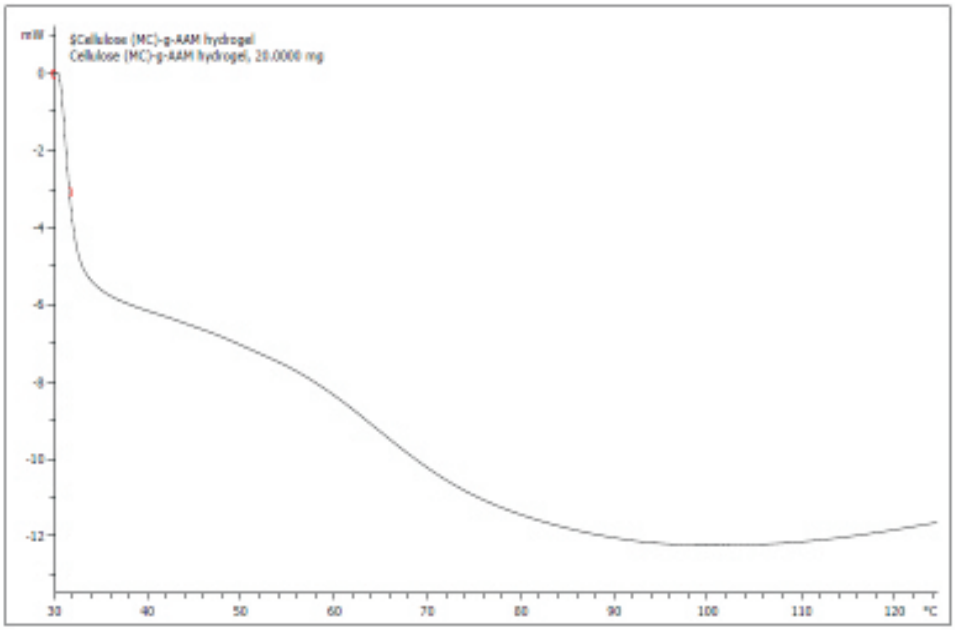

Figure 5. DSC Thermogram of Cellulose-g-(AAm) hydrogel

3.4.Swelling Studies

The effect of monomer and cross-linker concentration on the water swelling percentage of the synthesized hydrogel was studied and presented in fig. 6a and 6b respectively. The effect of pH on the water swelling characteristics of the hydrogel was studied and presented in fig. 6c.

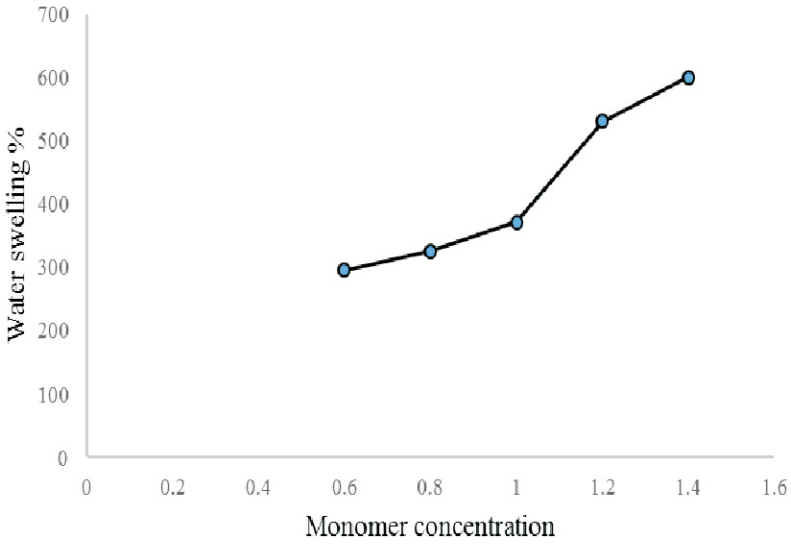

Fig 6a. Effect of monomer concentration on the concentration on the swelling property of hydrogel

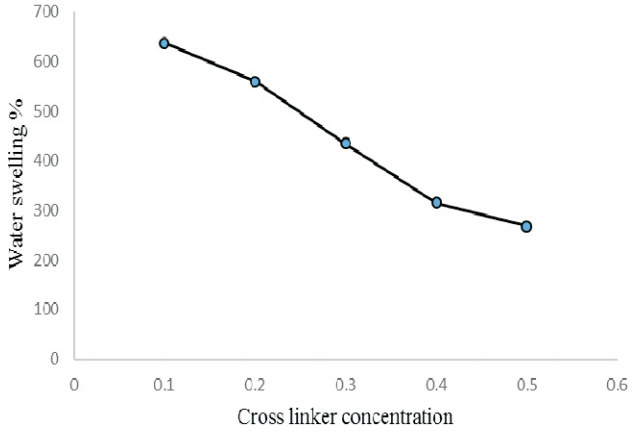

Fig 6b. Effect of crosslinker swelling property of hydrogel

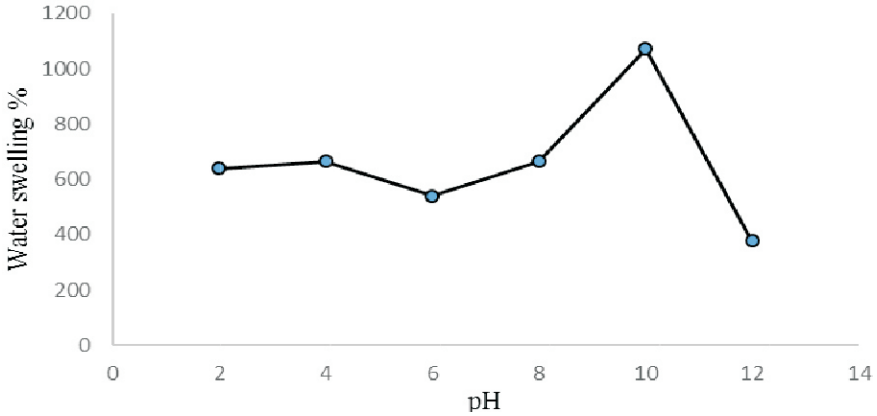

Fig 6c. pH sensitivity of synthesize hydrogel

3.4.1 Effect of Monomer Concentration on the Swelling Property of Hydrogel

From fig. 6a, the swelling percentage of the hydrogel increases as the monomer concentration increases from 0.6g to 1.4g. This characteristic can be attributed to the increase in the concentration of hydrophilic carboxylic group of the monomer around the cellulose backbone as studied by Abdel Ghaffar (2016).

3.4.2 Effect of Crosslinker Concentration on the Swelling Property of Hydrogel

The effect of crosslinker on the swelling properties of the hydrogel is depicted in fig. 6b and it can be seen that as the concentration of the crosslinker increases, the swelling of the hydrogel decreases accordingly. As the crosslinking density increased, the pore size of the hydrogel becomes narrow thereby reducing spaces required for the accumulation of water which will also decrease the osmotic pressure driving the water into the hydrogel network and this similar phenomenon was reported by (El-Arnaouty &M. Eid, 2010). This is due to the obvious fact that the swelling capability of the hydrogel is always dependent on the crosslinking agent. It can also be deduced that the higher the crosslinking agent in a hydrogel, the lower

the swelling capacity and vice versa.because crosslinking always prevents the liquid from penetrating into the hydrogels as it has been investigated by Chavda and Patel (2011).

3.4.2 Effect of pH on the Swelling Property of Hydrogel

The swelling behavior of the hydrogel was investigated at pH values of 2, 4, 6, 8, 10 and 12 and the result is presented in fig. 6c. As shown in fig. 6c, higher levels swelling was observed at pH of 4, 8 and 10 and this can be as a result of the presence of $–COONH_2$ in the polymeric chains (Saber-Samandari et al., 2013). The highest swelling level was observed under basic condition with a pH of 10 and this can be attributed to the carboxamide group ($-COONH_2$) undergoing hydrolysis and converting into carboxylate (-COONa) which are ionizable and resulting in an increase in the level of $–COO^-$ and then increased swelling (Ghobashy & Elhady, 2017).

This phenomenon will cause increase in water uptake because of the anionic and mutual repulsion among the carboxylate ions. As the pH increase above 10, the network structure collapse and swelling tendencies of the hydrogel drops rapidly.

This can also be attributed to charge screening effect of counter ions (N+) on the –COO- groups thereby generating and hindering electrostatic repulsion. Similar phenomenon was also reported by (Zhang et al., 2019, Saber-Samandari et al., 2013 & Dai et al., 2019).

3.5Adsorption Studies

The result of the physio-chemical parameters of the effluent analyzed are

presented in Table 3. The values obtained was compared with the World Health Organization (WHO) dye effluent standards (WHO, 2017). It can be seen that the effluents do not meet up with the standards specified by WHO and as such, should be treated prior to discharge to minimize possible environmental pollution.

Table 3. Physio-chemical Parameters of Effluents Before Adsorption

Parameters	Kofar Mata Dyeing Effluent	WHO
pH	11.6	6.5-8.5
TDS(mg/L)	53.2	50
Conductivity (µS/cm)	757	400
DO(mg/L)	4.5	7.5

The value of the maximum wavelength of the indigo blue and absorbance present in the dye effluent as recorded from the PerkinElmer UV/Vis Spectrum Lambda 35 is 663.61 nm and 1.9095 respectively. This result is in accordance withabsorbance of indigo blue which is at relatively long wavelengths (600-675nm) in the visible region as reported by RM Christie (2007).

Using the wavelength of the indigo blue present in the effluent as a reference, the absorbance of the standard indigo solutions was obtained from the machine and the absorbance values were plotted versus the specified specifications. As shown in fig. 8a and 8b, the unknown concentration of the indigo blue in the effluent was calculated using the eq. 1.

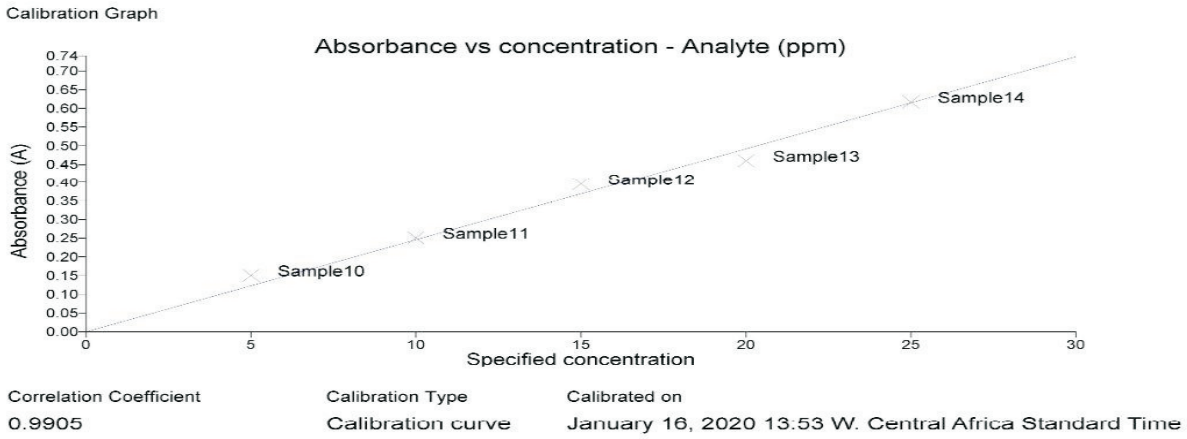

Fig 8a. Graph of absorbance versus lower concentrations of serial solutions

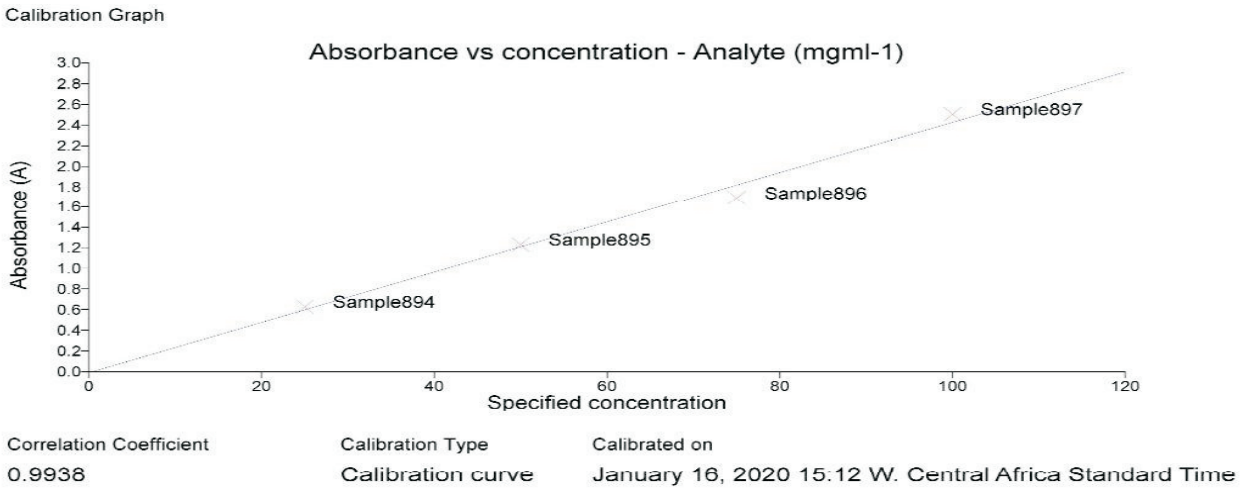

Fig 8b. Graph of absorbance versus higher concentrations of serial solutions

The slope obtained from both graphs are 0.024608 and 0.024371 respectively and the average was determined to be 0.0244895. Imputing the value of absorbance 1.9095 and slope of 0.0244985 in Eq. 1, the initial concentration of the indigo blue present in the dye effluent was calculated as 77.94 mg/L. The removal percentage of the prepared hydrogel was calculated using Eq. 4 taking into cognizance, the effect of contact time and temperature of the adsorption process.

3.5.1 Effect of Contact Time on the Percentage Removal of Indigo Blue from the Effluent Solution

The adopted contact time was 40, 60, 80, 100 and 120 minutes. As shown in fig. 9,

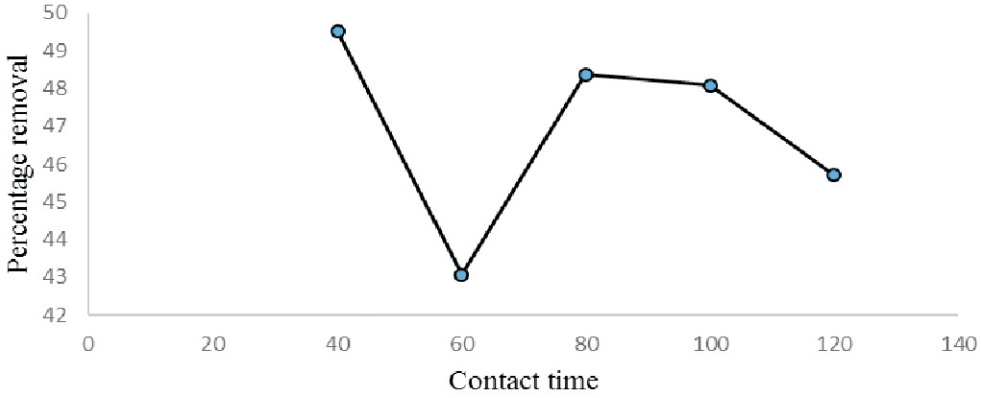

Fig 9. Effect of contact time on the percentage removal of indigo blue from the effluent solution

From fig. 9 and table 4, the optimum contact time required for the maximum percentage removal of the indigo blue from the effluent solution by the synthesized hydrogel at a constant pH of 11 and 0.1g of adsorbent is 40 minutes with corresponding percentage removal of 49.53%. Other notable optimum contact times were observed at 80 and 100 minutes with corresponding swelling

percentages of 48.38% and 48.09%. The residual indigo blue after testing with hydrogel was determined by repeating the same procedure adopted in determining the initial indigo blue in the die and removal percentage was calculated using Eq. 4.

The initial rapid adsorption was ascribed to the large pore size of the hydrogel networks and availability of carboxylate group thereby facilitating an initial bulk diffusion of the effluent into the hydrogel.

The intermediate decline in removal percentage at contact time of 60 minutes can be ascribed to the intra-particle diffusion as well as electrostatic interaction between the dye and the adsorbent similar to a report by (Yuan et al., 2019).

Table 4. Effect of contact time on the percentage removal of indigo blue from the effluent solution

Time (min)	Absorbance(A)	Concentration (mg/ml)	%Removal
40	0.9637	39.16	49.53
60	1.0872	44.18	43.06
80	0.9859	40.06	48.38
100	0.9913	40.28	48.09
120	1.0366	42.12	45.71

3.5.2 Effect of Contact Temperature on the Percentage Removal of Indigo Blue from the Effluent Solution

The effect of temperature on the adsorbent efficiency of the hydrogel was tested and the results obtained are depicted in table. 4 and fig. 9 respectively.

Table 4. Effect of temperature on percentage removal

Temperature (^oC)	Absorbance(A)	Concentration (mg/ml)	%Removal
30	1.017	41.33	46.73
35	0.9837	39.97	48.49
45	0.9539	38.76	50.1
55	1.132	46.00	40.71
60	1.315	45.98	40.74

The temperature was varied at 30^0C, 35^0C, 45^0C, 55^0C and 60^0C. It was observed that as the temperature increases from 30^0C to 35^0C the percentage removal increases gradually with the highest percentage obtained at 45^0C. the percentage removal increases. At higher temperatures such as; 55^0C and 60^0C, the

percentage removal was low. This characteristic can be attributed to the high decomposition rate of the initiator (potassium persulphate) leading to a higher crosslinking density and denser network which will then hinder the hydrogel from absorbing more effluent which is in accordance with the studies of Cheng *et al*., (2017).

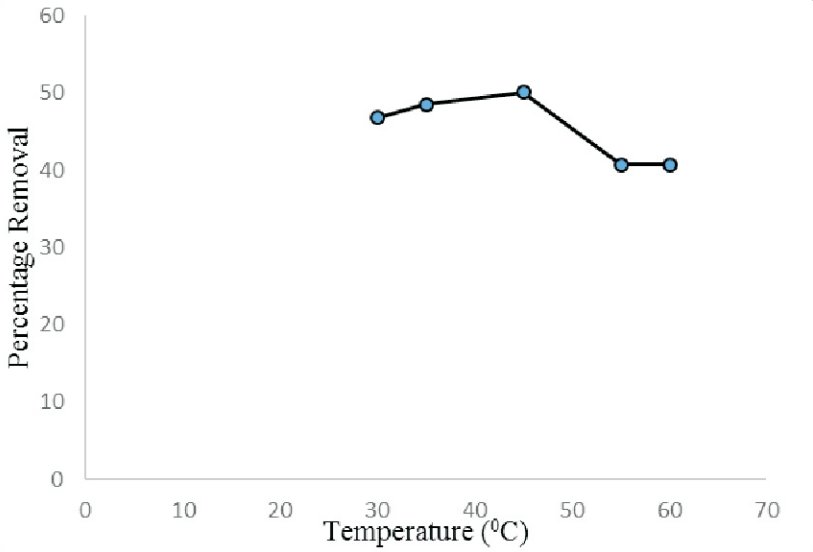

Figure 10. Effect of Temperature on the Percentage Removal of Indigo from Effluent Solution

3.5.3 Effect of Hydrogel Dosage on the Percentage Removal of Indigo Blue from the Effluent Solution and Physio-chemical Parameters of the Effluent.

The effect of hydrogel dosage on the percentage removal of the indigo blue from the effluent was investigated. This is also an important parameter as it helps optimize the behavior of removing dyes. As shown in table 5, the percentage removal of the indigo blue from the effluent increases as the hydrogel dosage is increased. This can be attributed to the availability of vacant adsorptive sites on the adsorbent for indigo blue under osmotic pressure as stated by Hu *et al*., (2018) in their investigation of superabsorbent hydrogel for removal of methylene blue dye from aqueous solution.

Table 5. Effect of hydrogel dosages on percentage removal

Hydrogel (g)	Absorbance (A)	Concentration (mg/ml)	%Removal
0.1	0.9539	38.76	50.1
0.2	0.6760	27.47	64.6
0.3	0.6441	26.17	66.27
0.4	0.5340	21.70	72.03

0.5	0.4878	19.82	74.46

Table 6 shows the effect of hydrogel dosages on the physiochemical parameters of the remaining effluent after adsorption studies. As shown below, it can be seen that though the physiochemical parameters obtained does not tallies with the WHO standard as tabulated in table 3 but it shows more prospect than the dye effluent before adsorption.

Table 6. Effect of the Hydrogel Dosages on the Physiochemical Parameters of Local Indigo Blue dye from the Effluent

Hydrogel dosages	Conductivity ($\mu S/cm^{-1}$)	TDS (mg/L)	DO (mg/L)	pH
0.1g	756	5.14	5.5	11.1
0.2g	754	5.14	6.5	11.0
0.3g	752.5	5.17	6.5	10.9
0.4g	752	5.08	6.1	10.7
0.5g	752	4.83	5.7	10.1

4. Conclusion

In this study, hydrogel was synthesized using cellulose from maize cob as raw materials while N,N'-methylene bisacrylamide was used as a crosslinking agent and potassium persulphate as initiator in the presence of acrylamide. The developed hydrogel was characterized using FTIR, SEM, XRD and EDS. Swelling studies was conducted with the hydrogel and it was observed that the swelling capacity decreases with increase in crosslinker concentration and increases with decrease in monomer concentration. The hydrogel also presented considerable removal of indigo blue from local dye effluent. Effect of hydrogel dosage, contact time and temperature on effluent removal was investigated and the result showed that the developed hydrogel is a promising candidate for application as an efficient adsorbent in wastewater treatment.

References

Abdel Ghaffar, A. M., El-Arnaouty, M. B., Abdel Baky, A. A., & Shama, S. A. (2016). Radiation-induced grafting of acrylamide and methacrylic acid individually onto carboxymethyl cellulose for removal of hazardous water pollutants. *Designed monomers and polymers,* 19(8), 706-718.

Abdul Razak N. I., Ibrahim N. A., Zainuddin N., Rayung M. and Saad W. Z (2014). "The Influence of Chemical Surface Modification of Kenaf Fiber using Hydrogen Peroxide on the Mechanical Properties of Biodegradable Kenaf Fiber Poly (Lactic Acid) composites". *Int J Mol Sci.* 15(8): 14728-14742.

Abe K., & Yano H. (2010). Comparison of the characteristics of cellulose microfibril aggregates isolated from fiber and parenchyma cells of Moso bamboo (Phyllostachyspubescens). *Cellulose*, 17, 271–277.

Anuka A., Mamphweli S., Reddy P., & Okoh O. (2017). Characterization and the effect of lignocellulosic biomass value addition on gasification efficiency. *Energy Exploration and Exploitation*, 1–16.

Chavda H.V. and Patel C.N. (2011). "Effect of Crosslinker Concentration on Characteristics of Superporous Hydrogel". *International Journal of Pharmaceutical Investigation.* DOI: 10.4103/2230-973X. 76724

Cheng W.-M., Hu X.-M., Zhao Y. -Y., W, M.-Y., Hu Z.-X., & Yu X.-T. (2017). Preparation and swelling properties of poly (acrylic acid-co-acrylamide) composite hydrogels. *e-Polymers,* 17(1), 95-106.

Christie R.M (2007). Why is Indigo Blue. *Biotechnic & Histochemistry. 82(2): 51-56.*

Dai H., Zhang, Y., Maa L., Zhan, H., & Huang H. (2019). Synthesis and response of pineapple peel carboxymethyl cellulose-g-poly (acrylic acid-co-acrylamide)/graphene oxide hydrogels. *Carbohydrate Polymers,* 215, 366–376.

Dongzhuo M., Baodong Z., Bo C., Jian W.&Jianwei Z. (2017). Fabrication of the novel hydrogel based on waste corn stalk for removal of methylene blue dye from aqueous solution. *Applied Surface Science* http://dx.doi.org/10.1016/j.apsusc.2017.06.072

Dong W., Qi, X., Wu L., Su T., & Zhang J. (2018). "Polysaccharide-based cationic hydrogels for dye adsorption". *Colloids and Surfaces. B, Biointerfaces,* 170, 364 – 372.

El-Arnaouty M. B., &Eid M. (2010). Synthesis of Grafted Hydrogels as Mono-Divalent Cation Exchange for Drug Delivery. *Polymer-Plastics Technology and Engineering,* 49(2), 182 – 190.

Ghobashy M. M., & Elhady M. A. (2017). pH-sensitive wax emulsion copolymerizationwith acrylamide hydrogel using gamma irradiation for dye removal. *Radiation Physics and Chemistry,* 134, 47–55.

Hu X., Liang R., & Sun G. (2018). Superadsorbent hydrogel for removal of methylene blue dye from aqueous solution. *Journal of Materials Chemistry,* 6, 17612-17624.

Huang H., Dai H., Zhang, Y., Ma, L. and Zhang, H. (2019). "Synthesis and Response of Pineapple Peel Carboxymethyl Cellulose-g-Poly (Acrylic Acid-Co-Acrylamide)/Graphene Oxide Hydrogels". *Carbohydrate Polymers* https://doi.org/10.1016/j.carbpol.2019.03.090

Huang S., Wu L., Li T., Xu D., Lin X. and Wu C. (2019). "Facile Preparation of Biomass Lignin-Based Hydroxyethyl Cellulose Super-Adsorbent Hydrogel for Dye Pollutant Removal". *International Journal of Biological macromolecules.* Vol 13: 939-947

Ibrahim M. M. and El-Zawawy W. K. (2013). "Cellulose and Microcrystalline Cellulose from Rice Straw and Banana Plant Waste: Preparation and Characterization". *Cellulose* 20:2403–2416

Ibrahim M. M, AAglevor F.A and El-Zawawy W.K (2010). "Isolation and Characterization of Cellulose and Lignin from Steam Exploded Lignocellulosic Biomass". *Bioresources* I5(1): Pp.397-418

Kang H, Song X, Wang Z and Zhang W. (2016). "High performance and Fully Renewable Low Protein Isolate-Based Film from Microcrystalline Cellulose via Bio-inspired Poly (dopamine)". *Surface Modification ASC Sustainable Chem. Eng.* Vol. 4(8), pp. 4354- 4360.

Karadag C., Uzum O. B, Saraydin D. and Guven O (2015). "Dynamic Swelling Behaviour of Gamma-Radiation Induced Polyelectrolyte Poly (AAm-co-CA) Hydrogels in Urea Solutions. *International J. of Pharmaceutics* 301; 102-111.

Kim J., Jayaramudu T., Ko H.U., Kim H.C. and Kim J. W (2019). "Swelling Behavior of Polyacrylamide Cellulose Nanocrystal Hydrogels: Swelling, Kinetics, Temperature and pH Effects". *Materials* 12; 2080: 10.3390/ma12132080.

Mondal I. H. and Harque O. (2019). "Cellullose hydrogels: A Greener Solution of Sustainability Cellulose-Based Superabsorbent Hydrogels". *Polymers and Polymeric Composites: A Reference Series*, https://doi.org/10.1007/978-3-319-77830-3-4

Morgan J.L.W., Strumillo J., Zimmer J. (2012). Crystallographic snapshot of cellulose synthesis and membrane translocation. *Nature* 493 (2012) 181–186.

Muhammad A.F., Hanif M. and Ranjha N.M. (2016). "Method of Synthesis of Hydrogels (A Review)" *Saudi Pharmaceutical Journal.* Vol. 24: 554 – 559.

Nurfadila, Maddu A, Winarti and Kurniati (2019). Cellulose-based Nano Hydrogel from Corncob by Gamma Radiation. *Earth and Environmental Science.* 299. doi: 10.1088/1755-1315/299/1/012003

Saber-Samandaria, S., Saber-Samandarib, S., & Gazi, M. (2013). Cellulose-graft-polyacrylamide/hydroxyapatite composite hydrogelwith possible application in removal of Cu (II) ions.*Reactive & Functional Polymers*, 73, 1523 – 1530.

Sami A. J., Khalid, M., Iqbal, S., Afzal, M., & Shkoori, A.R. (2017). Synthesis and Application of Chitosan-Starch Based Nanocomposite in Wastewater Treatment for the Removal of Anionic Commercial Dyes. *Pakistan Journal of Zoology,* 49(1), 21- 26.

Shogren, R. L., Peterson, S. C., Evans, K. O., & Kenarc, J. A. (2011). Preparation and characterization of cellulose gels from corn cobs. *Carbohydrate Polymers,* 86, 1351 - 1357.

Song Y., Peng R., Chen S. and Xiong Y . (2019). "Adsorption of Crystal violent onto Epicholohydrin Modified Corncob". *Desalination and Water Treatment* . Vol. 154, pp. 376-384.

Suhas Gupta V.K., Carrott P.JM., Singh R., Chaudhary M., and Kushwaha S. (2016). "Cellulose: A Review as Natural, Modified and Activated Carbon Adsorbent. *Bioresource Technology* 216:1066–1076.https://doi.org/10.1016/j.biortech.2016.05.106.

Xu H.T., Zhang H.J., Yang Y.O., Liu L. & Wang Y. (2016). Two - dimensional hierarchical porous carbon composites derived from corn stalks for electrode materials with high performance. *Electrochem. Acta* 214: 119–128.

Wang, Z., Ning, A., Xie, L., Xie, P., Gao, G., & Li, X. (2017). Synthesis and swelling behaviors of carboxymethyl cellulose-based superabsorbent resin hybridized with graphene oxide. *Carbohydrate Polymers,* 157, 48–56.

Wu, H. F., Chen-Ruoya, D. H., Zhang, J., Shi, L. Q., Yue, L. and Wang, J. (2018). Synthesis of activated carbon from peanut shell as dye adsorbents for wastewater treatment. *Adsorption Science and Technology*, 37(1-2), 34-48.

WHO (2017). *Guidelines for drinking-water quality* (Fourth ed.). Geneva: World Health Organization. Retrieved from http://apps.who.int/iris/bitstream/handle/10665/254637/9789241549950-eng.pdf;jsessionid=50C6132EBB51C726A13FBCDE4545385E?sequence=1

Winarti, C., Kurniati, M., Arif, A. B., Sasmitaloka K. S., & Nurfadila (2018). Cellulose-Based Nanohydrogel from Corncob with Chemical Crosslinking Methods. *IOP Conf. Series: Earth and Environmental Science,* 209, 012043. doi:10.1088/1755-1315/209/1/012043.

Yuan, Z., Wang, J., Wang, Y., Liu, Q., Zhong, Y., Wang, Y., Li, L., Lincoln, S. F., & Guo, X. (2019). Preparation of a poly (acrylic acid) based hydrogel with fast adsorption rate and high adsorption capacity for the removal of cationic dyes. *RSC Advances,* 9, 21075–21085.

Zhong G. T., Yang B, Hua W. Q, Li L., Zhou Z. H, Xu L., Bian F. G, Ji X and Li Z. H (2019). "Robust Hydrogel of Regenerated- Cellulose by Chemical Crosslinking Coupled with Polyacrylamide Network". *J. Appl. Polym-Sci.* DOI: 10.10021app. 47811.

Nigerian Journal of Polymer Science and Technology, 2021, Vol. 16, pp23-33
Received: 09/03/2021 Accepted: 12/10/2021

PREPARATION, CHARACTERISATION AND APPLICATION OF SHEA BUTTER ALKYD RESINS AS BINDER IN PAINTS

[1]Sharif N. U, [2]Haruna Musa, [3]H. Y. Umar, [4]Umar Bala Yakasai,

[1]Department of Chemical Sciences, Fed. University Kashere, P.M.B. 0182, Gombe, Nigeria
[2]Department of Pure and Ind. Chemistry, Bayero University, P.M.B. 3011, Kano -Nigeria
[3]Chemistry Department, School of Sciences, Fed. College of Education (Technical), Gombe
[4]Department of Chemistry, College of Remedial & Preliminary Studies Kano State.

*Corresponding author: nafiu.sharif@fukashere.edu.ng, sharifnafiuusman@ymail.com

ABSTRACT

The physico-chemical properties of Shea butter was determined and used in the synthesis of alkyd resin using glycerol and phthalic anhydride at 230-250^{o}c. The prepared alkyd resin was characterized using FT-IR spectroscopy, titrimetric analysis and its properties such as solubility, viscosity was measured. The antimicrobial activity was determined using well diffusion method. The resin microbial analysis shows some activity against some selected bacterial specie particularly at 100mg/ml and 50mg/ml in DMSO solvent. The paints containing 0%, 10%, 20% resin concentration were formulated. The resins content formulations were found to possess desired fastness properties to certain agencies. The antimicrobial activity results revealed SBAR can be utilized for the production of antimicrobial paints.

Keywords*: Shea butter oil (SBO), Shea butter Alkyd resin (SBAR), Paint, Binder.*

Introduction

The forest reserve of Nigeria accommodate a lot of edible and non-edible seeds bearing oil like Shea butter tree which known for its pharmaceutical and industrial uses, however, danger and rapid depletion of crude oil reserve, adverse environmental impacts, unstable nature of international oil market compel economic diversification for the country (Eze and Elijah 2010 and Uzo *et al.,* 2013). Ghana, Burkina Faso is an exporter of Shea butter, Nigeria with highest tree density is the major exporter despite setback of 70% rot away in a bush due to poor collection mechanism (Obibuzor *et al.,* 2014). Shea nut is an oil rich plant with 45-60% oil content which mainly used in the manufacture of candle, soap, cosmetics and pharmaceutical products (Warra *et al.,* 2013). Large quantities of oil are needed for the production of alkyd resin, like linseed oil was mostly imported which resulting in high cost of production. In Nigeria, the demand of alkyd resin is always increasing even though technical information on local production is scanty (Onuwli and Igbokwe 2008). Good drying performance rate, resistance to certain agencies having negative effects on paints necessitate using alkyd resin as binders for gloss finishes, varnishes, wood primers, enamels and lacquers instead of using drying oils (Ogunniyi and Njikang 1998). The alkyd resin which is prepared by polycondensation polymerization of polyhydric alcohol, polybasic acid and modified fatty acid is referred as oil modified alkyd resins and contribute about 70% of conventional binders which determined performance of surface coating against abrasion, chemical invading and UV-light attacks (Oladipo *et al.,* 2013; Blaise *et al.,* 2012; Hlaing and Oo 2008). The biodegradabilitys nature of major component of alkyd resins (plant oil, phthalic anhydride and glycerol) makes them quite interesting binders from an

ecological point of view (Shaker *et al.,* 2012). However, Nigeria blessed with oil-bearing seeds available in tropical plants that are important sources of industrial oil which if well harnessed can enhance the supply vegetable oil as raw materials (Odetoye *et al.,* 2008). Paints essentially consist of pigment dispersed in a resinous binder reduced to an acceptable viscosity with a solvent; in most cases organic components determine the physical and chemical properties of the paints (Opara *et al.,* 2013). The necessity of releasing the polymer industry from its dependence on depleting resources and searching for industrially renewable alternative is a major concern. Since, plant oils offer many advantage in term of their renewability, availability, low price makes them industrially acceptable (Meier and Lucas 2010). Despite the predominance of petroleum-based polymers, plants oil is increasingly demanded by coatings and chemical intermediate industries (Aigbodion *et al.,* 2000).

There is need for Nigeria to intensify research on some indigenous plants seed in order to reduce importation cost and generate wealth considering high demand of alkyd resin by coating industries due to rapid economic growth of the sector.

2.0 Material and Methods

The SBO sample was obtained from Kurmi Market, Kano State. Phthalic anhydride, glycerol, ethanol, methanol, white spirit, iron (III) oxide, calcium carbonate, calcium acetate were all purchased from Sigma Aldrich.

The apparatus and equipment used include; three-neck flask equipped with Dean and Stark apparatus, Reflux Condenser, Brookfield Viscometer, Oswald Viscometer, Suction filtration apparatus, pH meter Jenway Model 3320, FTIR Spectrophotometer Agilent Technologies and nitrogen source.

2.1. Moisture Content Determination

The oil samples weighed 100g in a pre-weighed beaker and heated for one hour at 100^0C. The oils were allowed to cool at room temperature and weighed again to determine the weight loss using the relation below;

$$\% \text{ Moisture Content} = \frac{w_1 - w_2}{w_1} \times 100 \quad \text{.....eq.1}$$

W_1=Initial weight

W_2=Final weight

2.2. Determination of Acid value

5.0 g of fat or oil in a dried conical flask followed by 25 ml of absolute ethanol and (2-3) drops of phenolphthalein indicator was added. Heat with shaking in water bath (65%) for 10 minutes, then cooled followed by titrating the solution against 0.1 N KOH until pink colour appears (end point).

$$\text{AV} = \frac{ml\ of\ KOH \times N \times 56}{weight\ of\ sample} = \text{mg of KOH} \quad \text{.....eq. 2}$$

% Free Fatty Acid (FFA) = AV x 0.503

2.3. Iodine Value Determination

The hanus iodine reagent was prepared by dissolving iodine (13.2 gm) in glacial acetic acid (1litre) with the help of heat. The solution was cooled and 3 ml of bromine added. The hanus iodine reagent was then kept in a brown bottle until the analysis was complete. Oil sample (2g) was weighed into a 500ml conical flask and 10ml of chloroform added. By use of a pipette 25ml of hanus iodine reagent was added and left to stand in the dark for 30minutes with occasional shaking. After this 15% potassium iodine was added, shaken thoroughly and distilled water (100ml) added to rinse down any iodine on the stopper.

The solution was then titrated with 0.1N sodium thiosulphate until a yellow solution turned almost colourless (titration = S ml). Three drops of starch indicator (1%) was added towards the end point and titration was continued until the blue colour turned colourless. A blank determination was done

and results recorded (titration = B ml). All the analysis was done in duplicate using the formula:

$$\text{Iodine value} = \frac{(B - S) \times 0.1 \times 12.69}{(weight(g)\ of\ sample)} \times 100$$

.....eq. 3

2.4. Determination of Saponification Value

Shea butter/oil samples (2g) was weighed into a conical flask and 25ml of ethanolic potassium hydroxide added. The solution was refluxed in boiling water bath for 1 hour while being shaken 1frequently. One ml of phenolthalein indicator was added to the hot solution and titrated immediately with 0.5M hydrochloric acid (sample titration= s ml). A blank test was done and results recorded (blank titration = b ml). All the analysis were done in duplicate and the saponification value calculated as:

$$SP = \frac{56.1\ (B - S)\ x\ N\ of\ HCl}{(weight(g)\ of\ sample)} \times 100$$

.....eq. 4

Where B = ml of HCl required by the blank sample

S = ml of HCl required by the sample

2.5. Preparation of Alkyd Resin

Monoglyceride was first prepared by heating a mixture of 10g oil, 20g glycerol and 0.3g $CaCO_3$ (catalyst) in a 500ml three necked round bottom flask fitted with condenser, Dean and Stark apparatus. The mixture was heated to 240ºC and maintained at this temperature for 1-2 hours using fitted thermometer. An aliquot was taken at interval to check for solubility in methanol which indicates the formation of the monoglyceride. At the onset of the second phase, the temperature was lowered to about 180 ºC and measured quantity of phthalic anhydride (3:2 glycerol) was added, followed by addition of xylene (10% of total weight charged) into the reaction mixture. The water of esterification forms an azeotrope with xylene and removed. The temperature was increased to 230-250 ºC while the reaction lasted. Aliquots were withdrawn from the reaction mixture at intervals of 60 minutes to determine the drop in acid value. The reaction was stopped when the acid value attained about 15 mg KOH/g and the alkyd resin was allowed to cool (Onukwli and Igbokwe 2008).

2.2. The physicochemical parameters of SBAR; such as colour, acid value and viscosity, were determined. The FTIR of the resin was acquired using FTIR spectrophotometer (Agilent Technologies) while the antimicrobial properties were determined using well diffusion method.

2.5.1. Fourier Transform Infra-Red (FTIR) Spectroscopy

The FTIR test was conducted using Agilent Technologies Spectrophotometer over range of 4000.00-650.00 on resolution of 4 cm^{-1} at Bayero University, Kano-Nigeria.

2.5.2. Determination of Solubility

The solubility of the samples in different solvents such as white spirit, ethanol, methanol and xylene. 1 gram of resins was dissolved in 10ml and shakes vigorously in which the solubility was carefully observed and recorded.

2.5.3. Determination of Viscosity

Oswald Viscometer was used at 30 ^{0}C for viscosity measurements. Stock solution of 1.0 gram of resins in 100ml turpentine prepared. The viscometer was charged with pure solvent and the time taken for the solvent to follow through the bulb noted. Stock solution of 10ml was transferred into the empty viscometer and the time taken for the solution to pass the same mark noted. Three readings were taken and the average used to calculate the relative viscosity (Habibu, S, 2012). The average for shea butter resin taken as;

$$\frac{t}{t} = \frac{9.75}{7.33} =$$

1ǫ33.....eq. 5

Where

t_o= efflux time of turpentine

t = efflux time of resin

2.5.4. Antimicrobial activity

Antimicrobial activity of the products was conducted using standard methods. The

antimicrobial potential test was carried out using agar well diffusion method. The inhibition zones were measured and compared with the standard reference antibiotic ciprofloxin. The extracts were subjected to serial dilusion by using dimethyl sulphoxide (DMSO) as a solvent to give 100mg/ml, 50mg/ml, 25mg/ml solutions. The concentration of ciproflaxin standard used for this study was at 2mg/ml. Each prepared concentration of the different extracts was tested for it antimicrobial activity against *S. aureus, E. coli, S. typhi* on nutrient agar plates using disc diffusion method. All the plates were incubated at 37^0C for 24 hours. Evaluation of antibacterial activity was measured showing the diameter of the zones of inhibition against the tested bacteria (Sharif 2015).

2.5.5. Paint Formulation

At first, 100ml of white spirit was measured, followed by dissolving certain quantity of resin (0, 10 and 20g) then mixing and stirring. Pigment and extender in 15:5 gram ratio was added, followed by addition of calcium acetate (0.3 gram drying agent). The paint was then transferred to air tight container (Haruna and Sharif 2016).

3. Results and Discussion

The physico-chemical properties of the SBO sample was evaluated using standard methods and result of the analysis presented in table 1.

Table 1. Physico-chemical properties of SBO

Physico-chemical properties	Result
Colour	Yellowish-white
Refractive Index	1.4801
pH	5.37
Nature at room temperature	Solid
Moisture content (%)	0.06
Specific gravity at 25^0c (g/cm^3)	0.9251
Acid Value (mg/g)	4.451
Iodine Value (mg/g)	67.816
Saponification Value (mg/g)	227.02
%FFA	2.24
Ester Value	222.57

The FTIR spectrum of prepared SBAR revealed signal of carbonyl stretching due to an ester linkage band at 1723 cm^{-1} and disappearance of broad band of O-H in the range of 3300-3500cm^{-1} from one of the reactant (glycerol). The peaks of 1601, 1581 cm^{-1} were attributed to benzene ring from phthalic anhydride in the alkyd resin component.

Table 2: physical properties of SBAR

Properties	Specific Value
Colour	Blue-Black
Viscosity (absolute)	1.33
Solubility in;	
Xylene	Completely soluble
Turpentine	Completely soluble
Ethanol	Limited solubility
methanol	Limited solubility

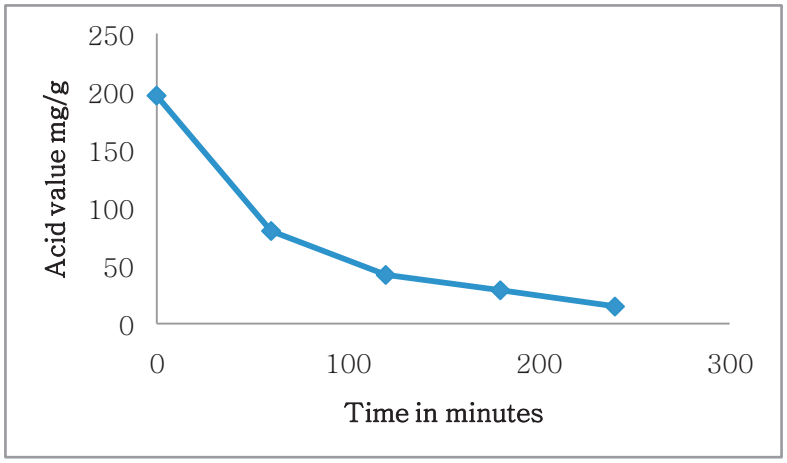

Figure 2: Drop of acid with polycondensation time

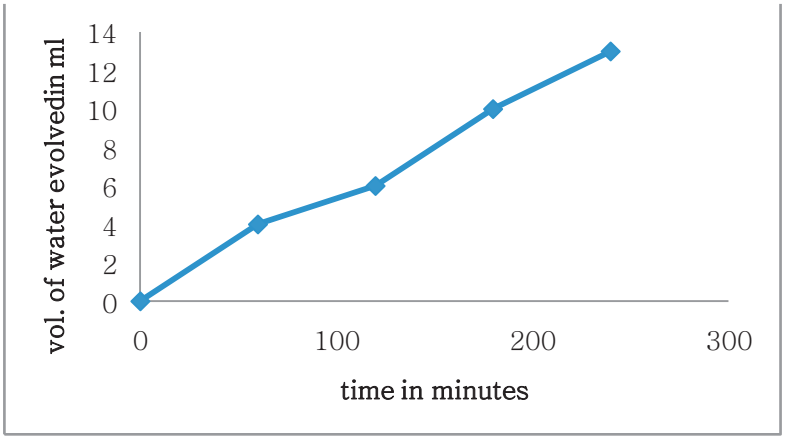

Figure 3: Volume of water evolved during synthesis of SBAR with time

The progressive decrease of acid value as in figure 2 can be linked to primary hydroxyl group (react at about 160^0c) and secondary hydroxyl group (react 230^0c) reaction with carboxylic group of phthalic anhydride. Also, step growth polymerization in which all the reactant are incorporated into a polymer chain characterized by decreased in acid value with time. Similar observation was reported by (Onukwli and Igbokwe 2008).

The reduced rate of water evolution as the reaction progress as seen in figure 3 was linked to esterification reaction of condensation process. Similar observation was reported by (Oladipo *et al.,* 2013). Also, there was decreasing in viscosity of the mixture as the reaction progresses.

Table 3: Antimicrobial Activities of SBAR

Isolates	100mg/ml (mm)	50mg/ml (mm)	25mg/ml (mm)	2mg/ml control (mm)
E. coli	8	7	0	35
S. typhi	12	9	7	32
S. aureus	8	7	7	31

*control= Ciprofloxacin.

The Shea butter resins show activities at various concentration of 100, 50 and 25mg/ml of SBAR as presented in Table 3 above.

In *Salmonella specie,* the inhibition zones were as 12, 9 and 7mm while the *Staphylococcus* was 8, 7, and 7mm both at 100, 50 and 25mg/ml respectively. It was observed that for *E. coli species,* the resin were only active against the species at 100 and 50mg/ml (8mm and 7mm inhibition zone) and inactive at 25mg/ml resin concentration.

Table 4: Properties of SBAR Paints

Mechanical/Physical test	0%w/v	10%w/v	20%w/v
Flexibility test	Crack observed	No crack observed	No crack observed
Light fastness at 94hrs	5(Good)	8(Outstanding)	8(Outstanding)
Chemical Resistance;			
Water	Good	Excellent	Excellent
Brine	Fair	Very good	Very good
Acid (H_2SO_4)	Fair	Good	Good
Alkali (NaOH)	Fair	Fair	Fair
Xylene	Poor	Poor	Poor
Viscosity (cp)		6.8	10.78

In the SBAR paint formulated, it was found that 10%w/v and 20%w/v passed flexibility test and showed excellent fastness to UV-light at 94hrs. The paints showed only poor resistance to xylene solvent thereby resistance to other liquids.

4. Conclusion

SBAR prepared from raw Shea butter and antimicrobial test shows it is active against some selected bacterial species. The resin used for the formulation of paint, the paints was found to be excellent and resistance to certain common agencies. Therefore, SBAR can be used for the production of antimicrobial paint which has promising application in public places to avoid contaminations by infectious diseases.

References

Aigbodion A. I., & Pillai, C. S. K. (2000). Preparation, analysis and application of rubber Seed oil and its derivatives in surface coatings, *Progress in Organic Coatings, 38*, 187-192.

Blaise V. I., Ogunniyi, D.S., Ongoka, P. R., Moussounga, J. E and Ouamba, J. M (2012); Physicochemical properties of alkyds resin and palm oil blends, *Malaysian polymer journal 7(2):42-45*

Eze, J. I. and Ejilah I. R., (2010): Tested performance of parameters of diesel fuel and transesterified shea nut oil blends in compression ignition engine, *Global Journal of Research in Engineering 10(1):84-92.*

Hlaing, N.N., Oo M.M. (2008): Manufacture of Alkyd Resin from Castor Oil, *World Academy of Science, Engineeing and Technology vol (2) 136-142.*

Haruna M. and Sharif, N. U. (2016). Preparation and

antimicrobial evaluation of Neem oil alkyd resin and its application as binder in oil-based paint, *Environmental and Natural Resources Research,* 6(2) 92-98.

Habibu, S., (2012): Synthesis, characterization and application and application of some monoazo disperse polymerizable dyes, unpublished MSc. Thesis submitted to Department of Pure and Applied Chemistry, Bayero University Kano.

Meier A. R. M., & Lu cas, M. E. (2010). Plants oil: The Perfect Renewable Resource for Polymer Science, *European Polymer Journal,* 47, 837-852.

Obibuzor, J. U., Abigor R. D., Omamor I., Omeriyekemwen V., Okogbenin E. A. and Okunwaye T., (2014): A two-*year* seasonal survey of the quality of shea butter produced in Niger State of Nigeria, *African Journal of Food Science 8(5):660-667.*

Odetoye, T. E., Ogunniyi D. S and Olatuji (2008): Vegetable oil as industrial raw material; Proceeding of the 1st Kwara Conference of Chemical of Chemical Society of Nigeria, 2008 Ilorin-Nigeria.

Ogunniyi, D.S. and Njikang G. N., (1998): Industrial Utilization of Castior Oil in Alkyd Resin Synthesis and Evaluation, *Journal of the Nigerian Society of Chemical Engineers. (17) 44-50.*

Onukwli, O.D.,Igbokwe P. K. (2008): Production and Characterization of Castor Oil Modified Alkyd Resin, *Journal of Engineering and Applied Sciences 3(2):160-165*.

Oladipo, G. O., Eromosele I. C and Folarin O. M(2013): Formation and Characterization of Paint Based on Alkyd Resin Derivative of Ximenia americana (wild olive) Seed Oil, *Environmental and Natural Resources Research 3(3) 52-62.*

Opara, C. C., Sokore Bekere, Ugwo, P. N., (2013): Production and Study of Factors Affecting the Flexibility of Polyester Paint Using Local Materials, Greener Journal of Science, Engineering and Technology Research 3(5):146-152.

Shaker N. O., Alian N. A., and Elsawy M. M. (2012): Preparation and Characterization and Evaluation of Jojoba seed oil modified alkyd resins, *Pelagia research library 3(5): 1157-1162.*

Sharif, N. U., (2016): Synthesis, characterization of alkyd resins derived from Neem oil and Shea butter and their application as binder in oil-based paints, unpublished MSc. Thesis submitted to Department of Pure and Applied Chemistry, Bayero University Kano.

Uzor C. F., Onukwuli, Odera R. S., Okey-Onyesolu C. F., (2013): Synthesis and characterization of palm oil based air-drying

alkyd resin for surface coating, *Research journal in engineering and applied science 2(3):187-191*

Warra A. A., Jega S. A., Ahmad A. J., and Abbas M. Y., (2013); Comparative physicochemical analysis of traditional and hexane extract of Shea nut fat, *Applied Science Reports 3(1):100-102*.

Appendix A

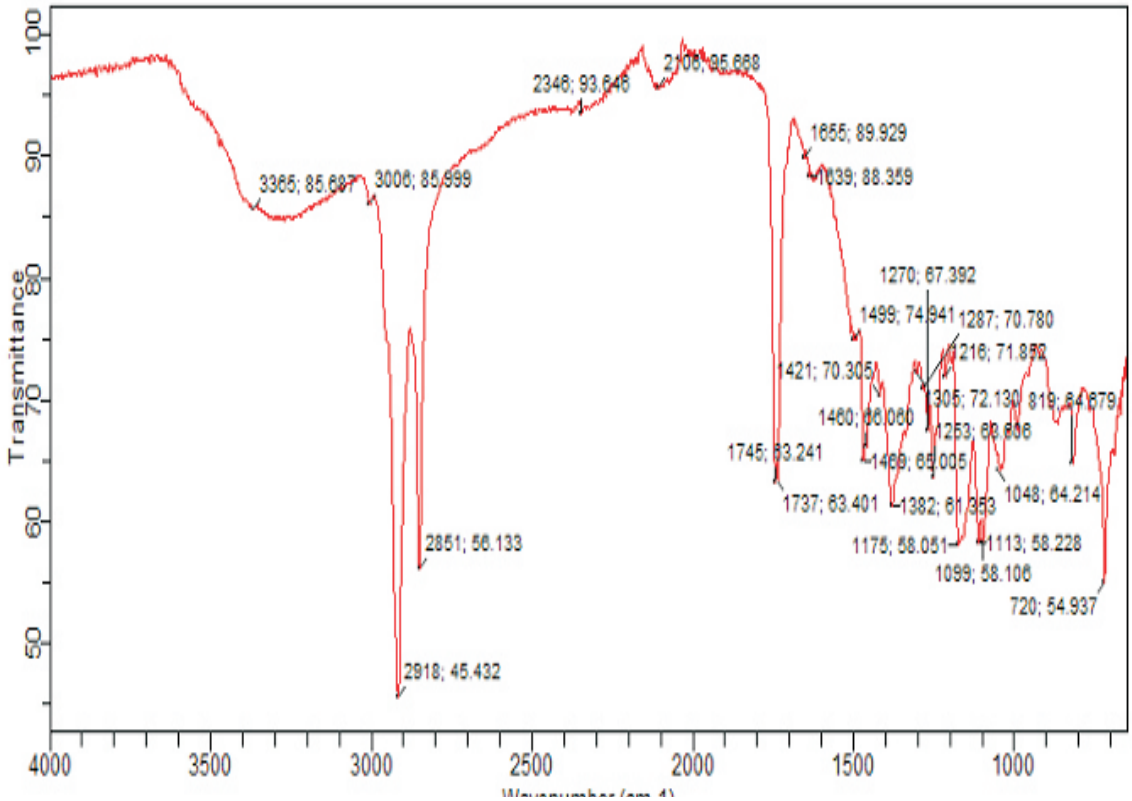

Figure 1: Shea Butter FTIR Spectra

Appendix B

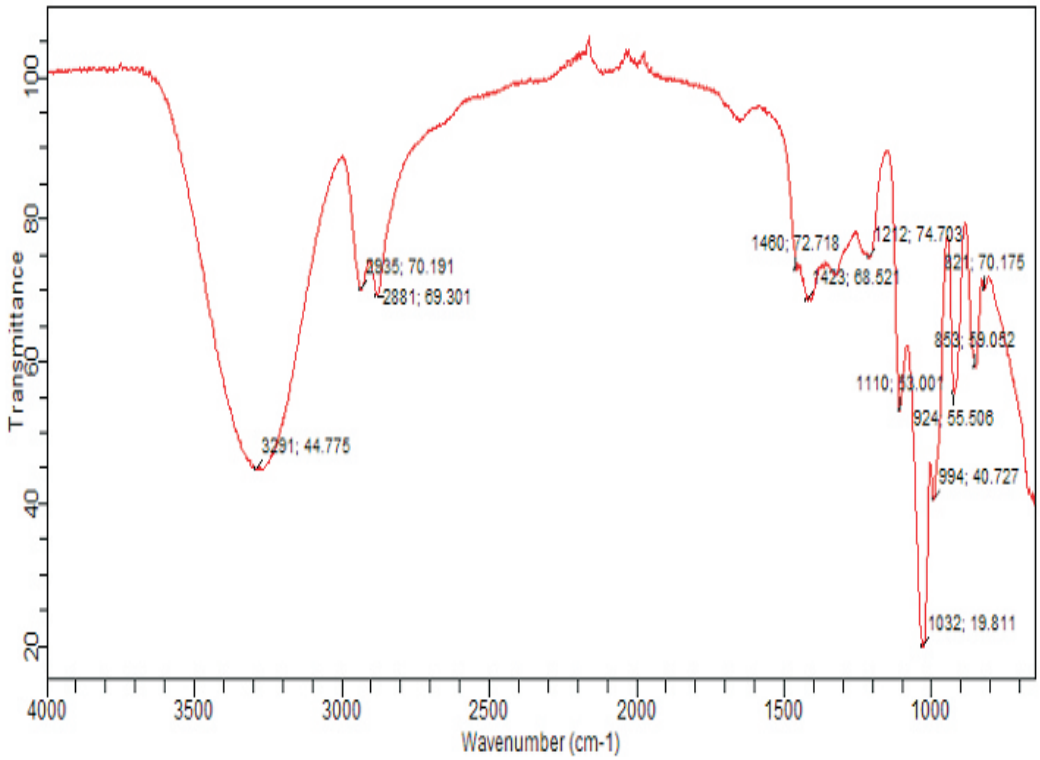

Figure 2: Glycerol FTIR Spectra

Appendix C

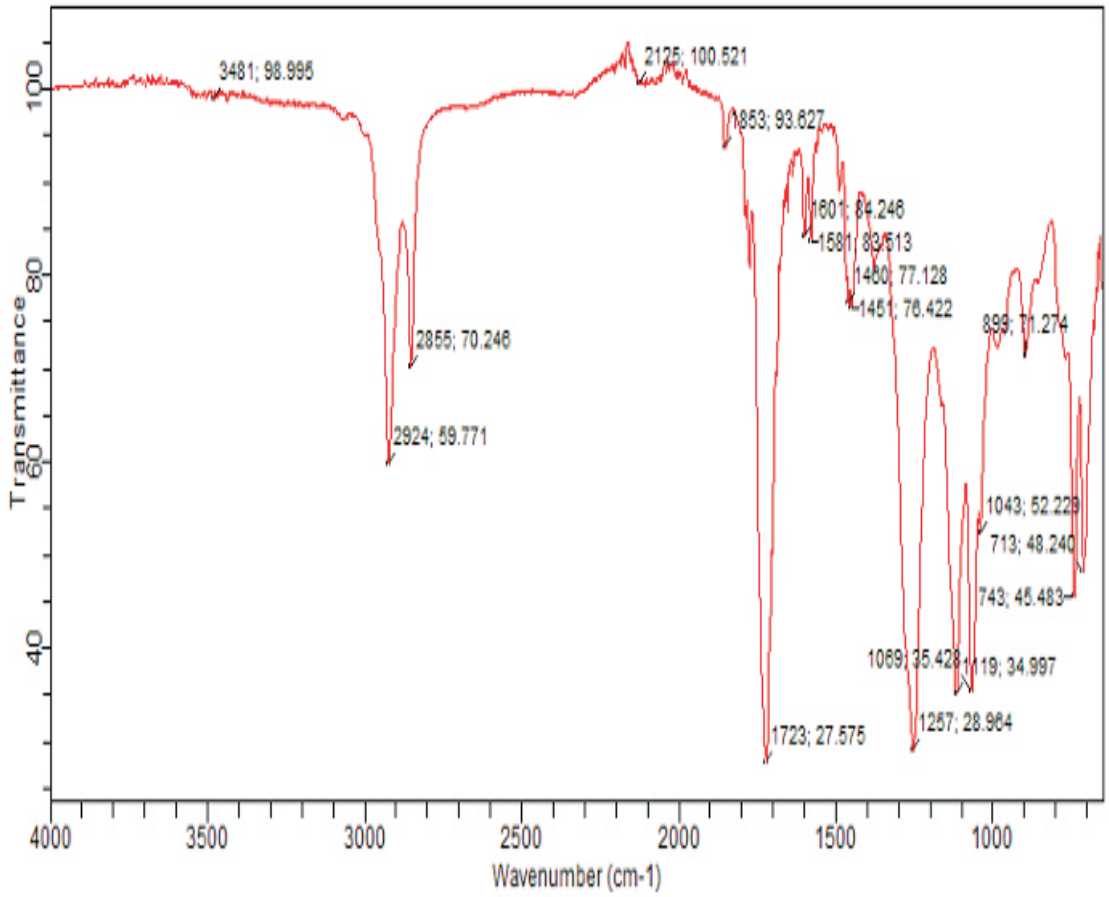

Figure 3: SBAR FTIR Spectra

Nigerian Journal of Polymer Science and Technology, 2021, Vol. 16, pp34-42
Received: 10/10/2020 Accepted: 06/06/2021

PREPARATION OF SPENT CHROME LIQUOR FOR REUSE AS RETAINING AGENT FOR VEGETABLE TANNED LEATHER

S.F. Tanko, [1*]E.N. Oparah[1], J.D. Putshaka[2], R.Z. Victor[1],P.L. Pascalina[1] and A.D. Kalip[1]

[1]Department of Pollution and Environmental Technology;
[2]Centre Manager/HOD, Jos Extension Nigerian Institute of Leather and Science Technology (NILEST) P.M.B.1034, Zaria.
Email: solomontanko0@gmail.com,

Abstract

Full vegetable tanned upper leathers were produced according to standard procedures with shrinkage temperature of 72°C. They were cleared with 0.5% oxalic acid to pH 3.0 and re-tanned with spent chrome liquor adjusted to pH of 2.0, 2.5 and 3.0 respectively with 40% NaOH solution. The initial chrome oxide content of the wastewater was determined before and after each process. Three (3) pieces of samples vegetable tanned leather measuring 7cm by 5cm were placed in 500 ml conical flask containing 400 ml of the conditioned spent chrome liquor and mechanically shaken continuously for4hours. After every batch, 1.0 ml of the reused spent chrome liquor and one (1) leather sample was withdrawn for chromium oxidecontent determination. The process was repeated three times, for each batch of spent liquor. The Chromium content of each retanned leather sample and the corresponding reused spent chrome liquor were determined using Atomic Absorption Spectroscopy. The Uv-spectroscopic method was also used to determine the exhaustion of the chromium from the used liquor to 78%. Results show a general reduction of Chromium content of the conditioned spent chrome liquor while it was increasing in the semi-chrome leather samples. The sample leathers produced from the conditioned spent chrome liquor after piling for four days gave an average of 1.6% Cr_2O_3 content and shrinkage temperatures of (T^S) 79^{O}C, 81^{O}C, and 82^{O}C below the CTL having 102^{O}C. Other results indicate the reduction of chrome oxide content of the liquor which should have been discharged to the environment.

Key words: reuse, retanned, semi-chrome; spent-chrome liquor,

INTRODUCTION

Chrome tanned leathers are characterized by high hydrothermal stability and excellent physical properties. This has been the envious attraction for leather producers, so till now chrome is still the best tanning agent. However, discharge of chromium tannery effluent without treatment is a serious threat to environment, posing great challenge to aquatic life, soil fertility and humanhealth due to bioaccumulation of the heavy metals in agricultural products from contaminated soil.

Minimization of chromewastewater or reuse, recycle and recover are techniques very important in combating this risk to the environment and to reduce cost of production [1, 2]. The presence of chrome salts in effluent is undesirable not only does it represent a waste of chrome salt but minimum discharge limits expected are not

made by tanning industries.Chrome oxide content of waste liquor often discharge vary widely from tannery to tannery, but an average chrome loss to effluent of about 30% of the total chrome used has been reported, [3, 4].

Reuse of spent chrome liquor in combination with vegetable tannins which is one of the most promising options in tanning, it is capable of achieving increase hydrothermal stability and it is based on a renewable resource, which is perceived to be environmentally friendly. The ideal combination of two tannages connotes the addition of desirable qualities.

Whilst it is true that not all end uses of leather requires high hydrothermal stability, majority do, shoe upper leather must be able to withstand lasting, heat setting and direct bonding of synthetic soles, garment leathers must withstand steam pressing and automotive upholstery leathers are frequently subjected to high temperatures, combined with the actions of light and perspiration. Therefore, it is important that any option in the method of tanning does not compromise boil fastness test, [5].

Direct reuse of chrome wastewater for retanning of full vegetable tanned leather will reduce its concentration in the wastewater often discharge without proper treatment. The objective of this research is to retann vegetable processed leather using conditioned spent chrome liquor so as to minimize the quantity being discharged and consequently reduce harmful effects of chromium to the environment. The cost of production of semi-chrome can be reduce, particularly for tanneries that produce both chrome and semi-chrome leathers

It has been reported that only 65-70% chromium applied in the form of units developed and adopted in large scale tanneries is absorbed, the remaining is discharged as waste in the effluent [6].Tanneries in India currently discharge large quantity of chromium salt, estimated at 17,000 tons per year as waste.Similar cases are also found in Nigeria where a lot of tannery wastewater is either without or poorly treated and discharged with high values of this heavy metal.High concentration of chromium in the spent liquor is considered a waste and poses as serious environmental hazards, besides complicating and increasing the cost of treatment.

The chromium concentration in terms of total chromium (Cr) in the exhaust chrome liquor ranges from 1,500 – 5000 mg/liter and the volume of exhaust chrome liquor is 4 to 6% of the total volume of wastewater discharged from the tanning process[7, 8]. This exhaust chrome liquor is generally mixed with other streams of effluent in the tannery and the concentration of chromium as Cr in the composite streams ranged from 100-300mg/liter. In most countries control authorities insist that the treated effluent should contain less than 2 mg/liter of chromium as Cr [9].

MATERIAL AND METHODS

Spent chromium liquor was collected from Nigerian institute of leather and science technology(NILEST) tannery Zaria was stored until required.Full vegetable tanned leather was tanned with (Bagaruwa) through convention process, having a shrinkage temperature of $72^{O}C$. The leathers were cleared with 0.5% oxalic acid to a pH of 3.0 and retanned with chrome wastewater adjusted to pH 2.0, 2, 5 and 3.0. Samples of the cleared vegetable tanned leather measuring 7.0 cm x 5.0 cm were retanned in acidified spent chrome liquor for 4 hours for every batch. Chrome oxide content

wasdetermined before and after each retanning. This was repeated three times in each liquor. Samples A, B and C containing 400mls of spent chrome liquor, sample vegetable tanned leather labeled A_I, A_{II} and A_{III} was introduce and agitated for 4 hours. The second batch was labelled as B_I, B_{II} and B_{III}. 1.0 ml of reused spent liquor was also taken corresponding to each leather sample and labelled as X_I, X_{II} and X_{III}; Y_I, Y_{II} and Y_{III} respectively. The control was a normal full vegetable retanned with 4.0% fresh chrome powder. Shrinkage temperatures of all sample leathers were carried out after horsing for four days according to the standard procedures, as reported by [10].

Atomic Absorption Spectroscopic Analysis the Reused Spent Liquor and Tanned Leather.

Crushed sample leather weighing 1.0g was digested with 10ml of the aquaragia then another 15.0 ml of de-ionised water was added and boil under a fumed cupboard for fifteen minutes. Thesolution was filtered and filtrate was transferred quantitatively, rinse andmade up to100ml sample bottle with de-ioned water according to the procedure reported by [9]. The procedure was repeated for each sample of used spentchrome liquor before and after every batch of retanning. The chromium oxide content was determinedusing Atomic Absorption Spectroscopy (AAS) at Multiuser Laboratory, Ahmadu Belo University (ABU), Zaria, similarly each ml of reused spent liquor withdrawn from the process was digested by the wet process in preparation for the same AAS analysis.

RESULTS

Table 1.0: Atomic Absorption Spectroscopic Analysis

Sample Identity	Mass of MgO (gm)	Conc. of Cr_2O_3 mg/L	Mean Absorbance	Standard Deviation (SD)
A	0.8	5256.98	0.4602	0.0016
B	0.9	3815.36	0.3340	0.0010
C	1.0	2258.38	0.1977	0.0007
D	1.10	504.91	0.0442	0.0003
E	1.20	245.59	0.0215	0.0002
F	1.30	110.81	0.0097	0.0011
G	1.40	0.000	0.0022	0.0010
H	1.50	0.000	0.0011	0.0012
Original Chrome Liquor	-	6652.12	0.5823	0.0010

Table 2.0: Concentration of Chromium Absorbed by Vegetable Tanned Leathers (Semi chrome) at pH 2.0

Initial Cr_2O_3 of wastewater (mg/L)	A_I (mg/L)	A_{II} (mg/L)	A_{III} (mg/L)	Total Abs
6652.12	2195.30	2054.23	1940.00	6189.53
6652.12	2108.42	2001.21	1885.06	5994.69
6652.12	2125.04	2033.11	1505.52	5663.67

Mean % Absorption	32.21	30.51	26.71	89.43

Descriptive statistics	A_I (mg/L)	A_{II} (mg/L)	A_{III} (mg/L)
Mean	2142.92	2029.52	1776.86
Standard Error	26.63	15.41	136.59
Standard Deviation	46.12	26.69	236.59
Sample Variance	2126.80	712.46	55973.65
Sum	6428.76	6088.55	5330.58
Count	3	3	3
Confidence Level(95.0%)	114.56	66.31	587.72

Table 3.0: Concentration of Chromium Remaining in Recycled Spent Chrome Liquor at pH 2.0.

Initial Cr_2O_3 of wastewater (mg/L)	X_I (mg/L)	X_{II} (mg/L)	X_{III} (mg/L)
6652.12	4457.13	2403.43	863.00
6652.12	4544.32	2543.26	795.00
6652.12	4527.42	2494.21	989.00
Mean % Remaining	67.79	37.29	13.26
Mean % Absorbed	32.21	62.71	86.74

Descriptive statistics	X_I (mg/L)	X_{II} (mg/L)	X_{III} (mg/L)
Mean	4509.62	2480.30	882.33
Standard Error	26.70	40.96	56.83
Standard Deviation	46.24	70.95	98.43
Sample Variance	2138.07	5033.22	9689.33
Sum	13528.87	7440.90	2647.00
Count	3	3	3
Confidence Level(95.0%)	114.86	176.24	244.52

Table 4.0: Concentration of Chromium Absorbed Vegetable Tanned Leathers (Semi Chrome) at pH 2.5

Initial Cr_2O_3 of wastewater (mg/L)	B_I (mg/L)	B_{II} (mg/L)	B_{III}(mg/L)	Total Abs
6652.12	2263.34	2122.42	1675.38	6061.14
6652.12	2164.25	1989.32	1745.43	5899.00
6652.12	2192.25	2055.65	1613.37	5861.27
Mean % Absorption	33.17	30.90	25.23	89.30

Descriptive statistics	B_I (mg/L)	B_{II} (mg/L)	B_{III} (mg/L)

Mean	2206.61	2055.80	1776.86
Standard Error	29.49	38.42	38.15
Standard Deviation	51.08	66.55	66.07
Sample Variance	2609.44	4428.92	4365.35
Sum	6619.84	6167.39	5034.18
Count	3	3	3
Confidence Level(95.0%)	126.90	165.32	164.13

Table 5.0: Concentration of Chromium Remaining in Recycled Spent Chrome Liquor at pH 2.5.

Initial Cr_2O_3 of wastewater (mg/L)	Y_I (mg/L)	Y_{II} (mg/L)	Y_{III} (mg/L)
6652.12	4392.39	2272.29	602.00
6652.12	4492.56	2512.45	1062.00
6652.12	4462.33	2412.44	702.00
Mean % Remaining	66.88	36.06	11.86
Mean % Absorbed	33.12	63.94	88.14
Descriptive statistics	**Y_I (mg/L)**	**Y_{II} (mg/L)**	**Y_{III} (mg/L)**
Mean	4449.09	2399.06	788.67
Standard Error	29.66	69.65	139.68
Standard Deviation	51.38	120.64	241.94
Sample Variance	2639.91	14553.47	58533.33
Sum	13347.28	7197.18	2366.00
Count	3	3	3
Confidence Level(95.0%)	127.64	299.68	601.00

Table 6.0: Concentration of chromium Absorbed by Vegetable Tanned Leathers (semi chrome) at pH 3.0

Initial Cr_2O_3 of wastewater (mg/L)	C_I (mg/L)	C_{II} (mg/L)	C_{III} (mg/L)	Total Abs
6652.12	2236.51	2183.52	1877.52	6297.55
6652.12	2184.51	2093.23	1655.55	5933.29
6652.12	2215.50	2254.36	1837.62	6307.48
Mean % Absorption	33.26	32.73	26.91	92.89
Descriptive statistics	C_I (mg/L)	C_{II} (mg/L)	C_{III} (mg/L)	
Mean	2212.17	2177.04	1776.86	
Standard Error	15.10	46.63	68.32	
Standard Deviation	26.16	80.76	118.33	

Sample Variance	684.30	6522.24	14002.03
Sum	6636.52	6531.11	5370.69
Count	3	3	3
Confidence Level(95.0%)	64.98	200.62	293.95

Table 7.0: Concentration of Chromium Remaining in Recycled Spent Chrome Liquor at pH 3.0

Initial Cr_2O_3 of wastewater (mg/L)	Z_I (mg/L)	Z_{II} (mg/L)	Z_{III} (mg/L)
6652.12	4422.40	2262.56	692.00
6652.12	4472.07	2382.64	732.00
6652.12	4442.05	2192.58	562.00
Mean % Remaining	66.83	34.26	9.95
Descriptive statistics	Z_I (mg/L)	Z_{II} (mg/L)	Z_{III} (mg/L)
Mean	4445.51	2279.26	662.00
Standard Error	14.44	55.50	51.32
Standard Deviation	25.01	96.12	88.88
Sample Variance	625.74	9239.87	7900.00
Sum	13336.52	6837.78	1986.00
Count	3	3	3
Confidence Level(95.0%)	62.14	238.79	220.79

Table 8.0: Shrinkage Temperature (T^S) of Sample the Semi-chrome

S/N	Sample	T^s Value
1.	A_I	76.0ºC
2.	A_{II}	78.50ºC
3.	A_{III}	78.5.0ºC
4.	B_I	11.0ºC
5.	B_{II}	80.0ºC
6.	B_{III}	79.0ºC
7	C_I	71.5°C
8	C_{II}	70°C
9	C_{III}	82°C
10	$_{CTL}$	102

Table 9.0: Tensile Strength and Percentage Elongation at break

S/N	Sample	Tensile Strength N/mm^2	Percentage (%)
1	AI	13	60
2	AII	15	65
3	AIII	13	68
4	BI	14	66
5	BII	16	64
6	BIII	14	63
7	CI	15	67
8	CII	16	69
9	CIII	15	65
10	CTL	17	76

DISCUSSION

Vegetable tanned leather is a good substrate for chrome absorption particularly when it is conditioned at appropriate pH with oxalic acid as the most appropriate organic acid,which has a tendency of creating more reactive sites for chrome absorption and fixation. Retanning of full vegetable tanned leather with modifiedspent chromium liquor has resulted to semi-chrome uppers close to the desired properties. The sample leathers showed shrinkage temperature within the range of $76^{O}C$ – $82^{O}C$and a chromium oxide content of 1.65% compared with the control sample having $102^{o}C$ and a corresponding Cr_20_3 of 2.5%, the standard for shoe upper leathers. This means that the semi-chrome was able to absorbed chrome from the conditioned spent liquor but not as much as required to meet with the standard specification.Despite the high quantity of chrome oxide content in the wastewater which is often discharged after normal chrome tannage. The semi chrome was unable to absorbed the required chrome oxide, most probably because the spent chrome liquor had formed large macromolecule with the basifier used during the initial chrome tannage. It is observed that as pH of the spent chrome liquor increases the better the exhaustion of the chrome oxide content of the liquor (Table 2.0 – 7.0).

Reuse of spent chrome liquor for retanning has not been popular, most probably because of the quest to satisfy customers demand within specified periods.Another reason could be the poor rate of absorption by thevegetable tanned leather because of the large macromolecule of the chrome complex formed during basification in the initial tannage.Although chrome fixation takes place at the carboxylic side chain of the protein, penetration of chrome could still be difficult because the pore size of the fiber network which might have been blocked by the vegetable tannins. Possibly because ofsteric hindrance of the protein-vegetable complex. Hence the unpopular reuse or recycling of spent chrome liquor. However, when stringent measures are taken by the authorities' concern, the technique might be considered or adopted as the cheapest approach for reuse of chrome wastewater especially for tanneries that produce both wet blue and vegetable crust.With this approach or technique fresh chrome powder may not be necessary for the production of semi-chrome upper leathers.

The shrinkage temperature of the sample leathers indicates increase in the thermal stability of the retanned leathers with the spent chrome liquor, Table 8.0The control sample showed a chrome oxide content of 2653.85mg/L and shrinkage temperature of $102^{O}C$ which is significantly different from sample leathers, ($P < 0.05$).

CONCLUSION

Reuse of spent chrome liquor for retanning of full vegetable tanned leather is very possible.The process is equally

economical and environmentally friendly as the quantity of chrome that should have discharged to the environment posing as a thread to the environment is recovered for reused. Although the penetration of chromium was not excellent but could be said to be good even though significant quantity of chrome was still left in the conditioned spent chrome liquor. At pH 2.0, the total chromium absorbed by the vegetable leathers was 89.43% leaving 13.26% in the wastewater. At pH 2.5 the total absorbed similar at 89.30% and the remaining was 11.86%. Meanwhile, at pH 3.0 the total absorbed by the vegetable leathers was 92.89% leaving 9.95% of chromium in the liquor. It was observed that much of chrome was absorbed at pH 3.0, which is the possible reason for higher shrinkage temperature observed in Table 8.0.

RECOMMENDATION

Retanning of vegetable tanned leathers with spent chrome liquor in order to improve on the properties of vegetable leathers has yielded good results. It is therefore being recommended for tanning pickled pelts.

REFERENCES

[1]Kanagaraj, J., Jakov, B., (2008). Journal of clear production. V.16, issue 16, 187-1813.

[2] Gaythil, R., Senthil, P.K., (2010). Recovery and reuse of hexavalent chromium from aqueous solutions by hybrid technique of electrolysis and ion exchange. Journal of chemical engineers. V. 27, (1).

[3]Boddu, V. M., Abburi, K., Talbot, J. L. and Smith, E. D., (2003). Removal of Hexavalent Chromium from Wastewater Using a New Composite Chitosan Biosorbent.1 Environ Sci. Technol. v. 37, 4449-4456.

[4]Rajamani, S., Jakov, B., (2000). Technology package. A system for recovery and reuse of chromium from spent tanning liquor using magnesium oxide and sulphuric acid. United Nations Industrial Development Organization Viena, Austria.

[5] Covington T; (2012) Tanning Chemistry, The science of leather. Royal society of chemistry UK, 209.

[6] Geremew, L Tadesse, T. Kasa, G.(2017) Impacts of Tannery Effluent on Environments and Human Health Journal of Environment and Earth Science www.iiste.orgISSN 2224-3216 (Paper) ISSN 2225-0948 (Online)Vol.7, No.3, 2017

[7] Durai, G. and Rajasimman M., (2011). Biological treatment of tannery waste water, a Review. journal of environmental science and Technology, 4 (1): pp. 1-17.

[8] HayelomDargo and AdhenaAyalew (2014); Tannery Waste Water Treatment: A Review. International Journal of Emerging Trends in Science and Technology 1(9): pp. 1488-1494.

[9] Buljan J. and Kral I., (2011); Introduction to treatment of tannery effluents. United Nations

IndustrialDevelopment Organization (UNIDO) Vienna

[10]SLTC (2014). SLP8/IUC 10, *Determination of Chromic Oxide Content*. Official Method of Analysis.*J.soc.Leather Technol. Chem. 82; 200.*

Nigerian Journal of Polymer Science and Technology, 2021, Vol. 16, pp43-52
Received: 19/10/2021 Accepted: 07/11/2021

STUDY OF COMPARATIVE MECHANICAL CHARACTERIZATION OF AFRICA FAN PALM (*BORASSUS AETHIOPUM*) PETIOLES AND SAW DUST PARTICLE REINFORCED UREA-FORMALDEHYDE COMPOSITES

A.A. Salihu[a]*; C.E. Gimba[a] and P.A.P. Mamza [b]

[a,b]Department of Chemistry, Ahmadu Bello University, Zaria

ABSTRACT

A research work on the polymer particleboard composites using Africa fan palm petioles (AFPP) fibre and saw dust (SD) fibre as reinforcement and urea -formaldehyde (UF) as matrix was carried out. Composites of particleboard were formulated with varying weight fraction of reinforcements: 90%, 80%, 70%, 60% and 50% to 10%, 20%, 30%, 40% and 50% urea formaldehyde. The mechanical properties of the composites where ultimate tensile strength (UTS), young's modulus, elongation at break, hardness strength and impact strength were analysed. The results show an improvement in the mechanical properties with increased in weight fraction of urea - formaldehyde (UF) matrix. Optimum results were observed at 50% weight fraction of urea-formaldehyde (UF) matrix. The results indicated that the AFPP particleboards had better properties compared to SD particleboards, thus AFPP can serve as a better substitute for wood in high-performing composites.

Keywords: *Africa fan palm petioles, Mechanical properties, Morphology, Particleboards, Saw dust.*

*Corresponding author: E-Mail salihuaudu4u@gmail.com Tel: +2348158391155; +2348092088651

INTRODUCTION

There has been an increasing environmental problem caused by the use of non-renewable, non-biodegradable materials such as polymer based products (Morales-Zamudio *et al*., 2019), carbon fillers, glass fibres etc. However, because polymer composites usually comprised of two or more components, it is expensive to separate the components for recycling purposes (Pickering *et al*., 2016). Nowadays the most usual methods of disposing polymer composites are landfill and incineration (Hassan *et al*., 2019), both methods cause environmental pollution. The main problems with polymers used as composites matrix such as urea-formaldehyde (UF) is its non-degradability and non-renewability. This problem can only be reduced by incorporating much quantity of reinforcement (natural fibre) in the composite formulation. UF is a hard, rigid and a three dimensional structural material, its properties can be improved by the introduction of natural fibres (Hassan *et al*., 2019) to form composites. Natural fibres have gained attention because of their many advantages such as low cost, low density, cheapness, renewability, biodegradability, high strength, enhanced energy recovery, etc (Jacob *et al*., 2016; Singha and Thakur, 2008 and Espinach *et al*., 2019). Natural fibres composites have proven to be environmental friendly than artificial fibre such as glass fibre reinforced polyolefin (Kong and Park, 2016; Singha and Thakur, 2009 and Pil *et al*., 2016). Over few years back, different types of waste materials (natural fibres and plastic waste) have been utilized in composite production; which offers an opportunity for waste materials re-utilization and thereby reduce environmental pollution (Eze *et al*., 2013).

Many research work have been reported on natural fibres based composites; examples are Palmyra palm petioles, bagasse, bamboo, Jute, Africa fan palm petioles, wheat straw rape straw and wood particles (Srinivasababu *et al*., 2014; Naguib *et al*., 2015; Qiu *et al*., 2019; Gupta, 2018; Salihu *et al*., 2019; Silva *et al*,. 2019 and Casereanu *et al*., 2019) among others.

Particleboards are produced from wood products but because of the pressure on the wood reserve, efforts are being made to save the forest by finding alternative raw materials such as Africa fan palm petioles.

Africa fan palm petioles are annually renewable agro-waste. The tree has many uses: It is used globally for both medicinal (Sarkodie *et al*., 2015) and structural applications because of its strength and resistance to various attacks such as chemical, climate, termite, etc. Fibres can be obtained from the leaves, petioles and wood (which is reported to be termite-proof) can be used in construction (Bailey *et al*., 1976). Virtually all parts of African fan tree are useful to greater extent but there is not much reported economic application of the petioles in Nigeria. The development of economically viable products in form of composites from these materials has prompted the need for this study.

Thus the aim of this work is to develop Africa fan palm petioles fibre composites with low proportion of UF matrix to reduce the effects of environmental pollution and also comparing their mechanical properties with the conventional saw dust particleboards composites.

Table 1: Designation of symbols and their meaning as used in this work

Symbol	Meaning
10HW	10wt% saw dust fibre reinforced 90wt% urea formaldehyde matrix
20HW	20wt% saw fibre dust reinforced 80wt% urea formaldehyde matrix
30HW	30wt% saw fibre dust reinforced 70wt% urea formaldehyde matrix
40HW	40wt% saw fibre dust reinforced 60wt% urea formaldehyde matrix
50HW	50wt% saw fibre dust reinforced 50wt% urea formaldehyde matrix
10F	10wt% saw Africa fan palm petioles fibre reinforced 90wt% urea formaldehyde matrix
20F	20wt% saw Africa fan palm petioles fibre reinforced 80wt% urea formaldehyde matrix
30F	30wt% saw Africa fan palm petioles fibre reinforced 70wt% urea formaldehyde matrix
40F	40wt% saw Africa fan palm petioles fibre reinforced 60wt% urea formaldehyde matrix
50F	50wt% saw Africa fan palm petioles fibre reinforced 50wt% urea formaldehyde matrix

MATERIALS AND METHOD

Materials

The materials used in this work are BDH-grade urea, formaldehyde, ammonium chloride, sodium hydroxide, Saw dust and Africa fan palm petiole (Salihu *et al*., 2019).

Method

Sample collection and preparation

Borassus aethiopum petioles were sourced from Mazhaga village, in Toto Local Government Area of Nasarawa State of Nigeria and saw dust was sourced from Samaru Sawmill, Zaria-Nigeria. They were both sun-dried for three weeks and finally reduced to 0.6mm particle size using a mechanical grinder as reported in (Salihu *et al*., 2019)..

Preparation of Urea Formaldehyde (UF)

400ml of 45% formaldehyde solution was measured into a clean dried 1000ml beaker with 200g of 99% urea place on the

heating mantle, 22% NaOH solution was added to moderate the pH to 8.5 and the temperature was raised in 50 min from ambient to 90 ^{0}C while maintaining pH in the range 7.6 by small additions of 22% NaOH. The temperature was maintained at 90 ^{0}C until the turbidity point is reached for 20 min. 5ml of 30% concentrated tetraoxosulphate (vi) acid (H_2SO_4) was added to adjust it acidic medium of 5.5 pH and the temperature was raised to 98^{0}C. The pH was finally brought to 8.5 using sodium hydroxide solution to terminate the polymerization reaction (Salihu *et al.*, 2019)..

Chemistry of UF resin:

The reaction of urea and formaldehyde is basically a two-step process: usually an alkaline methylolation followed by an acid condensation.

Step 1: Formation of methylol urea derivative

Methylolation refers to the addition of up to three (four in theory) molecules of the bifunctional formaldehyde to one molecule of urea to give the so-called methylolureas.

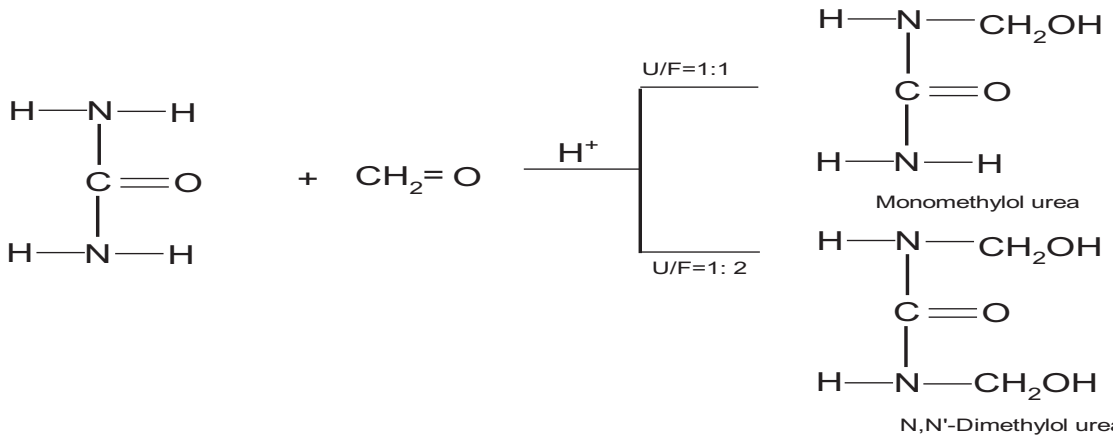

Step 2: Polymerization of methylol urea

The second stage is the acid condensation of the methylolureas, Several molecules of methylol urea derivatives condense with loss of water molecules to form a highly cross linked urea formaldehyde resin through polymerization process.

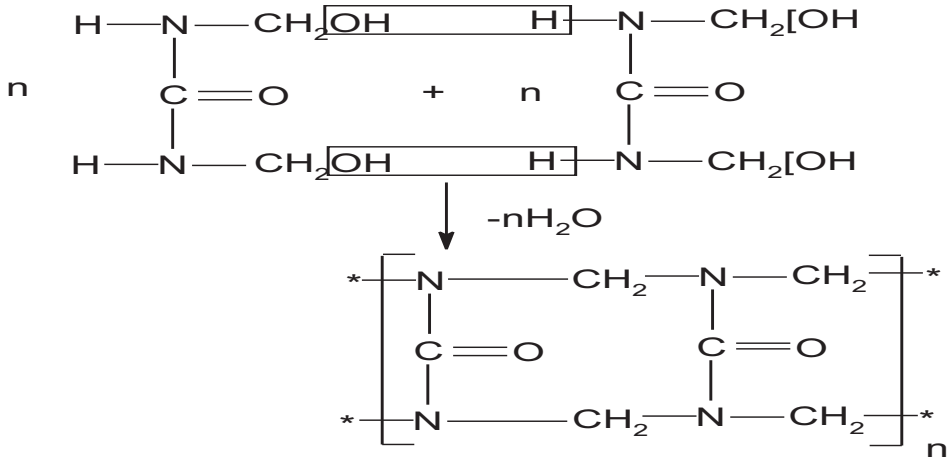

Formulation of saw dust (SD) and Africa fan palm petioles (AFPP) composites

The saw dust (SD) and Africa fan palm petioles (AFPP) fibres particleboards were formed by mixing each fibre with urea formaldehyde separately using hand layup method until proper mixture was obtained. The percentage urea formaldehyde resin loading was varied from 10%, 20%, 30%, 40% and 50%; and 90%, 80%, 70%, 60% and 50% of the fibre respectively as shown in table 2. The amount of ammonium chloride salt that was added to each formulation as a curing agent (CA) at 5% of Urea Formaldehyde (UF) was calculated to ensure equal concentration [15].

Table 2: Weight fraction ratio for the composites (Salihu *et al*., 2019)..

Sample	UF (%)	Filler (%)	CA (NH_4Cl)g
10H	10.00	90.00	0.50
20H	20.00	80.00	1.00
30H	30.00	70.00	1.50
40H	40.00	60.00	2.00
50H	50.00	50.00	2.50
10F	10.00	90.00	0.50
20F	20.00	80.00	1.00
30F	30.00	70.00	1.50
40F	40.00	60.00	2.00
50F	50.00	50.00	2.50

Curing

The composite samples were cured on a hydraulic machine with its platens electrically heated. The composites were wrapped in aluminum foil and cold-pressed into mat-form. The composites were cut into the metal mould with dimensions (25cm length, 25cm width, and 5mm thickness) and placed between heated platens of the compression molding in an electrically heated hydraulic press at the temperature of 160^0C, pressure of 12 MPa for 3mins (Salihu *et al*., 2019).

Impact Strength Test

Impact strength tests are measure of the toughness of a material or the ability of a material to resist sudden blow when dropped from a certain height and or a measure of the energy required to break a material. The izod impact test was carried out according to ASTM D256 in which the test sample was clamped upright in an anvil, with a V-notch at the level of the top of the clamp. The test piece was hit by a striker carried on a pendulum which was allowed to fall freely from a specific height to give a blow of 120ft-1b/ in energy. After the test piece fractured, the height at which the pendulum was rise to be recorded by a slave fraction pointer mounted on the dial. The energy E absorbed at fracture can be obtained by calculating the difference in potential energy of the pendulum before and after test as given below:

$E = m.g\ (h-h')$.

Where: E=Absorb energy, m = mass of pendulum, g = acceleration due to gravity and h=height.

Tensile test

The testing of the samples was done at Engineering Materials Development Institute, Akure, Ondo State, Nigeria in accordance with ASTM D638 standard. The samples were cut to dumb bell shape

and then placed in Instron universal tensile testing machine 3369 model and the tensile strength and modulus were evaluated.

RESULTS AND DISCUSSION

Impact test results

Figure 1 shows the impact strength of the particleboards, which is the ability of a plastic to withstand high energy impact without fracturing or breaking. In other word, it is a measure of the toughness of a material. It acts as a tool to study brittle-ductile transition. Brittle materials have low toughness and they can bear a small amount of plastic deformation. On impact, the energy of the pendulum is transferred to the test specimen and a part of the energy is consumed during fracture of the specimen. The total energy absorbed by the polymer composite is the sum of the energy consumed during plastic deformation and the energy needed for creating new surfaces. The impact properties of composite materials are directly related to its overall toughness. Composite fracture toughness is affected by interlaminar and interfacial strength parameters.

In figure1 shows that the impact strength of the AFPP filler composites shows an increase as the percentage resin increased. Similarly, the impact strength of the SD filler composites also shows an increase as the percentage resin increased with the minimum of 2.97 J/mm^2 at 20% weight fraction of matrix which could be as a result of voids present leading to poor impact strength (Danladi and Patrick, 2013). The increased in impact strength as the UF composition increased could be attributed to the saturation of the filler by the UF matrix which increased the interfacial bond. Similar observation has been reported by (Danladi and Patrick, 2013 and Suvana *et al*., 2015). The result shows that the impact strength of 90/10, 80/20, 70/30% fibre/UF matrix compositions for AFPP was 3.76, 4.24, 4.28 J/mm^2 and SD was 3.92, 2.97, 4.13 J/mm^2 lower than 5.50, 6.05, 7.00 Kgf.cm as reported by (Ghosh and Nayak, 2006) when the same particles/matrix compositions was used. This could be as a result of variations of the raw material. The AFPP and SD results was also observed to be higher than the value recorded for urea-formaldehyde resin (UFR)/maize cob (MC) particle boards range from 3.3 x 10^{-2} to 0.4 x 10^{-2} J/m^2. This could be as a result of variations of the raw material and particles/matrix composition. Optimum results were observed at 50% weight fraction filler for both AFPP and SD composites. AFPP (7.22 J/mm^2) particleboards showed better impact strength than SD (6.23 J/mm^2) particleboards. This could be attributed to the surface roughness of the AFPP particles than the SD fibres i.e smooth nature of SD particles (Srinivasababu *et al*., 2014) that encouraged better interfacial bonding in AFPP composites.

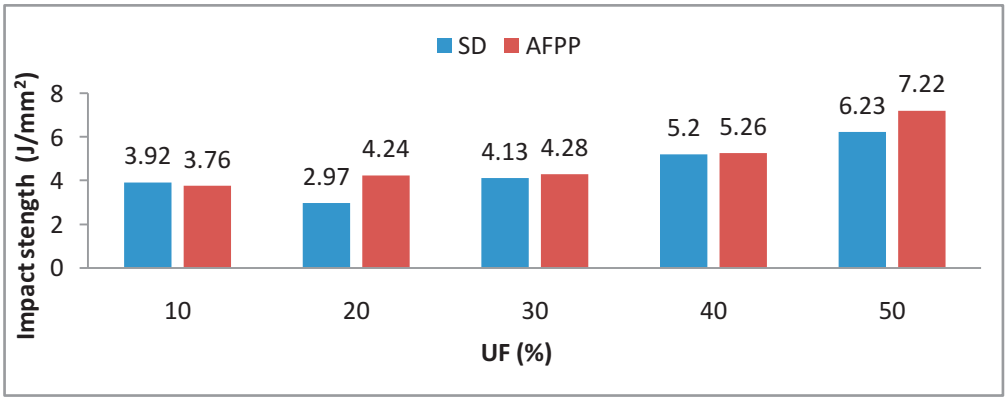

Figure 1: Impact test of the samples

Ultimate tensile strength test results

Figure 2 shows the ultimate tensile strength (UTS) of AFPP and SD particle composite samples. Ultimate tensile strength is the capacity of a material to withstand loads (stress) tending to elongate. Figure 4.7 shows that the tensile strength of AFPP and SD particle composites increased with decrease weight in fraction of UF matrix. This may be as a result of increase in wetting of the particles which lead to better compatibility of the particle/matrix composites. Similar observation was reported in (Mamza *et al*., 2014). This result was not in agreement with the work reported by (Jacob *et al*., 2018 and Abdulkareen and Adeniyi, 2017) which may be as a result of variation in percentage composition, raw materials and matrix. The AFPP composites UTS increases with increase in percentage resin more than SD filler composites UTS which could be as a result of high fibre matrix interaction in AFPP composites. Optimum results were observed at 50 % weight fraction of reinforcement for both AFPP and SD composites. AFPP (31.07 MPa) particleboards showed better tensile strength than SD (13.63 MPa) particleboards. This variation may be due to the variation in properties of the raw materials which leads to high compatibility in AFPP composites. The result shows higher values than BIS specification of 0.8 N/mm^2 (Mamza *et al*., 2014).

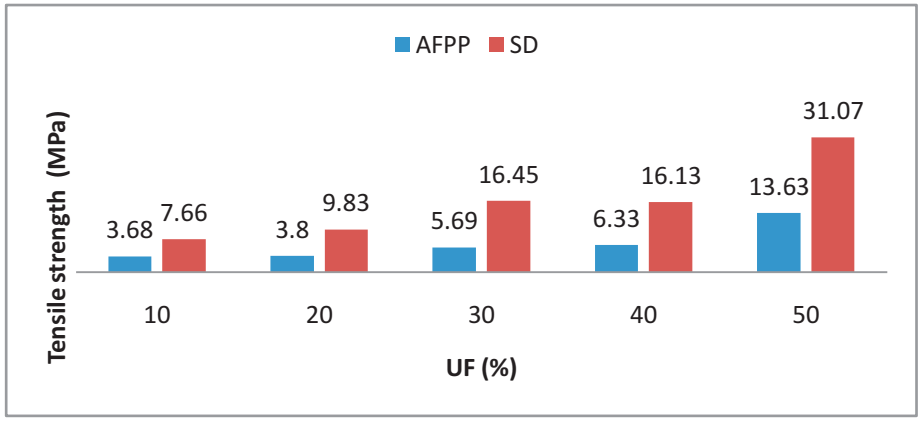

Figure 2: Ultimate tensile strength of the samples

Young's Modulus test results

Figure 3 shows the Young's modulus of AFPP and SD which is a measure of elastic deformation when stress is applied on the object or substance. The result shows that the Young's modulus of AFPP and SD particle composite increased with increased in weight fraction of UF matrix. This could be as result of proper wetting of the particles by the UF matrix which increased the interfacial bond. Decrease in Young's modulus was observed in AFPP composites from 671.90 MPa to 412.09 MPa at 30 % to 40 % percentage resin increases which could be as a result of poor particle distribution in the UF matrix during mixing. Similar observation was reported in (Salihu *et al*., 2019).

An optimum result was observed at 50% weight fraction of reinforcement for both AFPP (859.27MPa) and SD (506.92MPa)

composites. This could be as result of increase in wetting of the fibres by the UF matrix which increased the interfacial bonding strength of composites. AFPP (859.27MPa) particleboards showed better Young's modulus (stiffness) than SD (506.92MPa) particleboards. This variation may be due to the variation in properties of the raw materials which leads to high compatibility in AFPP composites.

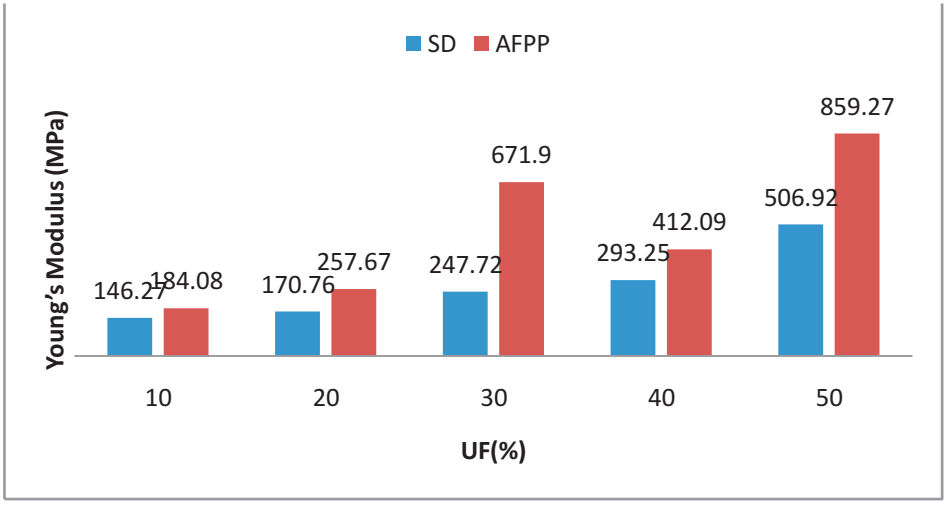

Figure 3: Young's Modulus of the samples

Elongation at break

Figure 4 shows the elongation at break of AFPP and SD particle composite which shows the ductility of composites. The ductile behaviour of AFPP composites shows that the elongation of the AFPP filler composites shows a decrease as the percentage resin increased from 20 %wt fraction of UF matrix. Similarly the elongation of the SD filler composites also shows a decrease as the percentage resin increased from 20 %wt fraction of UF matrix. SD composites show higher elongation than AFPP filler composites elongation. This could be as a result of particle variation. The highest ductile behaviour was observed in SD composite (3.99mm) than AFPP fibre composite (3.41mm) at 20% weight fraction of UF matrix.

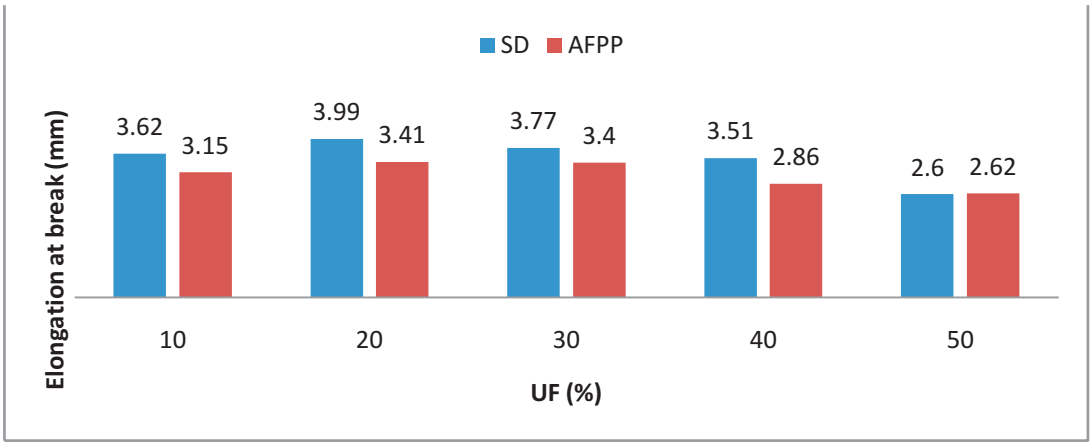

Figure 4: elongation at break of the samples

CONCLUSIONS

Particleboard from AFPP and SD reinforced UF was successfully developed

and characterized, the following conclusions were made.

(i). Optimum mechanical properties of both AFPP and SD composites was obtained at 50/50 matrix/reinforcement
(ii). AFPP-UF composites showed better mechanical properties compared to SD-UF composites.
(vi) The experimental results have shown that production of general purpose and furniture grade particleboard in dry conditions using AFPP is technically viable and therefore can be used as wood replacement.

RECOMMENDATIONS

(i). More research should be carried out on Africa Fan Palm so that small scale and large scale industries can be set up for particleboards production across the country. This can provide job for teaming Nigeria youth.
(ii). The AFPP fibres need to be modified via chemical treatment in order to increase its compatibility with the urea formaldehyde matrix.
(iii). Other characterizations such as creep compliance and dynamic mechanical analysis should be carried on AFPP-UF composites.

ACKNOWLEDGEMENT

The authors are grateful to Directorate of Research and Development, Nigerian Institute of Leather and Science Technology, Zaria and Staff of Strength of Materials Laboratory, Department of Mechanical Engineering for providing us with equipment used in this research.

REFERENCES

Abdulkareem, S.A. and Adeniyi, A.G. (2017) Production of Particleboards Using Polystyrene and Bamboo Wastes. *Nigerian Journal of Technology, 36*(3), 788 – 793.

ASTM D256, Standard Test Method for Determining the Izod pendulum Impact Resistance of plastics.

ASTM D638, 2014 Standard Testing Method for the tensile properties of polymer matrix composite materials. ASTM International West Conshohocken, PA.

Bailey, L.H. and Bailey, E.Z. (1976). Hortus Third i–xiv, 1–1290. MacMillan, New York.

Cosereanu, C. And Cerbu, C. (2019) Morphology, Physical and Mechanical Properties of Particleboard Made from Rape Straw and Wood Particles Glued with Urea-Formaldehyde Resin. *BioResources, 14*(2), 2903-2918.

Danladi, A. and Patrick, I.O. (2013). Mechanical Properties of Particle Boards from Maize Cob and Urea-Formaldehyde Resin. World Academy of Science, Engineering and Technology. *International Journal of Materials and Metallurgical Engineering 7*(10), 751-753.

Espinach, F.X., Chamorro.Trenado, M.A., Llorens, J., Tresserras, J., Pellicer, N., Vilaseca, F. and Pelach A. (2019) Study of Flexural Modulus and the Micromechanics of Old Newspaper Reinforced Polypropylene Composites. *BioResources, 14*(2), 3578-3593.

Eze, I.O., madufor, I.C. and Obidiegwu, M.U. (2013) A comparative Study of some Mechanical Properties of bamboo powder filled Virgin and Recycled Low Density Polyethylene Composites. *Academic Research International 4*(1), 420-430

Ghosh, S.K. and Nayak, L.K. (2006). Date-palm leaf particle boards – a wood substitute for various applications. *International Journal Agricultural. Sciences. 2*(2), 421-424

Gupta, M.K. (2018) Effect of Variation in Frequencies on Dynamic mechanical properties of Jute fibre Reinforced Epoxy Composites *Journal of Materials and Environmental Sciences, 9*(1), 100-106.

Hassan, A., Isa, M.R.M. and Ishaq, Z.A.M. (2019) Improving Thermal and Mechanical Properties of Injection Moulded Kenaf Fibre-reinforced Polyhydroxybutyrane Composites through Fibre Surface Treatment. *BioResources, 14*(2), 3101-3116.

Jacob, J., Mamza, P.A.P., Ahmed, A.S. and Yaro , S.A. (2018) Mechanical and Viscoelastic Properties of Plantain Powder Reinforced Recycled High Density Polyethylene Composites. *Nigeria Journal of Polymer Science and Technology*, *13*(2), 55-66

Jacob, M., Francis, B., Thomas, S. and Varughese, K.T. (2006) ''Dynamical mechanical analysis of sisa/oil palm hybrid fibre-reinforced natural rubber composites''. *Polymer Composites, 27*(6), 671-680.

Kong, C., Lee, H. and Park, H. (2016) ''Design and manufacturing of automobile hood using natural composite structure''. *Composites Part B: Engineering, 91*, 18-26.

Mamza, P.A.P., Emmanuel, C.E., Gimba, E.C. and David, E.A. (2014) Comparative Study of Phenol Formaldehyde and Urea Formaldehyde Particleboards From Wood Waste For Sustainable Environment. *International Journal of Scientific & Technology* Research, *3* (9).

Morales-Zamudio, L., Lopez-Marure, A., Garcia-Hernandez, M., Rodriguez-Gonzalez, F., Flores-Gallardo, S. and Lopez-Martinez E. (2019) Isolation, Characterization , and Incorporation of Microfibrils and Microcrystals from *Typha domingensis* Pers. As Impact Strength Reinforcer of Polypropylene Matrix Composite Using Stearic Acid as Interfacial Modifier. *BioResources, 14*(2), 2513-2535

Naguib, H.M., Kandil, U.F., Hashim, A.I., and Boghdadi, Y.M. (2015) Effect of Fibre Loading on the Mechanical and Physical Properties of Gren Bagasse-Polyester Composite. *Elsevier Journal of Radiation Research and Applied Sciences, 8*, 544-548

Pickering, K.L., Efendy, M.G.A., and Le, T.M. (2016) ''A review of recent developments in natural fibre composite and their mechanical performance''. *Composites Part A: Applied Science and Manufacturing,83*, 98-112.

Pil, L., Bensadoum, F., Pariset, J. and Verpoest, I. (2016) ''Why are designers fascinated by fax and hemp fibre composites?''. *Composites Part A: Applied Science, 83,* 193-205.

Qiu, H., Xu, J., He, Z., Long, L. and Yue, X. (2019) Bamboo as an Emerginng Source of Raw Material for Housedhold and Building Products. *BioResources, 14*(2), 2465-2467.

Salihu, A.A., Gimba, C.E. and Mamza, P.A.P. (2019) Characterization of Africa Fan Palm Petioles Fibre for Particleboard Production as Wood Substitute for various Application. *Journal of Science, Technology & Education, 7*(2), 281-289.

Sarkodie, A.J., Squire, A.S., Kretchy, A.I. (2015) Borassus aethiopum, A Potential Medicinal Source of Antioxidants, Anti-Inflammatory and Antimicrobial Agents. *Herbal Medicine*, *2*(1).

Silva, J.V.F., Bianchi, N.A., Oliveira, C.A.B., Caraschi, J.C., de souza, A.J.D., Molina, J.C. and de Campos, C.I. (2019)

Characterizatin of Composite Formed by Cement and Wheat Straw Treated with Sodium Hydroxide. *BioResources,14*(2), 2472-2479.

Singha, A.S. and Thakur, V.K. (2008) ''Mechanical properties of natural fibre reinforced polymer composites". *Bulletin of material Science, 31*(3), 991-999.

Singha, A.S. and Thakur, V.K. (2009) Study of Mechanical Properties of Urea formaldehyde Thermosets Reinforced by Pine Needle Powder. *BioResoures, 4*(1), 292-308.

Srinivasababu, N., Kumarb, J.S. and Reddyc, K.V.K. (2014) Manufacturing and Characterization of Long Palmyra Palm/ Borassus Flabellifer Petiole Fibre Reinforced Polyester Composites. *Procedia Technology*, *14*, 252 – 259.

Suvarna, A.S., Katagi, A., Pasanna, J., Badyankal P.V., Vasudeya, S.K. and Bennehalli, B. (2015). Mechanical Properties of Abaca Fibre reinforced Urea Formaldehyde composites. *Material Science Research*, *12*(1), 54-59.

Nigerian Journal of Polymer Science and Technology, 2021, Vol. 16, pp53-62
Received: 22/10/2021 Accepted: 07/11?2021

UTILIZATION OF RESPONSE SURFACE METHODOLOGY IN THE SORPTION OF CRUDE OIL BY WASTE POLYPROPYLENE PLASTICS

Okpanachi, C. B.[1], Agbaji, E. B.[2], Mamza, P. A. P. [2] and Yaro, S. A. [3]

[1]Department of Pure and Industrial Chemistry, Kogi State University, Anyigba
[2]Department of Chemistry, Ahmadu Bello University, Zaria
[2]Department of Chemistry, Ahmadu Bello University, Zaria
[3]Department of Metallurgical and Materials Engineering, Ahmadu Bello University, Zaria

ABSTRACT

In this study, waste propylene plastics (WPP) were used as sorbents for the removal of crude oil. The reactions were described by the use of central composite design as the function of factors namely; sorbent dosage, contact time, initial oil concentration and temperature. Results revealed that the best experimental run for the crude oil sorption was obtained at conditions of high sorbent dosage of 3.5 g, high contact time of 30 mins, high initial oil concentration of 75 g/L and low temperature of 25 ^{o}C which produced a maximum sorption capacity of 17.23 g/g. Relative effects of interaction between the process variables from the interaction plot and cube plot showed significant interaction between the factors. Statistical analysis revealed that the model of the WPP sorbents had high R^2 value of 0.9824, high AP value of 32.14 and low CV value of 1.47, indicating a very good precision and reliabilty of the model.

KEYWORDS: *Central composite design, Crude oil, Pollution, Polypropylene*, *Sorption*

Introduction

Over the past few years, oil pollution has become one of the most serious global concerns due to its impact on the environment and economy. Accidental and intentional oil discharges have been reported frequently during the exploration, transportation and refining of oil, and these have severe negative impact on organisms and the wider environment (Sabir, 2015). Stringent environmental policies worldwide have generated great interest in the development of cost-effective and efficient methods for the treatment of oily water. Among these methods, sorbent materials are more attractive for oil-spill cleanup because of the possibility of collection and complete removal of the oil from the water surface while bringing no adverse effect to the environment (Ge *et al*., 2016).

A large amount of plastic wastes get generated everyday with the main crucial concern as to how efficiently and effectively these wastes can be managed for the sustenance of mankind and the environment. In order to reduce plastic disposal to the landfill, another alternative method to manage plastic waste directly is to use it to produce value-added products such as sorbents. Most of the research on plastic waste has been focused on its elimination in a low cost approach rather than its beneficial, value-added reuse.

Response surface methodology (RSM) is an effective tool for optimizing

a factor process when a combination of several independent variables and their interactions affect desired responses (Thani *et al*., 2017). This methodology has the advantage of being less expensive and time consuming than other classical methods (Khosravi and Arabi, 2016). Hence, the aim of this study is to explore the viability of converting waste polypropylene plastics (WPP) into oil-sorbents and the application of RSM to identify the optimum conditions of the oil sorption capacity.

2.0 MATERIALS AND METHODS

Waste plastics made from commercial polypropylene (PP) were collected from refuse dumps and plastic waste collection centre in Tipper garage, Lokoja, Kogi State, Nigeria. The waste plastics were thoroughly washed with water, dried, shredded into particles and sieved with laboratory sieves to obtain a homogenous particle size of 300 μm.

2.1 Experimental Design Using Response Surface Methodology

A face-centered central composite design was applied for the study of the factor processes of the oil sorption capacity. Four different parameters namely sorbent dosage (1.5 – 3.5 g), contact time (10 – 30 mins), Initial oil concentration (25 – 75 g/L) and temperature (25 - 45 ^{o}C) were selected as the critical variables. The 30 experimental runs were conducted and the oil sorption capacity for each experiment was calculated.

The effects of sorbent dosage, contact time, initial oil concentration and temperature at three variable levels (-1, 0, 1) were evaluated in Table 1:

Table 1: Process factors and levels considered for the oil sorption

Factors	Units	Symbol	Levels				
			-α	Low (-1)	Center (0)	High (+1)	+α
Sorbent dosage	g	A	1.5	1.5	2.5	3.5	3.5
Contact time	min	B	10	10	20	30	30
Initial oil concentration	g/L	C	25	25	50	75	75
Temperature	^{o}C	D	25	25	35	45	45

2.2. Oil Sorption Capacity (OSC)

The waste polypropylene plastics (WPP) were subjected to crude oil sorption test, and in order to simulate the situation of oil spill and minimize experimental variation, the crude oil sample was held in beakers for a day in open air to release volatile hydrocarbon contents. The 30 experimental runs with the various combinations of the different factors were randomly performed according to Table 3.

To one liter of distilled water, a concentration (25, 50, 75 g/L) of crude oil was added. A mass of the sorbent (1.5, 2.5, 3.5g) was added into the mixture in the beaker and left unperturbed at a contact time (10, 20, 30 min) in a water bath at a temperature (25, 35, 45 ^{o}C).

After the contact time had elapsed, the sorbent was removed using sieving net and left to drain by hanging the net over the beaker in an oven for 4 hours at 60 °C in order to remove the excessive unsorbed oil (Onwuka *et al*., 2016).

$$\text{Oil sorption capacity} = \frac{\text{New Weight Gained (g)}}{\text{Original weight (g)}} \quad (1)$$

3.0 RESULTS AND DISCUSSIONS

3.1. Fit Summary

Presented in table 2 is the fit summary values for the oil sorpion capacity by WPP. Results revealed high R^2 values of 0.9824, thus suggesting adequate fitting of the WPP sorbents to the data model.

The WPP sorbents had adequate precision (AP) values of 32.14. With AP values greater than 4, it meant that the CCD model gave an adequate signal and a very good prediction to the oil sorption capacity. The coefficient of variation (CV) value of the sorbents was 1.47 % which was lower than the standard value of 10%, thus indicating a very good precision and reliabilty.

Table 2: Fit summary Values for the Oil Sorption C apacity by Waste Polypropylene Plastics (WPP)

Std. Dev.	0.22	R-Squared	0.9816
Mean	14.98	Adj.R-Squared	0.9644
C.V.(%)	1.47	Pred.R-Squared	0.9184
		Adeq. Precision	32.14

3.2. CCD Response for the WPP sorbents

Presented in table 3 is the CCD response of the oil sorption capacity by the WPP sorbents. Results indicated that the highest oil sorption capacity was obtained at the 9th experimental run which had a high level of sorbent dosage (3.5g), high level of contact time (30 mins), high level of initial oil concentration (75 g/L) and a low level of temperature (25^{o}C) corresponding to 17.23 g/g, while the lowest oil sorption capacity was obtained at the 23rd experimental run which had a low level of sorbent dosage (1.5 g), low level of contact time (10 mins), low level of initial oil concentration (25 g/L) and a high level of temperature (45^{o}C) corresponding to 12.34 g/g.

Table 2: Design Matrix and Response for the Oil Sorption capacity by WPP Sorbents

Run	Dosage (g)	Time (min)	Conc. (g/L)	Temp (^{o}C)	OSC WPP (g/g)
1	3.50	10.00	75.00	25.00	**17.02**
2	3.50	30.00	25.00	45.00	**14.68**
3	2.50	20.00	75.00	35.00	**16.51**
4	2.50	10.00	50.00	35.00	**15.27**
5	1.50	10.00	75.00	45.00	**13.89**
6	2.50	20.00	25.00	35.00	**14.72**

7	3.50	30.00	75.00	45.00	**15.89**
8	1.50	20.00	50.00	35.00	**13.56**
9	3.50	30.00	75.00	25.00	**17.13**
10	2.50	30.00	50.00	35.00	**15.71**
11	2.50	20.00	50.00	35.00	**15.53**
12	3.50	10.00	25.00	25.00	**15.06**
13	1.50	30.00	25.00	45.00	**12.68**
14	1.50	30.00	75.00	25.00	**15.81**
15	3.50	30.00	25.00	25.00	**15.40**
16	1.50	30.00	75.00	45.00	**14.48**
17	2.50	20.00	50.00	35.00	**15.53**
18	1.50	10.00	25.00	25.00	**13.32**
19	1.50	30.00	25.00	25.00	**13.42**
20	2.50	20.00	50.00	35.00	**15.53**
21	2.50	20.00	50.00	35.00	**15.52**
22	3.50	10.00	75.00	45.00	**15.03**
23	1.50	10.00	25.00	45.00	**12.34**
24	2.50	20.00	50.00	25.00	**15.14**
25	3.50	20.00	50.00	35.00	**15.99**
26	2.50	20.00	50.00	45.00	**13.68**
27	2.50	20.00	50.00	35.00	**15.51**
28	3.50	10.00	25.00	45.00	**14.34**
29	1.50	10.00	75.00	25.00	**15.33**
30	2.50	20.00	50.00	35.00	**15.51**

3.3. Development of regression model equations

The model equation for the oil sorption capacity of the waste polypropylene plastics (WPP) sorbents is:

$$15.38 + 0.87A + 0.20B + 0.84C - 0.59D - 0.46A^2 + 0.25B^2 + 0.38C^2 - 0.83D^2 + 8.750E\text{-}003AB - 0.13AC - 0.011AD + 0.058BC + 0.069BD - 0.18CD, \quad (2)$$

The sorption process model equation is presented from equation 2, from the equation it implies that an increase in the sorbent dosage, contact time and initial oil concentration will increase the oil sorption process while an increase in temperature will decrease the oil sorption process. It could also be seen from the equations that the quadratic terms of contact time (B^2) and initial oil concentration (C^2), the interaction terms of sorbent dosage and contact time (AB), contact time and initial oil concentration (BC) and finally contact time and temperature (BD) all had a synergistic relationship with the oil sorption process, while the quadratic terms of sorbent dosage (A^2) and temperature (D^2) and the interaction terms of sorbent dosage and initial oil concentration (AC), sorbent dosage and temperature (AD) and finally initial oil concentration and temperature (CD) had an antagonistic relationship with the oil sorption process.

3.4. Effect of Interaction of two Variables on the Oil Sorption Capacity

3.4.1. Effect of the Interaction of Sorbent dosage and Initial oil Concentration

The interaction effect of sorbent dosage and initial oil concentration on the oil sorption capacity is presented in Figure 1. Results showed that increasing the sorbent dosage at both high and low levels of the initial oil concentration produced an increase in the oil sorption capacities. The highest oil sorption capacity of the interactions occurred at high levels of initial oil concentration and sorbent dosage, this may be due to more enhancement of the bulk movement of the crude oil to an already receptive biosorbent (Ouasif *et al*., 2013). Also at high oil concentration, oil occupies the sorbent surface thus sorption is achieved much faster, and with an increase in the sorbent dosage, the active surface area is also increased thus increasing the sorption capacity.

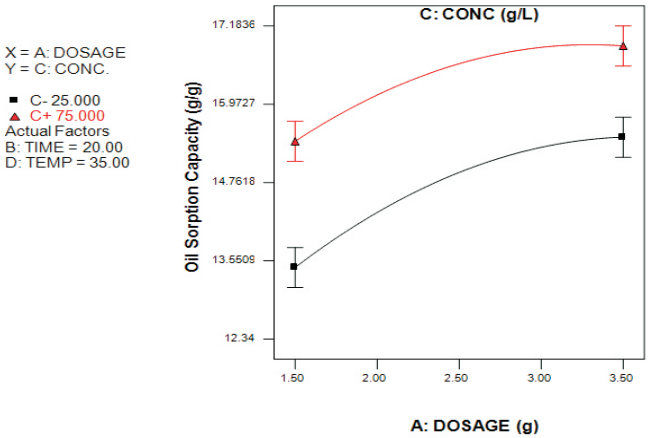

Figure 1: Interaction plot of Sorbate dosage and Initial oil concentration for the oil sorption capacity by WPP sorbents.

3.4.2. Effect of the interaction of Contact time and Temperature

Results presented in Figure 2 showed that increasing the contact time at both temperature levels resulted in an increase in the oil sorption capacities, with the low temperature level giving higher sorption capacity than the high temperature level. The lower sorption capacities at high temperature level could be probably due to the fact that at higher temperatures, oil starts to be very light which leads to release of oil from fibers, and an increase in the contact time may lead to more desorption from the fibers (Hussein *et al*., 2009).

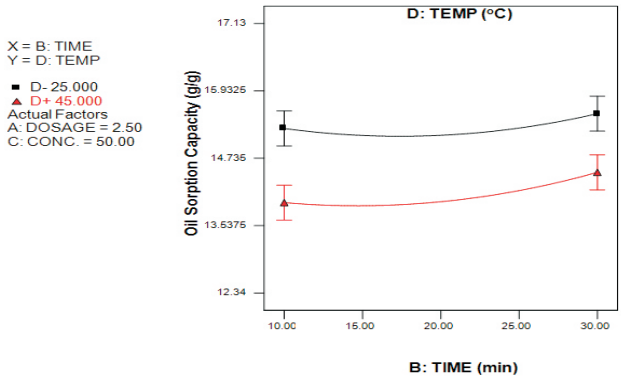

Figure 2: Interaction plot of Contact time and Temperature for the oil sorption capacity by WPP Sorbents

3.5. Effect of Interaction of Three Variables on the Oil Sorption Capacity

3.5.1. Effect of Interaction of Sorbent dosage, Initial Oil Concentration and Temperature on the Oil Sorption Capacity

The cube plot for the effect of interaction of sorbent dosage, initial oil concentration and temperature on the oil sorption capacity is shown in Figure 3. Results showed that the lowest oil sorption capacity (12.22 g/g) was achieved at low sorbent dosage of 1.5g, low initial oil concentration of 25 g/L and high temperature of 45°C (A-, C-, D+). This could be due to low available active sites for sorption, low sorbates present and low viscosity of the oil particles owing from the high temperature.

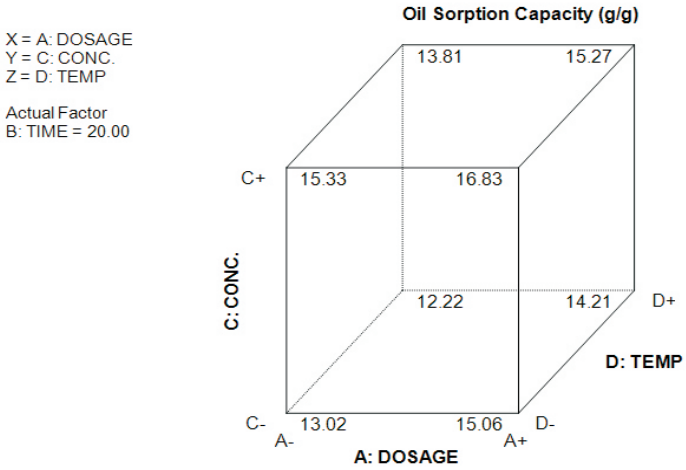

Figure 3: Cube plot of Sorbate dosage, Initial oil Concentration and Temperature on the oil sorption capacity by WPP sorbents

3.5.2. Effect of Interaction of Contact Time, Initial Oil Concentration and Temperature on the Oil Sorption Capacity

The cube plot for the effect of interaction of contact time, initial oil concentration and temperature on the oil sorption capacity is shown in Figure 4. It could be observed from the cube plot that the interaction factor of initial oil concentration produced the most positive effect since all the highest oil sorption capacities were obtained at high initial oil concentration. This could be due to the fact that increasing the initial oil concentration increases the number of collisions between oil and the sorbents which enhances the sorption process (Hameed and El-Khaiary, 2008).

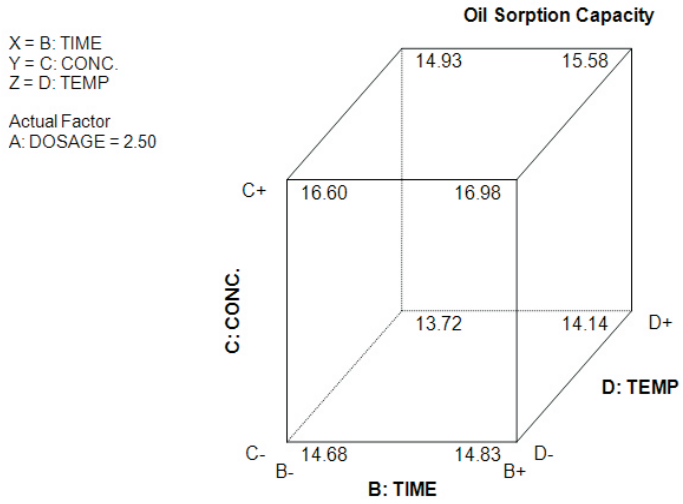

Figure 4: Cube plot of Contact time, Initial oil concentration and Temperature on the oil sorption capacity by WPP sorbents

3.6. Diagnostics

3.6.1 Residuals vs Predicted Values

The plot of residual versus predicted values is presented in Figure 5. From the figure, it was evident that there was randomly scattered points spread around mid-way line without an obvious pattern and unusual structure being made by this points, this suggests the adequacy of the sorption model by WPP sorbents.

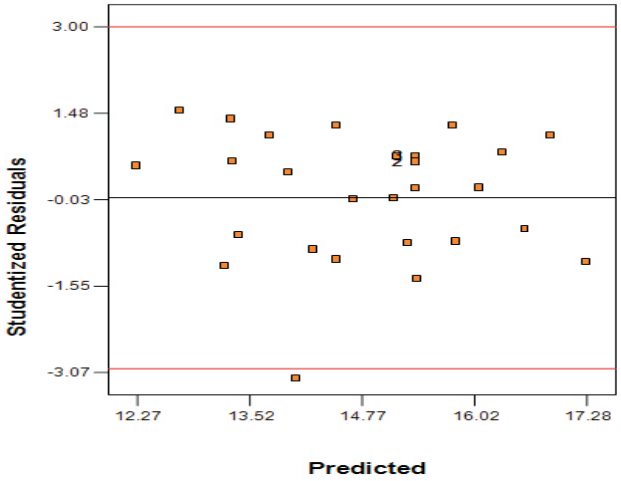

Figure 5: Residual vs Predicted Values Plot for the Oil Sorption Capacity by WPP sorbents

3.6.2. Outlier vs Run Number

The number of deviations of the actual value from the predicted value was determined from the outlier plot. Result from Figure 6 revealed that the plot of the WPP sorbents had all but one of its points within the control limits. Since only one outlier was located, it could be inferred that it was probably due to a slight experimental error inferring that the data in this study are acceptable.

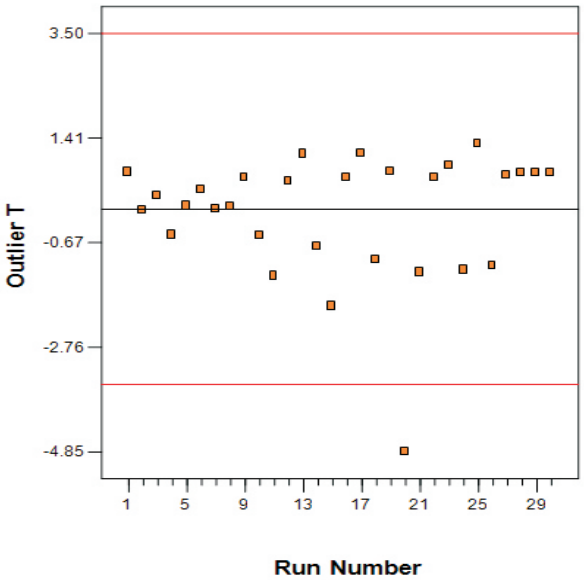

Figure 6: Outlier vs Run Number Plot for the Oil Sorption Capacity by WPP sorbents

Conclusion

The results of this study show that waste polypropylene plastics is an efficient sorbent for crude oil spillage with its maximum sorption capacity obtained at 17.23 g/g at conditions of 3.5g, 30 mins, 75 g/L and 45^{o}C. Results from the fit summary and the diagnostic studies also indicated adequate fitness of

the WPP sorbents for the face- entered CCD model.

The use of WPP as sorbents can benefit the oil pollution issue with a more affordable solution and can also reduce the abundance of household waste problems. WPP constitutes a cost-effective sorbent for oil-spill cleanup with additional merits of recycling and reusability. Further investigation on possible fabrication /combination with natural fibers which could enhance its oil sorption performance and incorporate the benefits of biodegradability should be encouraged.

REFERENCES

Abdel-Ghani, N. and El-Chaghaby, G. (2014). Biosorption for metal ions removal from aqueous solutions: A review of recent studies. *International Journal of Latest Research in Science and Technology*, 3(1), 24 – 42.

Ge, J., Zhao, H.-Y., Zhu, H.-W., Huang, J., Shi, L.-A. and Yu, S.-H. (2016). Advanced Sorbents for Oil-Spill Cleanup: Recent Advances and Future Perspectives. *Advanced Materials*, 28(47), 10459 – 10490.

Gecgel, U., Ozcan, G. and Gurpinar, G. C. (2013). Removal of methylene blue from aqueous solution by activated carbon prepared from pea shells (*Pisum sativum*). *Journal of chemistry*, 31(4), 11 – 19.

Hameed, B. H. and El-Khaiary, M. I. (2008). Malachite green adsorption by rattan sawdust: Isotherm, kinetic and mechanism modeling. *Journal of Hazardous Materials,* 159(2-3), 574 – 579.

Husseien, M., Amer, A. A., El -Maghraby, A. and Taha, N. A. (2009). Availability of barley straw application on oil spill cleanup, *International Journal of Environmental Science and Technology, 6(1),* 123 - 130.

Khosravi, M. and Arabi, S. (2016). Application of response surface methodology (RSM) for the removal of methylene blue dye from water by nano zero-valent iron (NZVI). *Water Science and Technology,* 74(2), 343–352.

Onwuka, J. C, Agbaji, E. B., Ajibola, V. O. and Okibe, F. G. (2016). Kinetic studies of surface modification of lignocellulosic *Delonix regia* pods as sorbent for crude oil spill in water. *Journal of Applied Research and Technology*, 14, pp. 415 – 424.

Ouasif, H., Yousfi, S., Bouamrani, M. L., El Kouali, M., Benmokhtar, S. and Talbi, M. (2013). Removal of a cationic dye from wastewater by adsorption onto natural adsorbents. *Journal of Materials and Environmental Science*, 4(1), 1 - 10.

Sabir, S. (2015). Approach of Cost-Effective Adsorbents for Oil Removal from Oily Water.

Critical Reviews in Environmental Science and Technology, 45(17), 1916 – 1945.

Thani, S. Y. M., Ghazi, R. M. and Ismail, N. (2017). Response surface methodology optimization of oil removal using banana peel as biosorbent. *Malaysian Journal of Analytical Sciences,* 21(5) 1101 – 1110.

Nigerian Journal of Polymer Science and Technology, 2021, Vol. 16, pp63-76
Received: 11/08/2020 Accepted: 09/08/2021

Reinforcing potential of acetone pretreated *Calamusdeerratus* fibre as filler in Natural Rubber and Epoxidized Natural Rubber Vulcanizates

***Osabohien, E., Okoh, B.E. and Egboh, S.H.O.**

Department of Chemistry, Delta State University, Abraka Nigeria.
*Correspondence author's email: osabohieneemma@yahoo.com

Abstract

The present study investigated the potential of acetone pretreated Calamusdeerratus fibre (CDF) on the cure characteristics and physico-mechanical properties of natural rubber, standard Nigerian rubber (SNR_{10}) and epoxidized natural rubber, ENR - 20 vulcanizates. The results of the analyses revealed that both the untreated and acetone-treated CDF manifested reinforcing effects by enhancing the cure characteristics and physico-mechanical properties of the SNR_{10} and ENR-20 vulcanizates. The maximum torque, abrasion resistance, modulus, hardness and specific gravity of the filled vulcanizatesincreased while the cure time, scorch time, elongation at break and rebound resilience decreased with increasing filler loadings. The tensile strength increased to an optimum level, then decreasedthereafter with increasing filler loadings. Compared with the untreated CDF reinforced vulcanizates, the cure characteristics and physico-mechanical properties of the acetone treated CDF- filled SNR_{10} and ENR – 20 vulcanizates were significantly improved. The ENR-20 filled vulcanizates manifested higher tensile strength, maximum torque, abrasion resistance, modulus, hardness and specific gravity but lower elongation at break, scorch time, cure time and rebound resilience than SNR_{10}- filled vulcanizates.

Keywords: *Natural rubber, epoxidized natural rubber, acetone treatedCalamusdeerratusfibre, fillers and reinforcement.*

Introduction

Growing concerns about the negative impacts of polymers, especially carbon black-reinforced plastics, and the increasing competition in producing cost effective polymeric articles in the last couple of years have driven scientists, researchers and industry players to seek alternative reinforcing fillers that are environmentally friendly. Biodegrdability of plant fibres is generally regarded as the most important feature of their utilization in polymeric reinforcement (Saba*et al*, 2014). This means that plant fibre-reinforced composites will pose less environmental pollution. However, natural fillers have some drawbacks; these include their hydrophilic nature,incompatibility with the polymer matrix, low thermal stability, tendency to agglomerateduring processing, high acidic content, poor wettability, relatively large particle size (hence, low surface area), poor dispersion, low impact strength and processing difficulty (Dakhal*et al*, 2007; Assarar*et al*, 2011; Abu-Bakar *et al*, 2012; Anike*et al*, 2014 and Shehu*et al*, 2014). All these factors will lead to weak interfacial bonding with the polymer resulting in poor mechanical strength properties of the vulcanizates. Nevertheless, research studies have shown that plant fibres are amenable to modifications because they bear hydroxyl groups from the constituent

polar molecules (cellulose, hemicelluloses and lignin) by different physical or chemical treatments (Alix*et al*, 2012; Pongdong*et al*, 2015).

Natural rubber exhibits several unique properties such as good elasticity, resilience, high strength and stiffness due to its ability to strain crystallize (Yoksan, 2008; Pongdong*et al*, 2015). However, most applications of natural rubber is limited due to its low stability to heat, oxygen, ozone, sunlight and high solubility in hydrocarbon oils due to the presence of unsaturation in it. The presence of unsaturation has long been exploited for possible chemical modification of natural rubber so as to improve its stability and durability(Hoon, 2006; Yoksan, 2008; Pongdong*et al*, 2015). One of the products of chemical modifications of natural is epoxidized natural rubber (ENR) derived from partial oxidation of natural rubber by reacting its molecules with performic or peracetic acid (Osabohien, 2012).

Past research works have revealed that the incorporation of plant fibres and wastes into the polymer matrices have resulted in enhanced physical and mechanical properties of the polymer vulcanizates(Imanah and Okiemen, 2004; Sogbaike*et al*, 2005; Osabohien*et al*, 2006; Imoisili*et al*, 2012 and Osabohien*et al*, 2015). The addition of plant fibres into the polymer matrix can reduce the overall usage of carbon black, thereby increasing the use of renewable, value-added, natural resources in our environment as fillers in rubber compounding. In addition, natural fillers have several other advantages over carbon black, amongst these are; natural abundance, light weight, sometimes hardness and stiffness, low cost, renewable, non-abrasive, carbon dioxide sequesteration, sustainable ecological and biodegradable features (Chandramohan and Marimuthu, 2011; Alix*et al*, 2012; Celino*et al*, 2014; Saba*et al*, 2014 and Okoh*et al*, 2014).

Previous study has shown that untreated (raw) *Calamusdeerratus* fibre manifested a reinforcing effect on natural rubber (SNR_{10}) vulcanizates although inferior to that of carbon black-reinforced natural rubber vulcanizates(Osabohien*et al*, 2015). The present study attempts to modify both the filler (CDF) by pre-treatment with acetone solution and the natural rubber by converting it to 20% epoxidized natural rubber (ENR-20). And then determine the cure characteristics and physico-mechanical properties of unmodified rubber, SNR_{10} and ENR-20 separately filled with industrial grade carbon black, N330, the raw and acetone-treated CDF.

Materials and Methods

Materials

The materials used for this study include *Calamusdeerratus* obtained from local farmers at Agbor, Delta State, Nigeria, the natural rubber, Standard Nigerian Rubber, constant viscosity, CV10 (SNR_{10}) was obtained from Footwear Accessories, Manufacturing and Distribution (FAMAD), Benin City, Nigeria. Industrial grade carbon black, N330 was obtained from Warri Refinery and Petrochemical Company (W.R.P.C.) Warri, Nigeria. The epoxidizednatural rubber with 20% epoxidation (ENR -20) was prepared in Polymer Chemistry Laboratory of the Department of Polymer Technology, Auchi Polytechnic, Auchi, Nigeria. Industrial grade compounding additives, rubber test equipment were obtained from the

Department of Polymer Technology, Auchi Polytechnic, Auchi, Edo State, Nigeria and Rubber Research Institute of Nigeria (RRIN), Iyanomo, Benin.

Methods

The epoxidized natural rubber (ENR) with 20 mole % epoxide group was prepared by directinsitu epoxidation reaction of the raw natural rubber in latex phase by the action of peracetic acid (Hoon, 2006; Osabohien, 2012). *Calamusdeerratus*fibre (CDF) was air dried and oven dried at 110 ^{0}C for about two hours. The pulverized specimen was sieved with a sieve of mesh size 212µm. The sieved sample was separately immersed in a 10% solution of acetone for two hours; washed with distilled water and dried to a constant mass at 120^{o}C. Both the acetone-treated and untreated CDF were separately packaged in plastic containers and labelled. Both samples were characterized relative to that of N330 by using standard test methods (ASTMD-1510, 1983; Horwitz, 2005). The SNR_{10} and ENR-20 were also characterized using standard methods (RRIM, 1989; SAR, 1998).

Compounding of the mixes

Table 1: Recipe for the formulation of SNR_{10} ENR – 20 Compounds

Ingredients	Phr
Natural Rubber (SNR_{10} or ENR- 20)	100.0
Zinc Oxide	4.0
Stearic acid	2.0
Processing oil	2.0
* filler	0 -70
N-cyclohexyl-2-benzothiazyl sulphonamide (CBS[a])	2.0
2, 2, 4- trimethyl -1, 2-dihydroquinoline (TMQ[b])	1.5
Sulphur	1.5

CBS[a] = N-cyclohexyl-2-benzothiazyl sulphonamide.
TMQ[b] = 2, 2, 4- trimethyl -1, 2-dihydroquinoline

The rubber compounds were prepared using efficient vulcanization (EV) system (Table 1). Both the untreated and acetone-treated CDF and the industrial grade carbon black, N330, were separately mixed with the $SNR_{10}$and ENR-20 rubbers together with other compounding additives at the different filler loadings and compounded on a laboratory size two roll mill (160mm x 320mm) maintained at 80^{o}C.The cure characteristics (scorch time, cure time and maximum torque) of each of the uncured compounded samples were determined by means of Monsanto rheomoter (MDR 2000, Wallace Instruments, UK). The various rubber compounds were cured by means of a hydraulically operated steam press at 180^{o}C and a pressure of 150 kg/cm^2.

Evaluation of the Physico-mechanical properties of the vulcanizates

The determination of the tensile properties (tensile strength, elongation at break and modulus at 100% strain) of the vulcanized rubber samples was carried out on Instrontensometer (Model 4301, Wallace instruments, UK) at room temperature at a cross-head speed of 500mm/min using the dumb-bell shaped test pieces punched out from the

moulded rubbers in accordance with standard procedure (ASTMD412-16, 2016) The hardness and specific gravity of the vulcanizates were tested using the Monsanto Duratron (Model 2001, Wallace Croydon, UK) and Monsanto Densitron (Model 2000, Wallace Instruments, UK) respectively. The rebound resilience and abrasion resistance of the vulcanizates were determined by means of Monsanto Tripsometer and the Akron abrader (Wallace Instruments, UK) respectively(BS 903, 1983).

RESULTS AND DISCUSSION

Physico-chemical properties of the rubbers, SNR_{10} and ENR-20

Table 2: Physico- chemical Properties of SNR_{10}, ENR – 20, SAR_{10} SMR_5

Natural Rubber	SNR-10	ENR-20	SAR_{10}	SMR_5
Dirt content (%)	0.03	0.01	0.02	0.05
Ash content (%)	0.20	0.25	0.22	0.50
Volatile matter	0.21	0.20	0.40	1.00
Nitrogen content	0.20	0.18	0.25	0.70
Plasticity Retention Index (PRI)	70.96	86.00	67.00	-
Mooney Viscosity, ML(1+4) 100 ^{O}C	85.00	96.00	70.00	60.00

The data in Table 2 summarize the physico-chemical properties of the natural rubber, Standard Nigerian Rubber (SNR_{10}) and Epoxidized Natural Rubber (ENR-20) used in this study in comparison with Standard African Rubber, CV 10 (SAR_{10}) and Standard Malaysian Rubber, CV 5 (SMR_5). The values of thedirt content, ash content, nitrogen content, volatile matter, plasticity retention index (PRI) and Mooney viscosity of the SNR_{10} and ENR – 20 rubbers compared favourably with those of SAR_{10} and SMR_5, thus suggesting that both rubbers are of good quality(RRIM, 1989;SAR, 1998).

Physico-chemical properties of the fillers

Table 3: Physico- chemical properties of CB (N330) and CDF Filler

Filler	CB(N330)	CDF	Acetone treated CDF
% moisture content at 120^{o}C	1.30	2.25	1.50
% loss on ignition at 1000^{o}C	93.0	80.0	85.0
Iodine Adsorption Number (mg/g)	78.50	56.20	62.10
pH of aqueous slurry	6.80	5.90	6.20
Magnesium (ppm)	Trace	53.10	31.30
Sodium (ppm)	Trace	51.20	20.10
Potassium (ppm)	Trace	16.10	10.50
Iron (ppm)	Trace	23.40	17.30
Chlorine (ppm)	Trace	17.80	10.10
Density (g/cm^3)	1.80	1.30	1.20

The data in Table 3 show the physico-chemical properties of the fillers, namely *Calamusdeerratus* fibre (CDF) and carbon black, N330. The parameters studied include moisture content, loss on ignition, iodine adsorption number, pH of the aqueous slurries, density,metallic and non-metallic contents. The results of the analyses revealed that the plant fibre,

CDF, had higher moisture content than N330.Similar observations have been documented in previous studies (Osabohien*et al*, 2006, 2015). Researchers have shown that the most relevant differences between plant fibres and carbon black is their response to humidity; carbon black is considered non-hygroscopic, whereas plant materials have pronounced hygroscopic behaviour (Dakhal, 2007; Celino*et al*, 2014).In plant fibres, the components which have polar groups that are responsible for absorbing moisture are cellulose, hemicelluloses, and lignin. In humid conditions, hygroscopic behaviour of such fibres leads to high level of moisture absorption. High moisture content of filler may lead to poor adhesion between the filler and polymer matrix, thereby resulting in poor mechanical properties of vulcanizates(Okoh*et al*, 2014).The hydroxyl groups in cellulose has the potential to associate with each other through hydrogen bonding to form a strong network thereby reducing the activity towards the polymer matrix. This can also lead to processing difficulty since the cellulose microfibrils tends to agglomerate during compounding(Dhakal*et al*, 2007; Celino*et al*, 2014).

The results also revealed that N330 had higher weight loss on ignition at 1000^{o}C than CDF, this means higher content of carbon orcarbonaceous materials, similar to previous reports (Imanah and Okieimen, 2004; Osabohien*et al*, 2006 & 2015). Several research studies have shown that the reinforcing potential of plant fibres and materials could be increased dramatically through carbonization (Okieimen and Imanah, 2005; Osabohien, 2010).

The iodine adsorption number of a filler is a relative measure of its surface area, hence its particle size. The results of the analyses showed that N330 had higher iodine adsorption number, meaning that N330 had a larger surface area (hence smaller particle size) than CDF. It has been well documented in related literatures that the particle size (surface area) of a filler is the most important parameter determining its reinforcing ability (Osabohien and Egboh, 2007). A reinforcing filler must have very small particle size of less than 1000nm in order to maintain a very strong surface contact with the polymer matrix. In a related study to investigate the effectiveness of powdered charcoal made from rice husk as a reinforcing filler for styrene-butadiene rubber (SBR), Yamashita and Ta naka (2005) did not observe any significant reinforcing effect by the unburnt rice husk due to its large particle size which was greater than 50nm, but powdered carbonized rice husk of particle size of about 1.0nm produced a reinforcing effect almost equivalent to that of carbon black. The larger the particle size of a filler, the weaker the filler-polymer matrix interactions and the poorer the mechanical strength properties of the resulting vulcanizates. Thus it has been postulated that the smaller the particle size of a filler,the higher the strength properties (Okieimen and Imanah, 2005; Osabohien, 2010).

The results of the analyses further revealed that the aqueous slurry of CDF with a pH of 5.90 was more acidic than that of N330 of pH 6.80. Acidity has been shown to affect reinforcement and vulcanization processes, highly acidic fillers retard both vulcanization and scorch time leading to poor mechanical properties of the vulcanizates(Okoh*et al*, 2014). The

results also showed the various metallic and non-metallic constituents of the plant fibre, CDF (Table 3). It has been observed in previous research studies that the presence of surface active groups could contribute to the surface activity of a filler and hence influence its reinforcing potential (Osabohien and Egboh, 2007; Osabohien*et al*, 2015).

Cure characteristics of SNR_{10} and ENR-20 vulcanizates

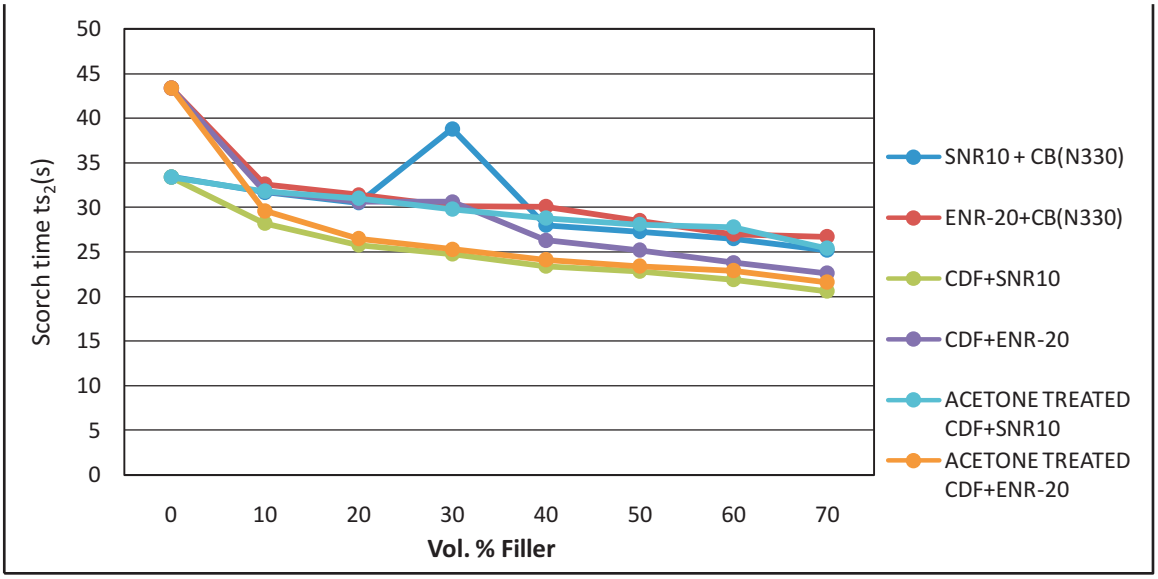

Figure 1: Scorch time of rubber composites as a function of volume fraction of fillers

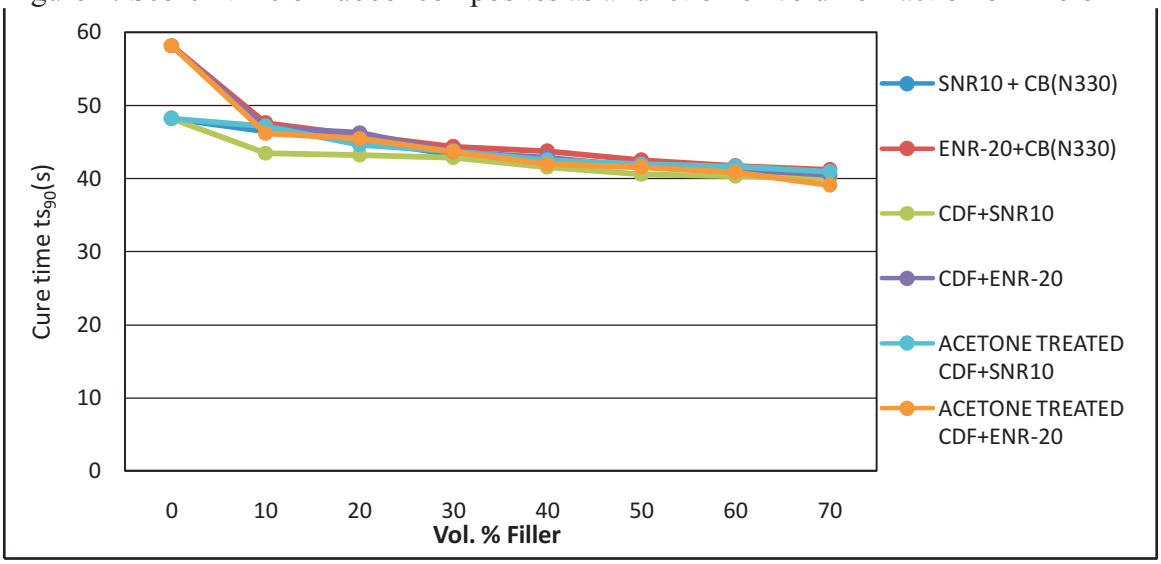

Figure 2: Cure time of rubber composites as a function of volume fraction of fillers

The data inFigures 1-3 showed the results of the analyses of the cure characteristics (scorch time, cure time and maximum torque, T_{max}) of SNR_{10} and ENR-20 vulcanizates filled with N330, untreated and acetone treated CDF at different filler loadings. The results revealed that the scorch time and cure time of both SNR_{10} and ENR-20 vulcanizates filled with N330 and both the untreated and acetone- treated CDF materials decreased while the maximum

torque (T_{max}) increased with increasing filler loadings consistent with earlier research reports (Sogbaike*et al*, 2005; Osabohien*et al*, 2015). The lower scorch times and cure times of N330-filled ENR-20 vulcanizatescompared to N330-filled SNR_{10}vulcanizates may be due to the additional (ether) crosslinks formed via the sulphur-acid catalyzed ring opening of the epoxide groups that occurred during vulcanization which probably produced cure enhancement. The results further showed that the scorch times and cure times of both the acetone-treated and untreated CDF filled ENR-20 and SNR_{10}vulcanizates were higher than N330 filled SNR_{10} and ENR-20 vulcanizates. This difference may probably be due to the larger particle size (hence lower surface area), higher moisture content, higher acidity, higher metal oxides content and other impurities of CDF as compared to N330 (Table 3). This observation has been asserted by earlier research reports (Okieimen and Imanah, 2005; Osabohien*et al*, 2015). It was also observed that the scorch times and cure times of the SNR_{10} and ENR-20 vulcanizates filled with untreated CDF were higher than SNR_{10} and ENR-20 vulcanizates filled with acetone – treated CDF. This may be due to the fact that the acetone solution activated or removed the metal oxides and the hydroxyl and other polar groups on the fibre surface that may interfere with the vulcanization process and slow down the curing (cure retardation). The increase in maximum torque (T_{max}) with increase in filler leadings suggests that there is a good interaction and good interfacial bonding between both fillers, N330and CDF with the rubber matrix. Maximum torque is a measure of stiffness and determines the degree of crosslinking in vulcanizates, the higher it is, the higher the crosslinking and stiffness.

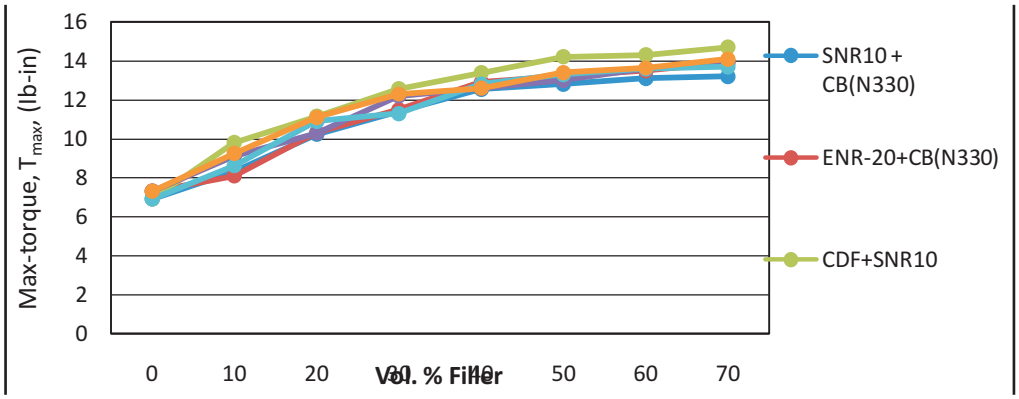

Figure 3: Maximum torque of rubber composites as a function of volume fraction of fillers

T_{max} values of N330- filled and CDF-filled ENR- 20 vulcanizates were higher than that of filled SNR_{10}vulcanizates. This may be due to the formation of additional (ether) crosslinks via the sulphur acid catalyzed ring opening of the epoxide groups during vulcanization which probably stiffened the ENR-20 vulcanizates, thus restricting the free mobility of the macromolecular chains. The larger particle size, higher moisture and acidic content of the CDF probably reducedthe degree of dispersion into the rubber matrix resulting in low degree of crosslinking and low restriction to the

flow of macromolecular chains and hence lower torque values (Osabohien*et al*, 2011; Osabohien, 2012; Okoh*et al*, 2014).

Physico-mechanical properties of filled SNR_{10} and ENR- 20vulcanizates

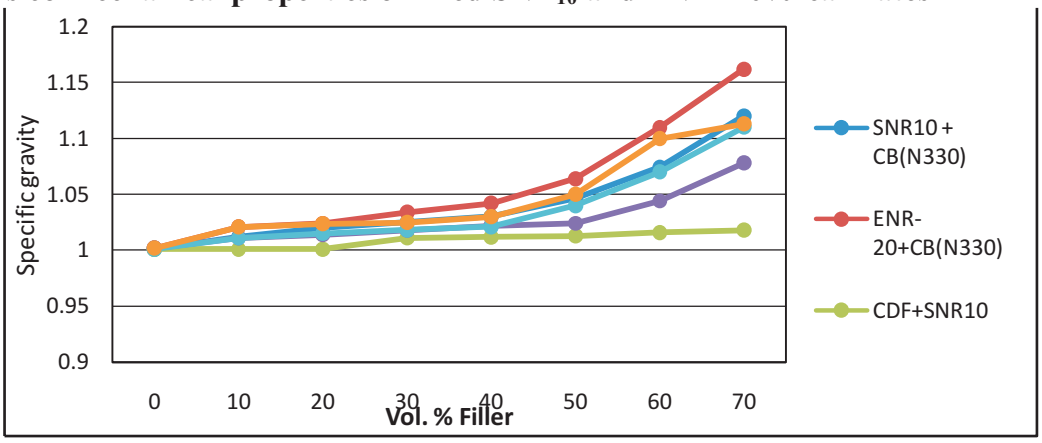

Figure 4: Specific gravity of rubber vulcanizatesas a function of volume fraction of fillers

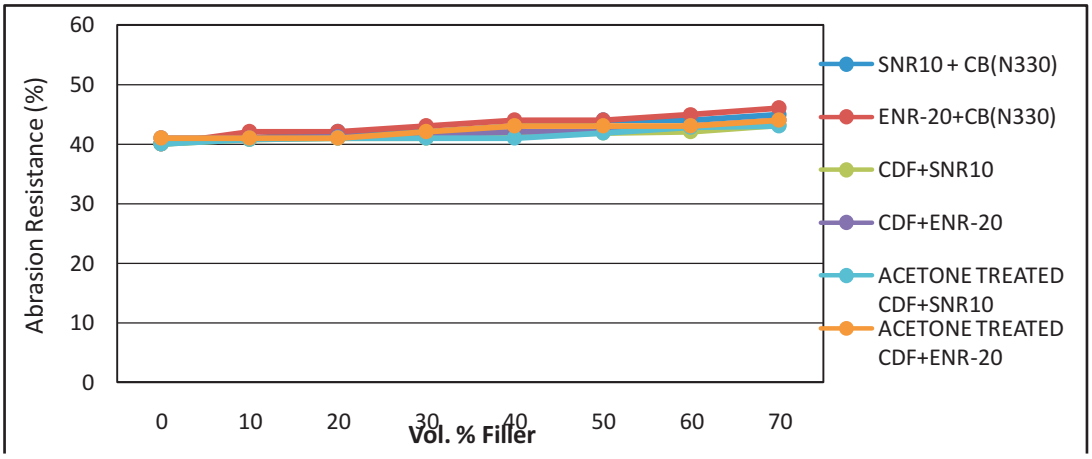

Figure 5: Abrasion resistance (%) of rubber vulcanizates as a function of volume of fraction of filler

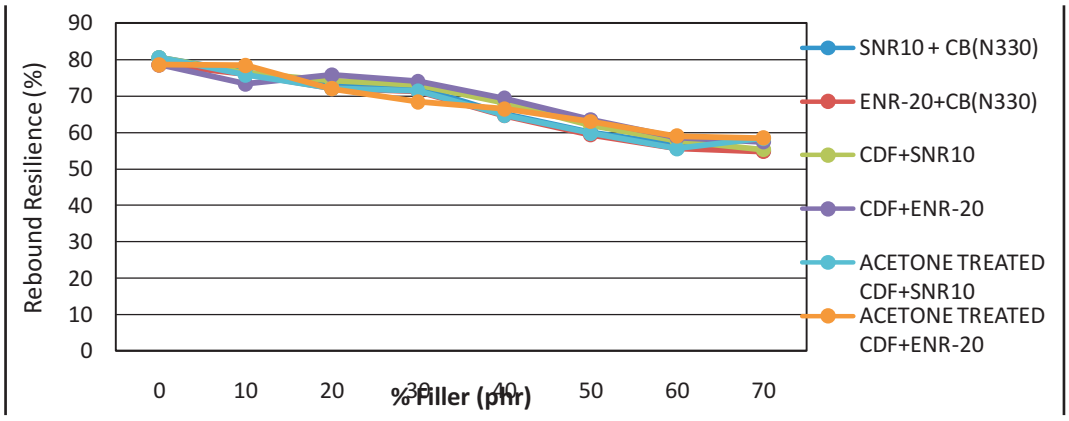

Figure 6: Rebound resilience (%) of rubber vulcanizates as a function of volume fraction of fillers

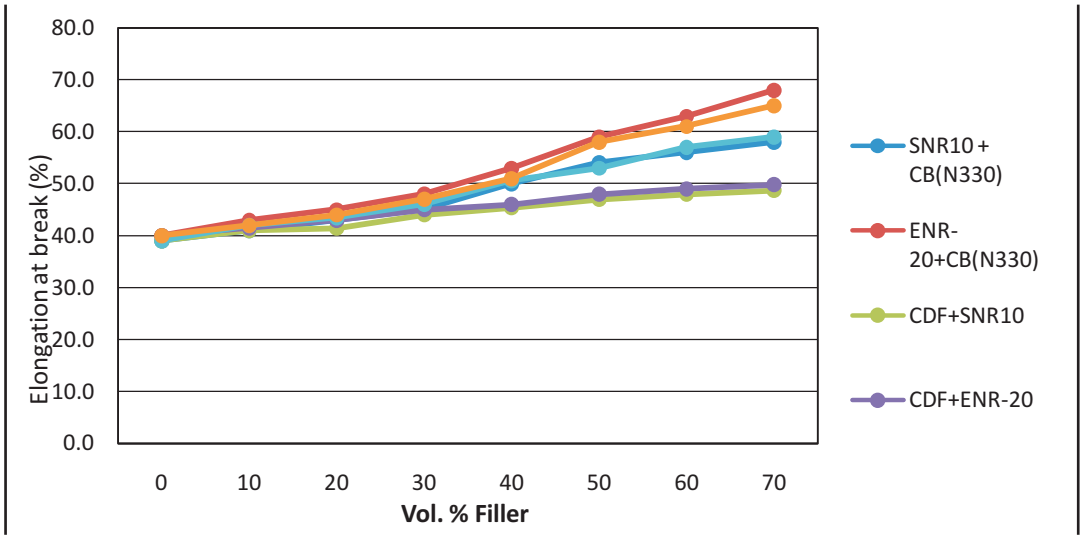

Figure 7: Hardness of rubber vulcanizates as a function of volume fraction of filler

The results of the specific gravity, abrasion resistance, rebound resilience, tensile strength, modulus, hardness and elongation at break of SNR_{10} and ENR-20 reinforced with N330, the untreated and acetone treated CDF fillers at different loadings were presented in Figures 4-10. The specific gravity, abrasion resistance, modulus and hardness increased while the rebound resilience and elongation at break of all the CDF and N330-reinforced SNR_{10} and ENR-20 vulcanizates decreased with increasing filler content consistent with documented research reports (Osabohien*et al*, 2011; Osabohien, 2012).

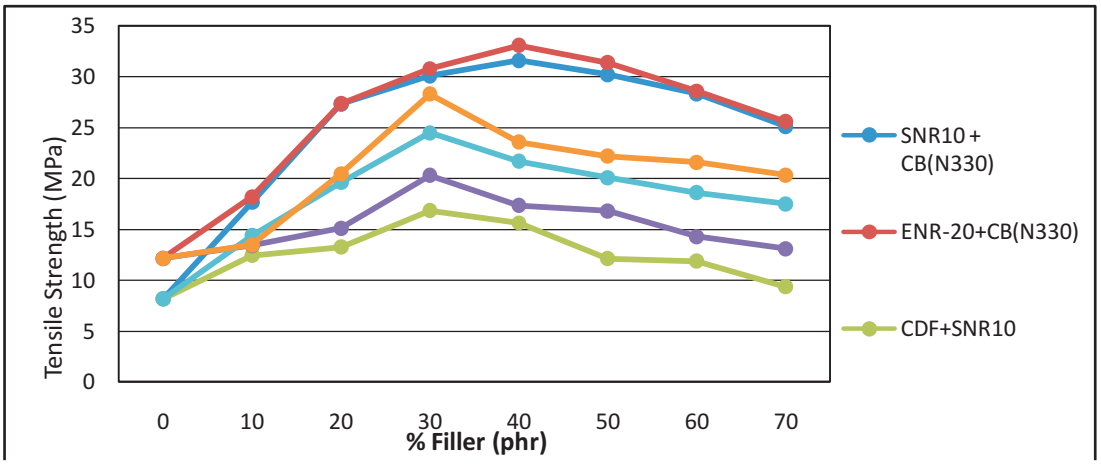

Figure 8: Tensile strength of rubber vulcanizates as a function of volume fraction of filler

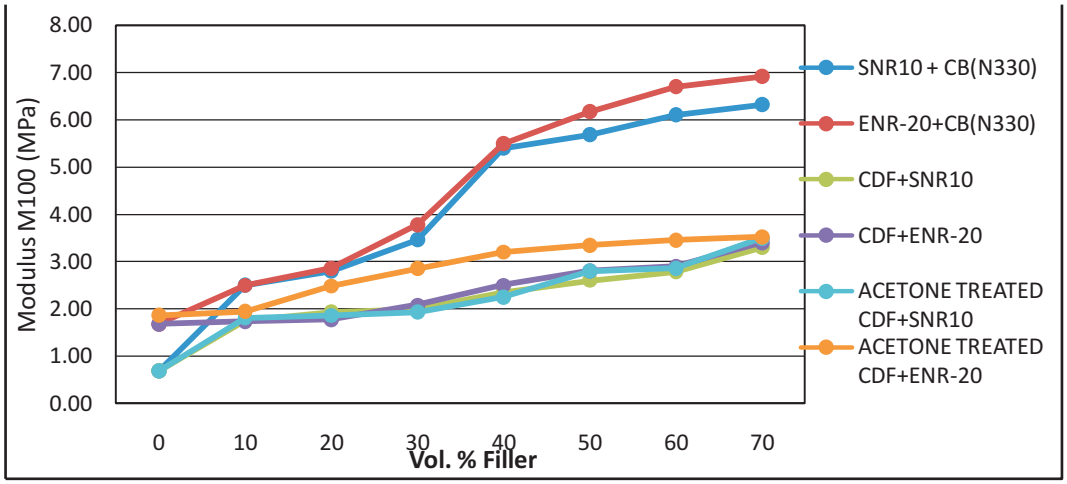

Figure 9: Modulus of rubber vulcanizates as a function of volume fraction of filler

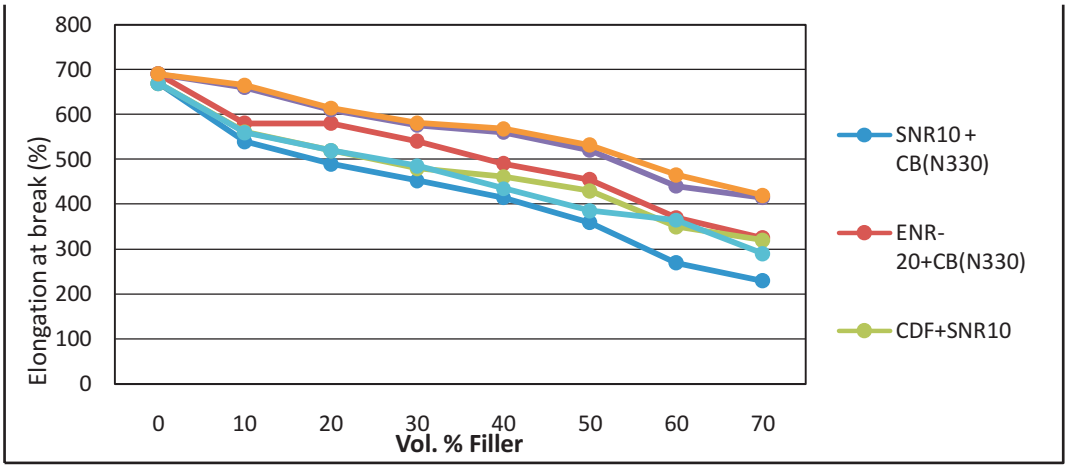

Figure 10: Elongation at break of rubber vulcanizates as a function of volume fraction of filler

The tensile strength of both reinforced systems increased with increasing filler content until certain critical levels (40phr and 30phr respectively for N330-filled and CDF-filled SNR_{10} and ENR-20 vulcanizates) were reached. A further increase in filler content decreased the tensile strength. These observations are consistent with earlier research findings (Imanah and Okieimen, 2004; Osabohien and Egboh, 2008; Okoh*et al*, 2014). The decrease in tensile strength after attaining certain optimum value may be attributed to dilution effect, common to all fillers, due to diminishing volume fraction of the rubbers in the vulcanizates or agglomeration of the filler particles which may occur during compounding to form a domain which can act to prevent or decrease filler-polymer matrix adhesion. The number of agglomerates increases as loading increases. Researchers have postulated that the dilution effect was due to lack of enough polymer matrix to hold the filler together which is a phenomenon of phase inversion (Osabohien and Egboh, 2007 & 2008; Osabohien, 2010). The results however showed that both the untreated and acetone-treated CDF manifested lower reinforcing effects than N330filler as indicated by

the lower tensile strength, modulus and abrasion resistance but higher elongation at break and rebound resilience of the SNR_{10} and ENR-20 filled vulcanizates. These differences may be due to filler- related parameters. The larger particle size (hence smaller surface area), higher acidic and moisture contents, greater tendency to agglomerate and metal oxide contents of CDF could have led to poor wetting and dispersion of the fibre with the rubber matrix leading to a weak interfacial bonding between the CDF and rubber matrix. The presence of agglomerates in fillers is believed to deteriorate the mechanical properties of the polymeric compounds (Mohamad *et al*, 2008). N330 has smaller particle size (larger surface area), lower acidic content (Table 3), and may have less tendency to agglomerate than CDF, hence it exhibits greater reinforcing effects than CDF. Also, the smaller the particle size (hence the larger its surface area), the greater the filler-elastomer interactions and the greater thetendency to impose extra resistance to the flow of macromolecular chains of the polymer(Wolff *et al*,1993; Osabohien*et al*, 2015).This implies an increased resistance of the vulcanizates to stretching on the application of strain. This probably explains why N330-filled ENR-20 and SNR_{10}vulcanizates had lower rebound resilience and elongation at break than both CDF-filled ENR-20 and SNR-vulcanizates. The results also showed that the untreated CDF manifested lowest tensile strength, modulus, abrasion resistance and hardness but highest rebound resilience and elongation at break than the acetone- treated CDF and N330 filledvulcanizates, which may be due to a weaker filler-polymer matrix adhesion and weaker interfacial bond strength of the untreated CDF. Several research reports have shown that physical or chemical treatment of plant fibres/materials prior to their incorporation into the polymer matrix not only decreases their hygroscopicitybut also concomitantly increases the interaction of the fibre/material with the polymer matrix (Yamashita and Tanaka, 2005; Abu - Bakar *et al*, 2012; Anike*et al*, 2004; Saba*et al*, 2014; Pongdong*et al*, 2015). Thus, pretreatment of CDF with acetone solution probably removed all acetone soluble constituents from the fibre. This would leave increased pore volumes and a surface which is both rough and irregular thereby increasing the fibre-polymer matrix interfacial adhesion, hence the observed higher strength properties of the acetone-treated ENR-20 and SNR_{10}vulcanizateswhen compared with the raw CDF-filled ENR-20 and SNR_{10}vulcanizates [Figures 4-10].

The results also showed that the physico-mechanical properties of SNR_{10}vulcanizates of both N330 and CDF were inferior to that of the ENR-20 vulcanizates. This observation may probably be due to the additional (ether) crosslinks produced in ENR-20 molecules as a result of the acid-catalyzed ring-opening of the epoxide groups in the ENR-20 backbone(Osabohien*et al*, 2011; Osabohien, 2012). The results further revealed that CDF- filled SNR_{10} and ENR-20 vulcanizates manifested slightly higher hardness property than the N330-filled SNR_{10} and ENR-20 vulcanizates. This may be due to some kind of fibre (polymer) – rubber (polymer) interactions between the filler (fibre) and the rubber to give enhanced stiffness and hardness results (Osabohien and Egbon, 2008; Osabohien, 2012).

CONCLUSION

The main objective of this study was to determine the potential of acetone- treated *Calamusdeerratus* fibre (CDF), as alternative reinforcing filler to carbon black in natural rubber and epoxidized natural rubber compounds. The results of the analyses showed that both the untreated and acetone treated CDF manifested reinforcing effects by enhancing physico-mechanical properties of the SNR_{10} and ENR-20 vulcanizates.

The physico-mechanical properties of ENR-20 and SNR_{10}vulcanizateswere however significantly improved by the incorporation of the acetone- treated CDF compared with the untreated (raw) CDF. Furthermore, the superior hardness results for CDF-filled vulcanizates coupled with the lower specific gravity could be advantageous in applications requiring light weight and improved hardness.

REFERENCES

Abu-Bakar, M. A., Almad, S. and Kuntjoro, W. (2012). Effect of epoxidized natural rubber on mechanical properties of epoxy reinforced kenaf fibre composites. *Pertanika J. Sci. Technol.* **20**(1): 129-137.

Alix, S., Leboun, L., Marais, S., Philippe, E., Bourmaud, A. and Baley, C. (2012). Pectinase treatments on technical fibres of flax: Effects of water sorption and mechanical properties. *Carbohy. Polym.* **87**: 177-185.

Anike, D. C., Onaegba, T. U., Ogbu, I. M. and Alaekwe, I. O. (2014). The effect of alkali treatment on tensile behaviour and hardness of raffia palm fibre reinforced composites. *American J. Polym. Sci.* **4**(4): 117-121.

Assarar, M., Seida, D., El Mahi, A., Poilare, C. and Ayed, R. (2011). Influence of water ageing on mechanical properties and damage events of two reinforced composite materials: Flax fibres and glass fibres. *Mater. Des.* **32**: 788-795.

ASTM D-1510 (1983). *Standard Test Method for Iodine Adsorption Number. American Society for Testing and Materials,* West Conshohocken, P. A.

ASTM D412-16 (2016). *Standard Test Methods for Tensile Properties of Elastomers.* ASTM International, West Conshohocken, P.A. www.astm.org

B.S 903 (1983). *British standard methods of Testing Vulcanized Rubber.* Part, A9 1-5.

Celino, A., Freour, S., Jacquemini, F. and Casari, P. (2014). The hygroscopic behaviour of plant fibres: A Review. *Frontiers in Chem.* **1**:43-48.

Chandramohan, D. and Marimuthu, K. (2011). A Review of Natural Fibres. *IJRRAS.* **8**(2): 194-206.

Dhakal, H. N., Zhang, Z. Y. and Richardson, M.O.W. (2007). Effect of water absorption on the mechanical properties of hemp fibre reinforced unsaturated polyester composites. *Compos. Sci. Technol.* **67**: 1674-1683.

Hoon, T. C. (2006). Epoxidized Natural Rubber (ENR-50) Stabilized Gold and Platinum Organosols. M.Sc. Thesis, UniversitiSains, Malaysia: 1-34.

Horwitz, W. (2005). *Official Methods of Analysis of AOAC International.* 17th ed. Maryland, USA: 7-9.

Imanah, J. E. and Okieimen, F. E. (2004). Studies on the mechanical properties of Natural Rubber reinforced with Agricultural by products. Benin City, *Proceedings of 27 Int. Conf. Chem. Soc. Nig.* 272-274.

Imoisili, P. E., Olunlade, B. A. and Tomori, W. B. (2012). Effect of silane coupling agent on the Tensile properties of Rice Husk Flour (RHF) polyester composites. *Pak. J. Sci. Tech.* **13**(1): 457-462.

Mohamad, N., Maditar, A., Ghazali, M. J., Muhd, D. and Azhari (2008). The effect of filler on Epoxidized natural rubber – Alumina Nanoparticle composites. *Euro. J. Sci. Res.***24** (2): 538-547.

Okieimen, F.E. and Imanah, J.E. (2005). Physico-mechanical and equilibrium swelling properties of Natural Rubber- Filled rubber seed shell carbon. *J. Polym. Mater.* **22**: 409-416.

Okoh, B. E., Osabohien, E. and Egboh, S.H.O. (2014). The Reinforcing potentials of *Velvet tamarind* seed shell as filler in natural rubber compounds *Int. J. Biol. Chem. Sci.***8**(5): 2367- 2376.

Osabobien, E., Egboh, S.H.O. and Okoh, B.E. (2006). The cure characteristics and physico-mechanical properties of natural rubber filled with Pineapple Leaf fibre. *Bio. Sci. Biotech. Res.Asia,***4**(1): 161-168.

Osabohien, E. (2010). Potential of carbonized cherry seed shell as filler in natural rubber vulcanizates. *J. Polym. Mater.* **27**(4): 379-389.

Osabohien, E. (2012). Bowstring hemp fiber reinforced epoxidized natural rubber compounds, *J. Polym. Mater.,* **29**(1): 423-435.

Osabohien, E. and Egboh, S.H.O. (2008). Utilization of bowstring hemp fiber as filler in natural rubber compounds, *J. Appl. Polym. Sci.,* **107**, 210-214.

Osabohien, E. andEgboh, S.H.O. (2007). An investigation on the reinforcing potential of red earth as filler in natural rubber compounds. *J. Appl. Polym.Sci*.**105**(2), 515-520.

Osabohien, E., Okoh, B. E. and Egboh, S. H. O. (2015). *Calamusdeerratus* fibre reinforced Natural Rubber Vulcanizates. *Int. J. Biol. Chem. Sci.***9**(2): 1094-1106.

Osabohien, E., Okoh, B.E., Imanah, J.E. and Egboh, S.H.O. (2011). The effects of epoxidation on the potentials of red earth natural rubber composites, *Nigerian J. Polym. Sci. Technol.,* **7**(1): 85-100.

Pongdong, W., Nakason, C., Claudia, K. and Vennemann, N. (2015). Influence of filler from a renewable resource and silane coupling agent on the properties of epoxidized natural rubber vulcanizates. *J. Chem.* 1-15.

RRIM (1989). *Rubber Research Institute of Malaysia*, SMR Bulletin No. 7: 9-40.

Saba, N., Tahri, P. M. and Jawaid, M. (2014). A review of the potentiality of nanofibre/natural fibre filled polymer hybrid composites. *Polymer*. **6**: 2247-2273.

SAR (1998). *Standard African Rubber.* Manual No. 2: Specification and Testing Methods, 1-10.

Shehu, U., Audu, H. I., Nwamara, M. A., Ade-Ajayi, A. F., Shittu, U. M. and Isa, M. T. (2014). Natural fibre as reinforcement for polymers: A review. *Nig. J. Polym. Sci. Technol.* **9**(1): 54-76.

Sogbaike, O. E., Okieimen, F. E. and Edojariogba, P. O. (2005). Effects of substitution of N330 carbon black on the cure characteristics, physico-mechanical and swelling properties of natural rubber vulcanizates. *Chem. Tech. J.* **1**:24-29.

Wolff, S., Wang, M.J. a nd Tan, E.H. (1993). Filler-elastomer interactions, Part X, *Kantschuk Gummi Kunststoffe*, **94**(2): 102-107.

Yamashita, Y. and Tanaka, A. (2005). Mechanical property of rubber reinforced with rice husk charcoal. Available at http://www.mat.usp. A.c. jp/polymer composites. Accessed 5 Jan. 2009. 1-10.

Yoksan, R. C. (2008). Epoxidized natural rubber for adhesive application. *Kasetsart J. Nat. Sci.***42**: 325-332.

Nigerian Journal of Polymer Science and Technology, 2021, Vol. 16, pp77-82
Received: 23/10/2021 Accepted: 08/11/2021

Mechanical Properties Utilization of a Leather Lubricated Using Modified *Lophira Lanceolata* Seed Oil for Footwear and Leather Goods Manufacturing

Habila, B[*1]., Mamza, P.A.P[2]., Gimba, C.E[2].

[1]Directorate of Research and Development, Nigerian Institute of Leather and Science Technology; P.M.B. 1034, Zaria*
[2]Department of Chemistry, Faculty of Physical Sciences, Ahmadu Bello University, Zaria.
bitrushabila@yahoo.com

Abstract:
Special mechanical performance properties of leather depends on the fields of use (especially shoes and leather goods) and specific performance characteristics of the leathers. In a process of choosing a quality leather product, people most are times pay close attention to its handle character, although its physical-mechanical properties contribute to capability of withstanding wear and tear. Mechanical properties such as tensile strength, percentage elongation and ball-burst of the fatliquored leathers increased with increase in the degree of sulphation. An optimum tensile strength of 16.40MPa at 10% degree of sulphation, percentage elongation of 105.30% and a distension of 13.75mm were obtained respectively. Therefore, as a result of the high tensile strength of 14.98 MPa and 16.40 MPa at 8% and 10% degree of sulphation respectively, the fatliquored leather can be used for leather goods such as: clothing leather, wallets, key holder, bags and Automated Teller Machine (ATM) card pack. Also, the distension properties of the leather at 13.75mm, indicated the use of the fatliquored leather for shoe upper leather.

Keywords: *Fatliquor, Ball-burst, Lophira lanceolata seeds oil, Sulphonic acid, ATM.*

1.0 INTRODUCTION

The term leather goods generally refer to leather accessories such as: wallets, bags, belts, key holders, ATM card pack etc. Leather and leather goods are one of the most widely traded goods in the world with an annual estimated global trade value of around $170 billion (Mohammad and Mahtab, 2018). Special mechanical performance properties of leather depends on the fields of use (especially shoes) and specific performance characteristics of the leathers (Urbanija *et al*., 2004). This is in relation to the body weight, comfort and health. In a process of choosing a quality leather product, people most are times pay close attention to its handle character, although its physical-mechanical properties contribute to capability of withstanding wear and tear (Xiao-Lei *et al*., 2006). Leather production involves the conversion of hide and skin into leather which requires several chemical and mechanical processes to remove non-collagenous matter in pre-tanning operation (Chen *et al.,* 2012). After the tanning operation, to produce a good leather of desirable quality, the tanned leather is lubricated in a fatliquoring processes (Cuq *et al*., 1998). Fatliquor is the largest amount of leather-chemistry material in leather industry and has extremely important impact on the performance of leather (Senait, 2014). It can penetrate to the collagen fibres, making the leather plastic and lubricant. The fatliquor can make the molecular chain segment easily move by separating the leather fibres from each other, giving the leather flexibility, water proof, moisture and softness (Hassan *et al.,* 2017).

2.0 MATERIALS AND METHODS

2.1 Materials

i. Modified *Lophira* seed oil
ii. Fatliquored leather

2.1 Tensile Strength

To determine the tensile strength of the leather, the test samples were cut according to a total length of 100 mm and gage length of 47 mm. The testing of the samples was done at Engineering Materials Development Institute, Akure, Ondo State, Nigeria in accordance with ASTM D638 (2014) standard. The samples were machined to dumb bell shape and then placed in Instron universal tensile testing machine 3369 model and the tensile strength and modulus were evaluated.

2.2 Lastometer (Bursting Ball Test)

To determine the grain crack distension and load when a circular leather test specimen is secured in between two circular rings of 25 mm diameter and stretched with the help of a spherical head. Unto grain crack appears on the grain surface of leather (IULTCS, 2002).

3.0 RESULTS AND DISCUSSIONS

3.1 Result of Tensile Strength (6% Offer)

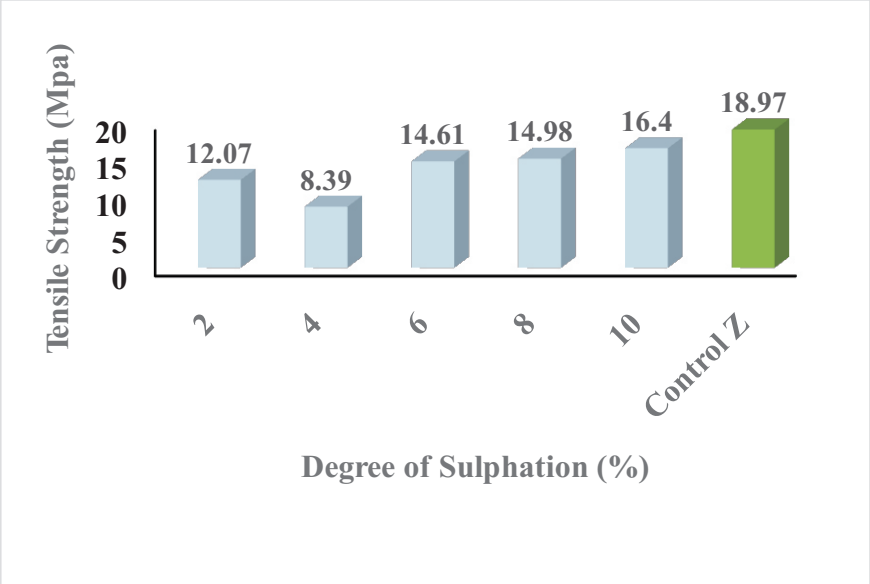

Figure 3.1: Tensile strength of leathers fatliquored with sulphated *Lophira* seed oil (6% Offer)

The tensile strength of the manufactured leather with the synthesized fatliquor increases with increase in the degree of sulphation, however Figure 4.6 illustrated the variation of tensile strength with increase in degree of sulphation, due to the fact that more of the emulsifying group (SO_3) is been added to the liquor. The decrease in the TS of the leather at 4% degree of sulphation could be due to the variation in the toughness of the animal skin before processing. The result 5% fatliquor offer of 2%, 4%, 6%, 8% and 10% degree of sulphation produced results that are less than that of the control fatliquor (commercial fatliquor). 18.97 MPa is the optimum tensile strength of the leather fatliquored with the manufactured fatliquored at 6% fatliquor offer. The results obtained is closely in agreement with the UNIDO recommendation of a 20 MPaminimum of tensile strength for shoe upper leathers(UNIDO, 1996).

3.2 Ball-burst Distension Properties of the Fatliquored Leather

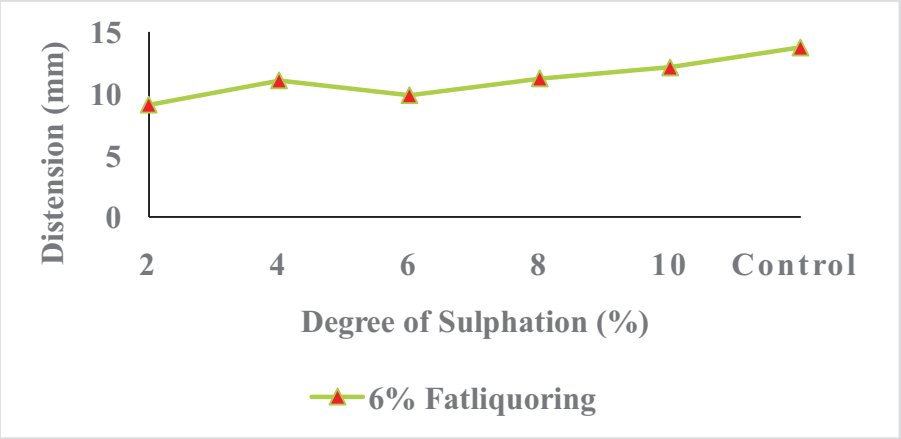

Figure 3.3: Distension of Leather fatliquored with sulphated *Lophira*oil (6% offer)

The reason for this test method is to determine the grain crack force (load) and distension of leather when used for shoe upper. Shoe upper leather often shows slight crack in the toe area at the time of lasting operation despite the fact that, the leather has good tensile strength. It could be observed from figure 4.7 and figure 4.8 that the highest distension of the fatliquored leather at various degree of sulphation and percentage offer was at 5% offer of the fatliquor and consequently at 8 and 10% degree of sulphation with a distension value of 12.13 mm, load of 48.12 Kg and 63.27 Kg. The commercial fatliquor yield a distension of 13.75 mm at 67.55Kg of load. Although, the highest load was 80.01 Kg at 4% offer and 10% degree of sulphation, but the distension value of 11.75 mm is low compared to 12.13mm at 5% offer and 10% degree of sulphation. This is an indication that fatliquor agent has the ability to enhanced the ball-burst property of the leather during retanning processes as reported by Wintana (2014).

Table 3.1: Percentage Elongation in relation to Percentage Degree of Sulphation/Percentage Offer of the Fatliquor

Degree of Sulphation (%)	Offer (%)	Elongation (%)
2	6	33.79
4	6	47.42
6	6	86.08
8	6	95.30
10	6	43.55
Control Z	6	64.63

The elongation at break of leathers is a useful index on the elastic properties of the leathers. The elongation is measured simultaneously with the measurement of tensile strength. Table 4.6 is the result of percentage elongation at 4, 5 and 6% offer for 2, 4, 6, 8 and 10% degree of sulphation. In the study, leathers fatliquored with the produced fatliquor gave the highest value 95.30% elongation at break at 6% offer and 8% Degree of sulphation. Whereas, the leather obtained with commercial fatliquor gave highest value of 64.63%. Sharphouse, (1989), reported that, the minimum level of elongation required for the manufacture of footwear and other leather goods is 40%, this being extensively completed by each

of the fatliquored leathers and this is a prove that, the leather fatliquored with *Lophira* fatliquor has a high percentage elongation as compared to the standard.

Conclusion

In conclusion, the production of sulphated fatliquor from locally available raw material of *Lophira lanceolata* seed oil through sulphation reaction has been investigated at five different degree of sulphation to determine their iodine value, saponification value, acid value, functional groups and stability. The outcome of the experiment conducted were analysed according to the sulphated fatliquor have the best stability which can be used for application on leather. The stability test indicated that 6%, 8% and 10% degree of sulphation are the most stable based on the different solution of salts and solvent.

Reference

A.O.A.C. (2000). Official Methods ofAnalysis of Association of OfficialAnalytical Chemists.

Affiang, S.D., Gamde, G., Okolo,V.N., Olabode, V. and Jekada, J.Z. (2018). Synthesis of sulphated-fatliquor from Neem (*Azadirachta indica*) seed oil for leather tannage. *American Journal of Engineering Research*, 7(4): 215-221.

Ariful H.Q., Uddin T.M., AbulKashem A., Murshid J.C., Amal K.D., Nazmul H. (2015). Fatliquor Preparation from *Karanja* seed Oil (*Pongamia pinnata* L.) and its Application for Leather Processing. *Journal of Applied Chemistry*. (8), 54 – 58.

Bin L.V. (2009).Characterization and properties of organic silicon modified amphoteric fatliquor, college of resource and environment, Shaanxi University of Science and Technology, Xi'an 710021, Shannxi, P.R. China. 175-311.

El-Shahat, H.A.N. and Mohamed, G.M. (2010). Ester phosphate of discarded palm oil from potato chip factories as fatliquoring agent. *Journal of American Science*, 12(6): 617-626

Girgis, A.Y. (2004). The utilization of discarded oil from potato chip factories in toilet soap making. Grasas Y Aceites (Sevilla, Spain), 55(3): 264-272.

Hashem, Md. and Shahruk, N.T. (2015). One step to prepare fatliquor from the extracted fat of cowhide fleshings for using in leather processing. XXXIII *International Union of Leather Technologists and Chemists Societies*. 162.

Helmy, H. E. and Megahed, M.G. (2010). Utilization of olein oil resulting from frying processes in soap manufacture. *Journal of Food and Dairy Science*, Mansoura University, 1(6): 367- 373.

Li, L.X., Li, J., Li, R., Yu , X.H. and Chen, W.Y. (2008). The synthesis and characterization of montmorillonite-amino resin nano-composite material. *Journal of Sichuan University*, 40(4): 95–99.

Society of Leather Technologists and Chemists (2001). SLC 115: Determination of total solubles. *Society of Leather Technologists and Chemists*, UK.

Wintana, K. (2014). Preparation of Leather Fatliquor cum Filler from Fleshing Waste for Retaning Process in Leather Manufacture. M.Sc. Thesis, Addis Ababa Institute of Technology, Ethiopia.

Appendix

Plate I: An ATM Card Pack manufactured from the fatliquored leather

Plate II: A wallet manufactured from the fatliquored leather

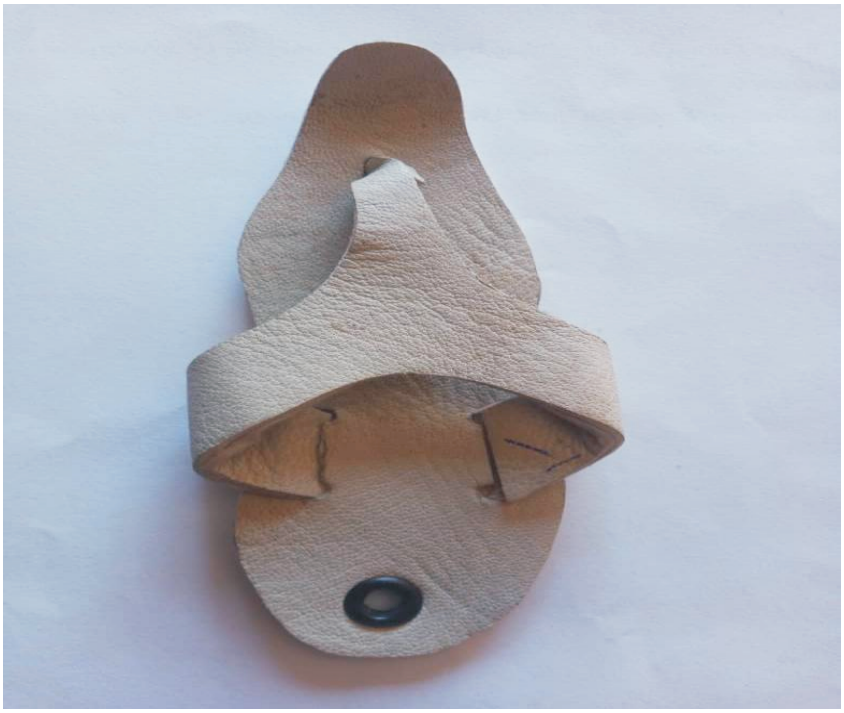

Plate III: A Key holder manufactured from the fatliquored leather

Nigerian Journal of Polymer Science and Technology, 2021, Vol. 16, pp83-97
Received: 19/10/2021 Accepted: 06/11/2021

EFFECT OF CALCIUM CARBONATE AND *FICUS POLITA* SEEDS POWDER ON THE CREEP RECOVERY AND THERMODYNAMIC MECHANICAL PROPERTIES OF POLYPROPYLENE, POLYSTYRENE AND POLVINYLACETATE TER -BLEND

***Shuaibu M.A[1] and Mamza P.A.P[1], Hamza A[1] and Isa M.T[2]**

[1]Department of Chemistry Ahmadu Bello University, Zaria, Nigeria
[2]Department of Chemical Engineering Ahmadu Bello University, Zaria, Nigeria

*Corresponding author's *E-mail: shuaibupolymer@gmail.com;* Phone no: +2348030570393

ABSTRACT

The creep recovery and thermodynamic mechanical properties of pristine polypropylene (PP), blends without filler (PP/PS/PVAc), blend with filled with calcium carbonate (B/$CaCO_3$) and that filled with Ficus polita seed powder (B/FPSP) were reported in this study. The blends with and without filler were prepared by melt blending and compression moulding technique. The prepared analytes with and without filler of different composition and filler loading (100/0, 80/15/5, 60/30/10, 40/40/20, $B_1/CaCO_3$, $B_2/CaCO_3$, B_1/FPSP and B_2/FPSP) were characterised for creep recovery and thermodynamic mechanical properties. Comparative studies were made on the creep measurement and the thermodynamic mechanical properties of the neat PP and the blends with and without fillers. Creep recovery, thermal Stability and stiffness of the blends were advanced for creep recovery, storage modulus and activation energy. The excellent results were found for bl end filled with 20 g Ficus polita seeds powder (B_2/FPSP) 1069.70 μm creep recovery, 2990.611 MPa storage modulus and 29844.119 kJmol^{-1} activation energy.

Keywords: *Blend, filler, creep recovery, thermodynamic mechanical analysis and compression moulding technique*

INTRODUCTION

The rapid increase in the use of blends is one of the most important features of the polymer industry over the last few years. More recently, considerable research effort in polymer blends and alloys in both academia and industry has led to a mushrooming growth of the patent and scientific literature. The miscibility between the constituents of the polymer mixture is an important factor in the development of new materials based on polymeric blends. Miscibility is defined as the ability to be mixed at molecular level to produce one homogenous mixture Mohan *et al.,* (2011). In the search for new polymeric materials, either new monomers are polymerised or co-polymerisation techniques are used to tailor a new product. An alternative method has been to blend existing polymers. Mixing together of two or more different polymers or co-polymers is known as blending. Blending is a process somewhat similar to compounding. In a polymer blend, the constituent polymers are usually present in significant weight or volume proportions with respect to each other, but seldom in equal proportions Mohan *et al.,* (2011). An obvious advantage of this approach is that it requires little or no extra capital expenditure relative to new polymers. It is also possible to produce a range of materials with properties completely different from those of the blend constituents. It is well known that the viscoelastic behaviour of polymers is determined by many factors, including the inherent structural factors which are mainly

related to the chain rigidity, crystalline structure, orientation and phase morphology, and the external factors which are mainly related to the environmental temperature, external force and the observation time (Liu *et al.,* 2016). Formal deformation is time-independent while the latter deformation is time-dependent. Generally, if the observation time is much smaller than the relaxation time during the creep measurement and the viscous flow of molecular chains is avoided, the sample mainly exhibits the instantaneous elastic deformation and viscoelastic deformation (Liu *et al.,* 2016).

According to Kumar *et al.,* (2016) Polymers are viscoelastic materials and exhibit time-dependent or temperature deformation or relaxation when subjected to a constant stress or strain. While creep is a measure of increase in strain with time under a constant stress, stress relaxation is the reduction of stress with time under a constant strain (Adeosun, 2013). Therefore, creep and stress relaxation tests measure the dimensional stability of a polymer over time. Such tests are of great importance for Chemists and engineers, particularly if a polymer must be in service under stress and strain for long periods. There are three major variables that affect the rate of creep and stress relaxation. These are molecular mobility, stress/strain level and time. Because increasing temperature generally increases molecular mobility, it is also a major factor. At very high stress/strain or temperature, creep/stress relaxation development is too fast to be qualified. Therefore, load and temperature should be suitably chosen for their studies in order that measurements can be made over a significant period of time (Liu *et al.,* 2016). Polypropylene (PP) and polystyrene (PS) and Polyvinylacetate (PVAc) are among the commodity polymers and the volume leader in the polymer industrial field. The non-sharp glass transition temperature, poor impact strength at low temperature and low environmental properties of PP can be improved by blending PP with PS and PVAc Jiang *et al.,* (2019). Dynamic mechanical analysis (DMA) is an important technique used to indicate molecular relaxation dynamics of polymeric materials Robert (2012). Dynamic mechanical analysis (DMA) tests were used to determine the shift factors with only the storage modulus curves ignoring other viscoelastic parameters (Dan-asabe, 2016). The principle of DMA measurement is such that, a sinusoidal stress is applied and the corresponding strain in the material is evaluated, allowing one to determine the storage modulus, loss modulus and loss tangent or damping Factor. By studying the dependence of these parameters on temperature or frequency, it is possible to show the dynamic mechanical properties (such as thermodynamic transitions and other molecular relaxation) of the materials and their applications Ji-Zhao (2020). and Jun (2018). The Elastic (Storage) Modulus: Measure of elasticity of material. Due to the visco-elastic nature of blend and composite materials, analysis of creep behaviour is vital in understanding equilibrium strain rate. Dan-asabe *et al.,* (2015), investigation of the thermo-mechanical characterisation of banana particulate reinforced PVC composite as piping material and established that, better creep stability was obtained at 50/50 polyvinylchloride to banana peeled particulate composite composition. It was also reported by Khan (2008) the viscoelasticity of polypropylene/polyethylene blends and the creep stress increases with increasing time at constant load. According to the report given by Razavi-Nouri, (2006) reported that the creep and creep relaxation time of PP/m-LLPE (50/50) composition were better than that of pure PP. Liu *et al.,* (2016) conducted a research on the Eenhancement of tensile creep stability of immiscible poly(L-

lactide)/poly(ethylene vinyl acetate) blends achieved by adding carbon nanotubes concluded that the creep stability of the immiscible blend is apparently enhanced by adding (Carbon nanotubes) CNTs. The mechanisms for the enhanced creep stability were are suggested to be related to the interfacial location of CNTs at the blend interface, the formation of the percolated CNT network structure. Liu *et al.,* (2016). Another research titled "creep behaviour of PS/PMMA blend by compression molding creep behaviour of PS/PMMA blend by compression molding, revealed that the creep deformation increases with increasing time at constant creep stress (100 Pa and 1000 s) and decreases at (100 Pa and 7000 s). Masaoki *et al.,* (2016). Martien and Karin (2019) carried out an investigation to determine the creep deflection of Wood Polymer Composite profiles (WPC) at 20 and at load 850 N conditions and reported that the creep deflection progresses steadily but slowly and creep deflection rate decreases with time proceeding, which is in particular visible for sample coded WPC-3. They further stated, at these conditions the creep deflections increase significantly for all three WPCs with WPC-3 showing high deflection rate during the first days, followed by much slower rate during the next period. WPC-1 shows high progressive creep deflection for 2 samples during the entire test temperature and period (50 and three weeks). At 20 the curves show steady but slow creep rate, whereas at 50 creep rates were are higher than of the neat PVAc, in particular for WPC-1 and WPC-3. WPC-3 shows high creep rate during early stage, but strain rate levels off at longer term. Other Authors observed similar results, epoxy plasticized with polyvinylacetate saturated with water had a higher creep compliance as compared to the plasticized blends without saturation with water in a research Time–Temperature–Plasticization Superposition Principle to Predict creep of a plasticized epoxy conducted by (Anstey *et al.,* 2019).

MATERIALS AND METHODS

Polypropylene was supplied by Dushanzi Chemical Company, China, as the major polymer with the trade name PP, T30s with density 0.91 g/cm^3 , melt flow index 2.8 g/ 10 min and 230 °C, 2.16 kg accordingly. The Polystyrene, PS, molecular weight of approximately 100, 000, (Trade name 5250) was purchased from BDH Chemical limited, England. The melt flow rate is 7 g/10 min (200 ^{o}C/5 kg). The Polyvinylacetate (PVAc), with chemical formula $(C_4H_6O_2)_n$ with molecular weight 1900, viscosity of 8.8 w/w % solution in toluene at 20 °C 5-7cS and its softening point is 105 °C, was supplied by Sigma Aldrich. The Calcium carbonate $CaCO_3$, with molecular weight of 100.09 gmol^{-1} was purchased from Fisons Plc, Middlesex, England, Scientific, Equipment Division. The *Ficus polita* seeds were obtained locally from Samaru in Sabon Gari Local Government, Kaduna State, Nigeria.

Sample Preparation

Preparation of Terna ry blends

Mixing, compounding and pressing of PP/PS/PVAc with and without filler

-A roller (two roll mill) was used the PP, PS and PVAc processing temperatures were set with that of PP at 170 , PS at 170 -180 and PVAc at 150 ^{o}C respectively. The nip of the rollers was adjusted and the polymers were subsequently poured on the nip, after total melting had been attained. When a homogeneous mixture was achieved, the compounded sample was sheeted out for further processing. The compounding was done based on the formulation proposed by Mamza (2011), according to Table 1 and 2. Pressing was done by compression moulding technique at the rate of 190 ^{o}C/4 Pa/hour.

Table of formulation (1)
The composition of poly (propylene)/poly (styrene)/poly (vinyl Acetate) blend without filler

S/NO	Blend ratios PP/PS/PVAc	Wt of PP	Wt of PS	Wt of PVAc
1	100/0/0	100	0	0
2	50/20/30	50	20	30
3	50/25/25	50	25	25
4	50/30/20	50	30	20
5	50/35/15	50	35	15
6	50/40/10	50	40	10
7	60/20/20	60	20	20

Table of formulation (2)
The composition of poly (propylene)/poly (styrene)/poly (vinyl acetate) blend with $CaCO_3$ and FPSP

S/N	Filler loading (g)	PP/PS/PVAc (g/g/g/)	B/$CaCO_{3(g)}$	B/FPSP
1	0	100/0/0	100/0/0/0	100/0/0/0
2	10	85/15/5	85/15/5/10	85/15/5/10
3	20	70/20/10	70/20/10/10	70/20/10/10
4	30	60/20/20	60/20/20/30	60/20/20/30
5	40	50/30/20	50/30/20/40	50/30/20/40

Key: FPSP = *Ficus polita* seed powder

Method
Creep measurements and dynamic mechanical analysis were conducted using DMA 242E machine in strength of materials laboratory of mechanical engineering, A.B.U. Zaria (ASTM D7028, 2015). The test parameters were first configured via the Proteus software using personal computer. Instruments set up comprised up of the sample holder (3-point-bending), furnace temperature (range of 30–70) thermocouple and measurement mode by using an apparatus equipped with a mechanical stress amplifier (lever) 10:1. A mechanical strain gauge (with an accuracy of about 2 mm) was connected with the upper clamp of the specimen to indicate the displacement. Specimen dimensions used during the creep and dynamic mechanical test, the static load was set at 2.18 N. Sample specimens of dimension of 50.000 × 11.5000 × 2.600 mm were produced for each test. The samples were loaded on to the machine using a three-point-bending sample holder and subsequently locked into the furnace Mechanical preconditioning preceding the series of short-term creeps consisted in applying a stress (for 90 min) equal to or higher than the highest stress applied in the series of the creep measurements dynamic mechanical analysis was used.

Results and Discussion

Table 3: Result of storage modulus of PP and blends with and without filler at (2.5 Hz, 5.0 Hz and 10.0 Hz)

S/N	Blend composition (g/g)	Onset temperature ((°C))	Tg (°C)	E'/MPa(2.5 Hz)	E'/MPa(5 Hz)	E'/MPa(10 Hz)
1	PP	49.1	67.1	843.3099	858.5347	871.1108
2	Bo/5 PVAc	56.0	64.9	2892.001	2945.014	2990.611
3	B_1/10 $CaCO_3$	48.3	52.2	1080.396	1127.326	1171.576
4	B_2/20 $CaCO_3$	48.6	57.8	2365.503	2457.247	2539.618
5	B_1/10 FPSP	48.5	51.1	1774.250	1856.733	1926.961
6	B_1/20 FPSP	47.8	52.3	2820.802	2902.509	2969.362

Table 4: Result of loss modulus of blends with and without filler at (2.5 Hz, 5.0 Hz and 10.0 Hz)

S/N	Blend composition (g/g)	Onset temperature ((°C))	Tg (°C)	E"/MPa (2.5 Hz)	E"/MPa (5 Hz)	E"/MPa (10 Hz)
1	PP	49.1	67.1	50.97819	48.77086	47.43922
2	Bo/5 PVAc	56.0	64.9	177.0054	167.3494	167.7713
3	B_1/10 $CaCO_3$	48.3	52.2	135.7481	123.7299	115.0259
4	B_2/20 $CaCO_3$	48.6	57.8	269.7594	242.2185	225.9903
5	B_1/10 FPSP	48.5	51.1	208.6029	190.8188	179.6307
6	B_1/20 FPSP	47.8	52.3	225.6885	203.0777	192.0895

Table 5: Result of Tan δ of blends with and without filler at (2.5 Hz, 5.0 Hz and 10.0 Hz)

S/N	Blend composition (g/g)	Onset temperature ((°C))	Tg (°C)	Tanδ (2.5 Hz)	Tanδ (5 Hz)	Tanδ (10 Hz)
1	PP	49.1	67.1	0.09880	0.08890	0.08770
2	Bo/5 PVAc	56.0	64.9	0.11226	0.10074	0.10053
3	B_1/10 $CaCO_3$	48.3	52.2	0.22722	0.19854	0.19804
4	B_2/20 $CaCO_3$	48.6	57.8	0.20635	0.17704	0.18269
5	B_1/10 FPSP	48.5	51.1	0.23827	0.20669	0.20947
6	B_1/20 FPSP	47.8	52.3	0.22797	0.20538	0.20539

Table 6: Results of Activation energy of the prepared blend with and without filler

Blend composition (g)	Maximum activation energy ($kJmol^{-1}$)	Temperature range ( )
PP	819.357	40-100
B/5 PVAc	2450.401	40-99.8
B_1/10 $CaCO_3$	6631..903	40-100
B_2/20 $CaCO_3$	1323.623	40-100
B_1/10 FPSP	10528.942	40-100
B_2/20 FPSP	98440.119	40-100

Table 7: Results creep recovery of the prepared blends with and without filler at constant temperature and at constant time range

S/N	Blend composition (g)	Creep deformation (μm)	Time range (min)	Temperature range ( )
1	100PP	325.00	42.2- 60.00	5 – 60.00
2	B_o/5 PVAc	312.90	42.5- 60.00	5 – 59.90
3	B_1/10 $CaCO_3$	289.70	45.7- 60.10	5 – 60.10
4	B_2/20 $CaCO_3$	875.10	42.1 – 60.0	5 – 60.00
5	B_1/10 FPSP	925.40	42.5- 60.00	5 – 60.00
6	B_2/10 FPSP	1069.70	45 – 60.10	5 – 60.00

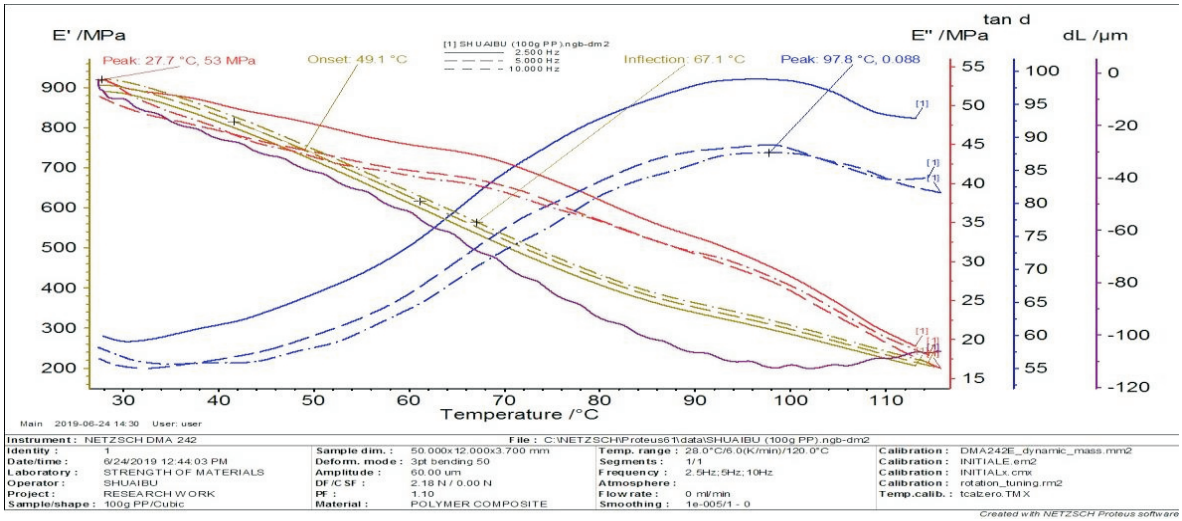

Figure 1: Dynamic Mechanical Analysis (DMA) test curves of 100 gPP

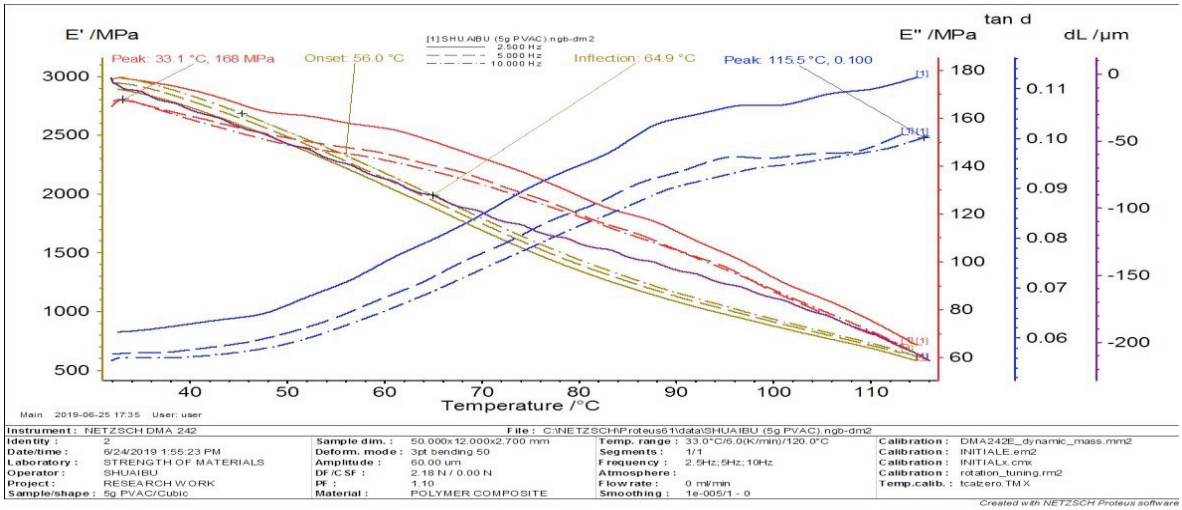

Figure 2: Combine curve of the Dynamic Mechanical Analysis of PP/PS/5 g PVAc

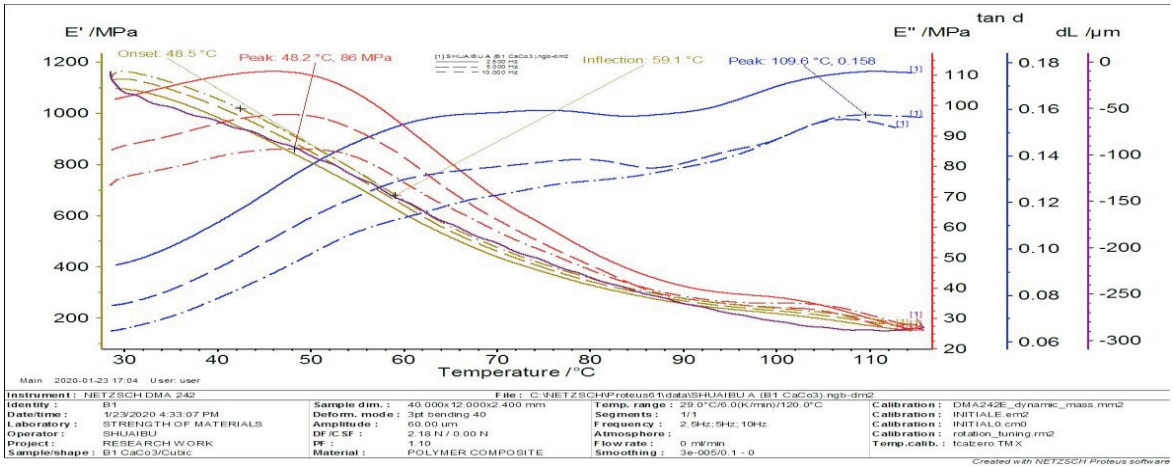

Figure 3: Combine curve of the Dynamic Mechanical Analysis of B_1/ $CaCO_3$

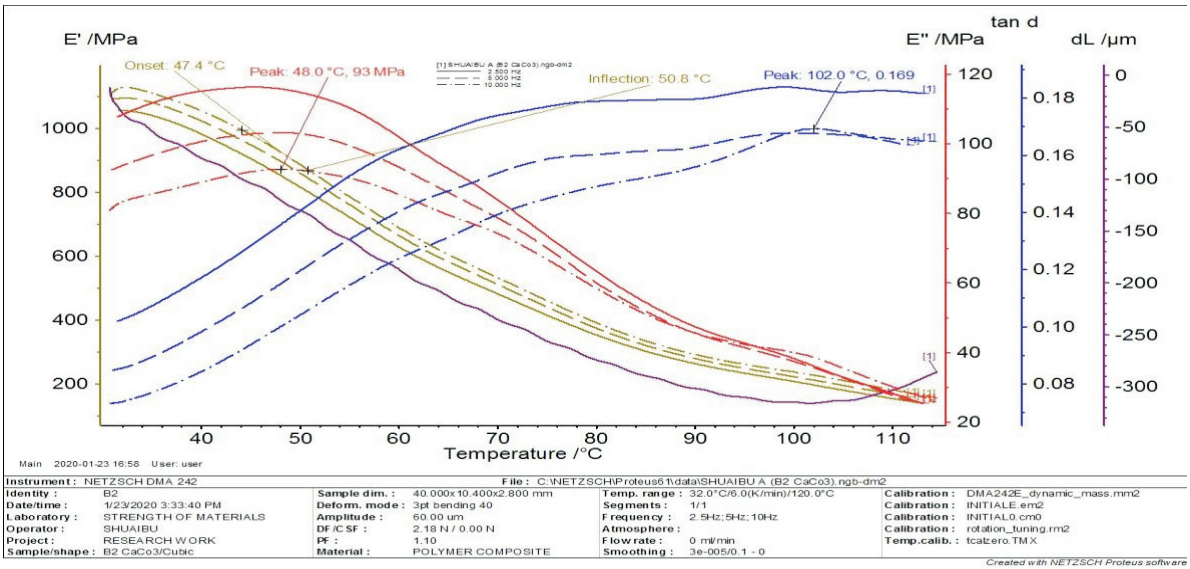

Figure 4: Combine curve of the Dynamic Mechanical Analysis of B_2/ $CaCO_3$

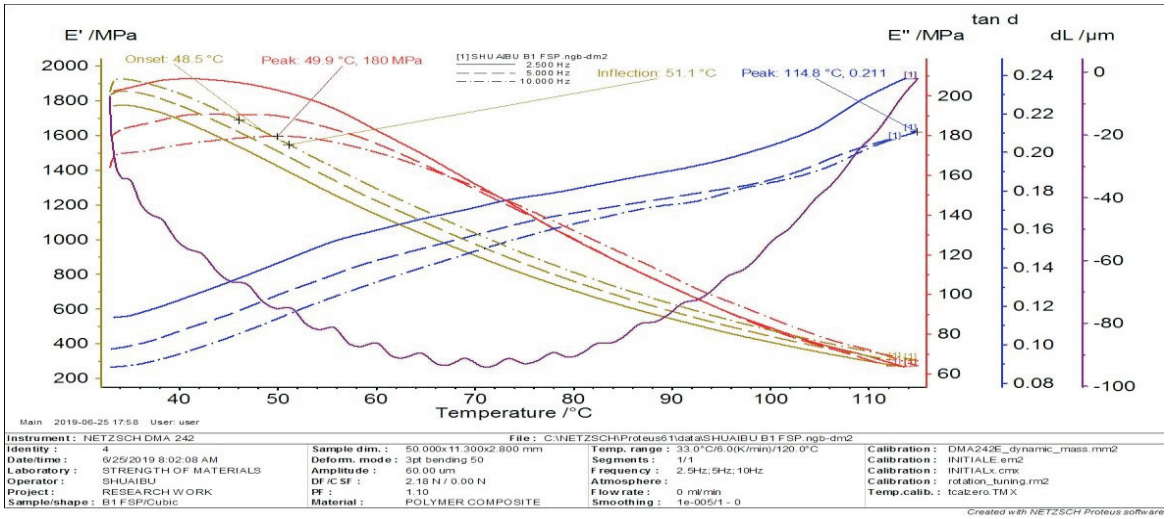

Figure 5: Combine curve of the Dynamic Mechanical Analysis of B_1/FPSP

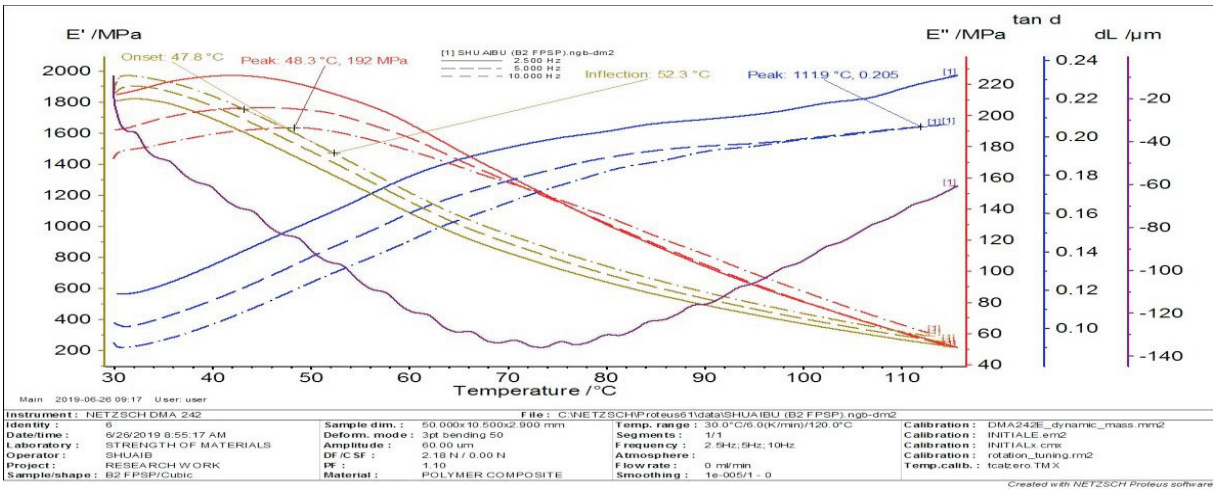

Figure 6: Combine curve of the Dynamic Mechanical Analysis of B_2/FPSP

Creep recovery

Due to the visco-elastic nature of the composite materials, analysis of creep strength or recovery is vital in understanding equilibrium strain rate. The result of the creep recovery for the blend with and without fillers at 70^{0}C was shown in Figure 1- 6 (purple lines). The creep test was conducted for 70 min at a constant loading stress of 2.18 N. The initial vertical large strain is due to the applied constant load after which the strain decreases with time up to about 50 min where the strain rate is very small known as the equilibrium strain rate. This stage is the secondary creep region and must be considered in load bearing capability of visco-elastic materials Dan-asabe (2018). The percentage strain during this period and temperature (60 ^{0}C) is 1.55 %. Similarly, these figures depict the creep curves for the pristine PP at 60^{0}C for 60 minutes. The strain rate is fairly constant (not steadily decreasing) throughout the experimental period and does not attain equilibrium. This shows that, the article produced with the neat PP is not a good load bearing material (it can break easily with prolong usage) as compared to the blends with and without fillers as it did not attain equilibrium state The blend with and without fillers depict has a corresponding percentage strain during the period of of the experiment for the blend with and without fillers ($CaCO_3$ or FPSP) of the article produced at all the blend and filler composition within the same time and temperature with the Bo/5 gPVAc having the highest creep strength rate percentage of 6.80 % compared to the pristine propylene. It has been established by Ghalia *et al.,* (2011) in their research, Viscoelasticity and viscoplasticity of polypropylene/polyethylene blends that the creep stress increases with increasing time at constant load.

-According to the report given by Razavi-Nouri (2006) reported that the creep and creep relaxation time of PP/m-LLPE (50/50) composition were better than that of pure PP in his research Creep and stress relaxation behavior of polypropylene, metallocene-prepared polyethylene and their blends. Similar results was reported by Dan-asabe *et al.,* (2018). They concluded that better creep stability was obtained at 50/50 polyvinylchloride to banana peeled particulate composite composition. Liu *et al.,* (2016) conducted a research on the enhancement of tensile creep stability of immiscible poly(L-lactide)/poly(ethylene

vinyl acetate) blends achieved by adding carbon nanotubes concluded that the creep stability of the immiscible blend is apparently enhanced by adding(Carbon nanotubes) CNTs. The mechanisms for the enhanced creep stability are suggested to be related to the interfacial location of CNTs at the blend interface, the formation of the percolated CNT network structure (Liu *et al.,* 2016). Another research titled "creep behavior of PS/PMMA blend by compression molding creep behavior of PS/PMMA blend by compression molding, revealed that the creep deformation increases with increasing time at constant creep stress (100 Pa and 1000 s) and decreases at (100 Pa and 7000 s). Martien and Karin (2019) carried out an investigation to determine the creep deflection of wood polymer composite profiles (WCP) at 20 and at load 850 N conditions and reported that the creep deflection progresses steadily but slowly and creep deflection rate decreases with time proceeding, which is in particular visible for sample coded WPC-3. They further stated, at these conditions the creep deflections increase significantly for all three WPCs with WPC-3 showing high deflection rate during the first days, followed by much slower rate during the next period. WPC-1 shows high progressive creep deflection for 2 samples during the entire test temperature and period (50 and three weeks). At 20 the curves show steady but slow creep rate, whereas at 50 creep rates are higher than of the neat PVAc, in particular for WPC-1 and WPC-3. WPC-3 shows high creep rate during early stage, but strain rate levels off at longer term. Other Authors observed similar results, epoxy plasticized with polyvinylacetate saturated with water had a higher creep compliance as compared to the plasticized blends without saturation with water in a research Time–Temperature–Plasticisation superposition principle to predict creep of a plasticised epoxy conducted by Ishigami *et al.,* (2019).

The storage modulus represents the elastic portion of the materials and is defines as the optimum quantity of stored in by the material during the period of one revolution of oscillation (Gupta, 2017; Rana, 2017; Jacob *et al.,* 2018). It can also be define as the capacity of the material to store energy Jacob *et al.,* (2018). The Viscous (loss) Modulus: The ability of the material to dissipate energy. Energy lost as heat Jacob *et al.,* (201. The dynamic thermal analysis (DMA) can also give the details explanation of the measure of the rigidity and stability of the blends with and without fillers temperature as a codomain, it's glass transition temperature and visco-elastic nature when feigns to dynamic loading Dan-asabe *et al.,* (2018 and Mustapha, *et al.*, (2020). Figure 1 to 6 described the visco-elastic parameters such as storage modulus (E') loss modulus (E''), and tan δ of the pristine Polypropylene (control), blends with and without fillers with increasing temperature at oscillation frequencies of 2.5, 5 and 10 Hz respectively. The $E'(MPa)$ curve shows (red curve) the stability of the pristine Polypropylene matrix under dynamic loading in which the onset temperature is 41.1^{0}C corresponding to storage modulus E', calculated and recorded value as 760 MPa (table 1) and its point of inflection (mid-point) with a corresponding temperature usually known as the glass transition temperature recorded as 67.1 qC at 10 Hz. It was also observed that the value of storage modulus E', of both the blend composition without filler and all the blends filled with the two fillers increased with increasing filler loading and increase in both frequency of oscillation compared to the pristine Polypropylene. This observation was generally recorded across all the temperature range of the experiments as well as the oscillating frequency range of the experiment this is due to the increased or improvement of the stiffness of the blends with and without

filler. This could be attributed to the structural changes associated with the addition of Polystyrene (PS) and Polyvinylacetate (PVAc), are blended in to the pure Polypropylene (PP) within the appropriate experimental conditions to form the specific blends which were filled with Calcium carbonate ($CaCO_3$) and *Ficus polita* seeds powder (FPSP) to form the composites the rigidity of the PP was enhanced, this implies that there was high interaction among the components of both the blend and the two fillers thus improving the capacity of the neat PP to resists deformation Dan-asabe *et al.,* (2018).

Other authours studied the Mechanical, Thermal, and degradation properties of biocomposites with biopolyesters filled with date seed powder prepared melt mixing of DSP with biopolymers using mini-twin conical screw extruder. They established equivalent results stating that the storage and loss modulus of the composites were enhanced with 30 and 40% filler loading, due to filler aggregates and low filler-polymer interfacial interactions Mittal *et al.,* (2014). Similar observation was made by Wu *et al.,* (2017) on Polypropylene/polystyrene/clay blends prepared by an innovative eccentric rotor extruder based on continuous elongational flow study the rheology property, morphology and crystallisation behaviour and they concluded that the T_g of the blend filled with MMT increased compared with that of the pure PP/PS blends, and the T_g value increased by 2.2 % when the MMT concentration was 3 wt%. The result suggested that the compatibility of PP/PS blends was improved with the addition of MMT, and the best compatibility for blends was obtained with 3wt % MMT concentration Wu *et al.,* (2017). Similarly, same effect of the addition of PS, PVAc and the two fillers used ($CaCO_3$ and FPSP) in PP on the miscibility of the blend composition of PP/PS/PVAc blends and give a more intuitive comparison between the blend with and without filler was also recorded. The loss factor (blue curve on the combined curves) as a function of temperature for PP/PS/PVAc, PP/PS/PVAc/$CaCO_3$ and PP/PS/PVAc/FPSP blends were obtained from dynamic mechanical thermal analysis, as shown in figure 1 to figure 6. The glass-transition temperature (T_g) gotten from these curves were illustrated in table 1 to 3.

In general, it can be suggested that the immiscible of the ternary blends were partially miscible and that some molecular interactions occurred between the three components if the difference between T_g, PS and T_g, PP for blends was reduced. Similar observations were made by Jia *et al.,* (2013) and Wu *et al.,* (2017). As earlier referred to Figure 4 and Table 1, it was clear that with increasing the dose/load of $CaCO_3$ or FPSP, the T_g value of PP/ PS/PVAc blends decreased at *fi*rst and then increased compared with that of PP, and the T_g value reduced 2.2 and 9.3 when the amount of $CaCO_3$ and FPSP added to blends were 10 g each respectively. The result suggested that the compatibility of PP/PS blends was improved with the addition of $CaCO_3$ or FPSP, and the best compatibility for blends was obtained with 10 g $CaCO_3$ or FPSP load. The reason may be that the PS or PVAc particle size in blends were reduced with the addition of $CaCO_3$ or FPSP which impliedly increased the surface area of the components of the blends there by increasing more chance of interaction between the polymer matrices and the fillers, which enhances the entanglement effect of PP, PS and PVAc.

However, when the $CaCO_3$ and FPSP amount exceeds 10 g, the $CaCO_3$ and FPSP particles are easier to reunite and stack in high concentration so that the miscibility of PP/PS/PVAc blends is gradually declined.

Therefore, the rational controlling of $CaCO_3$ or FPSP concentration is more effective in improving the miscibility of PP/PS/PVAc blends. It also can be clearly observed from figure 1-6 that the storage modulus (E') (*MPa*) and the loss modulus (E'') (*MPa*) of PP/PS/PVAc blends were obvious greater than those of pure PP. Moreover, with the addition of $CaCO_3$ or FPSP, the values of 'and '' of PP and PP/PS/PVAc blends were increased at all the experimental frequencies (2.5, 5 and 10 Hz) when the amount $CaCO_3$ or FPSP is less than 20 g. And interestingly, the enhancement of moduli was found to be proportional to $CaCO_3$ or FPSP load, which could be attributed to either compatibilising effects when PVAc resi ded at interface or reinforcing effect related to inter- and intraparticle of the blend-filler interactions as reported by Liu *et al.,* (2016) and Wu *et al.,* (2017). However, $CaCO_3$ or FPSP load reached 20 g, in the blends of different composition, the values of the storage modulus (E') and the loss modulus (E'') of the blends were declined compared with those of blends at 10 g $CaCO_3$ or FPSP load. The reason for this may be aggregated up in two approaches. Firstly, part of $CaCO_3$ or FPSP load particles are aggregated at the interface with the presence of high $CaCO_3$ or FPSP load, which leads to a relatively lower degree of intercalation and exfoliation. Therefore, the molecular chains of PP, PS and PVAc were not well inserted and dispersed in the $CaCO_3$ or FPSP galleries. Similar observation was given by Wu *et al.,* (2017). Secondly, some particles of $CaCO_3$ or FPSP selectively disperse into the dispersed phase, so the inhibition effect on the movement of PP macromolecular chain is decreased, resulting in a decline in the elasticity and stickiness of blends. In high frequency region, the 'and ''of all samples tended to be similar, indicating that under the effect of high frequency, the effect of $CaCO_3$ or FPSP on the elasticity and stability of blends were independent of the experimental frequencies and time, and they were mainly depended on the temperature range at which the experiment was performed. Damping or tan d/tan delta or loss factor is the dissipation of energy in a material under cyclic load. It is a measure of how well a material can get rid of energy and is reported as the tangent of the phase angle. It tells us how good a material will be at absorbing energy.

According to the results of the study carried out on the Mechanical, diffusion and degradation behaviour of polypropylene and cellulose blends prepared by melt mixing followed by injection moulding by Korir (2013), reported that, the storage modulus, loss modulus, damping properties of the blend were improved commingling of the cellulose in to the pure PP as compared to the values obtained for the fresh PP,. Thus, the improvement of the thermal stability increases with increase of the frequency, temperature and the amount of the cellulose in PP matrix. Storage modulus varies with the state of the material, its temperature, and with the frequency Xie *et al.,* (2017). Increasing the value of tan d means the material has more potential to dissipate energy and so the greater the tan d the higher dissipative the material is. In other word, decreasing tan d indicates material act more elastic and by applying load, the material has the ability to store energy rather than dissipating it. For polymer that is filled with fillers, increasing the content of the filler diminished the value of the tan d as the filler imposed restriction against molecular mobility of polymer chains due to the adsorption of particulate fillers on to the surface of the polymers as it results to interfacial adhesion between the polymer matrix and filler which often produces hydrogen bond between the components in a blend system. Similar result was reported by (Xie *et al.,* 2017; Jacob *et al.,* 2018; and

Mostafa *et al.*, 2020). With higher filler loading of both $CaCO_3$ and FPSP into the PP/PS/PVAc blend, higher dispersion of the fillers were more uniformly distributed as the storage modulus increased, strong correlation between this results and previous work on this blend on the mechanical properties can be established as the mechanical tests results depicted same trend, most especially at these blends composition filled with 10 to 20 g of either of $CaCO_3$ and FPSP, Ha and Jiang *et al.,* (2019) and Mamza *et al.,* (2020) reported similar results. Ha (2019) studied the Structure-Properties of Polypropylene/Liquid Crystalline Polymer Blends filled with Liquid Crystalline glass prepared by melt mixing and reported that the thermal stability of the blend increased with increasing the amount of the liquid crystalline glass into the polypropylene matrix, revealed similar result relative to the one established in this research. From these figures (figure 1 to 6), it can be seen that the blends $CaCO_3$ or FPSP showed lower Tan δ compared to that of fresh PP or the blend without filler. Low value of loss factor implies good loading bearing capacity of the blends and composites as reported by (Jacob *et al.,* 2018). The damping factor decreases with increasing temperature and frequency from neat PP and the blends with and without filler.

Since the damping peak occurs in the region of glass transition where the material changes from rigid to a more rubbery state, it is associated with the segmental mobility of the chains, which are initially in the frozen state. The higher the tan δ peak, the greater is the degree of molecular mobility. On comparing the tan δ peak values of the different fillers ($CaCO_3$ or FPSP) composition of the blends show the minimum value related to that of the unreinforced PP. This result is in agreement with the observation made by (Sui *et al.,* 2018). The observed decrease in damping factor is associated with the improvement in interface bonding (Sui *et al.,* 2018) reported that a composite with poor interface bonding tends to dissipate more energy than that with good interface bonding.

ACTIVATION ENERGY

The activation energy is found to increase with incorporation of $CaCO_3$ and FPSP and the maximum value was obtained at for B_2/FPSP blend that is, the blend filled with 20 g *Ficus polita* seed powder filler. This increase in the activation energy could be attributed to the two fillers commingled in the blend as compared to that obtained for the neat PP which is associated with high interaction between the fillers and the blend which accompanied by high interfacial adhesion between the filler and blend composition as compared to other blends composition and this result can be supported with the mechanical analyses results performed in this research.

CONCLUSION

The ter-blends containing polypropylene, polystyrene and polyvinylacetate (PP/PS/PVAc) with and without filler were successfully prepared with an inexpensive material with an exhaustive less dense weight material and a good thermo-mechanical and creep recovery characteristic property. The excellent Thermomechanical and creep recovery were measured with the optimum values at 10 g and 20 g of each of calcium carbonate ($CaCO_3$) and *Ficus polita* seed powder (FPSP) reinforcing fillers. Yielding corresponding storage modulus, loss modulus, activation energy and creep recovery, thermal Stability and stiffness of the of the blends with and without fillers were enhanced at B_o/5gPVAc, $B_1/CaCO_3$, $B_2/CaCO_3$, B_1/FPSP and B_2/FPSP blends compositions compared to the pristine PP (871.1108 Mpa) at 10 Hz. Creep recovery was improved for all the tested blend

compositions with the highest creep recovery recorded at B_2/20 g FPSP (1069.7 μm).

B_o/5gPVAc having the highest storage modulus (2990.611 MPa) followed by B_2/FPSP (2969.362 MPa) respectively. Activation Energy also increased for all the blend composition except for B_o/5gPVAc composition compared to that of the neat PP, the highest value was obtained at B_2/20 g FPSP (98440.119 $kJmol^{-1}$).

REFERENCES

Adeosun, S. O., Usman, M. A., Ayoola, W. A., and Bodud, M. A. (2013). Physico Mechanical Responses of Polypropylene-$CaCO_3$ Composite. *Journal of Minerals and Materials Characterizationand Engineering*, *1*(4), 145–152.https://doi.org/10.4236/jmmce.14025

Anstey, A., Codou, A., Misra, M., and Mohanty, A. K. (2018). Novel Compatibilized Nylon-Based Ternary Blends with Polypropylene and Poly (lactic acid): Fractionated Crystallization Phenomena and Mechanical Performance. *American chemical society,* 3, 2845-2854. https://doi.org/10.1021/acsomega.7b01569

Dan-asabe, B., Yaro, A. S., Yawas, D. S., and Aku, S. Y. (2018). Long Term Thermo- mechanical Prediction of Banana Stem Particulate Reinforced PVC Composite as Piping Material. *Pakistan Journal of Engineering Applied Science*, *23*(2), 8–16.

Ghalia, M. A., Hassan, A., and Yussuf, A. (2011). Mechanical and thermal properties of calcium carbonate-filled PP/LLDPE composite. *Journal of Applied Polymer Science*, *121*(4), 2413–2421. https://doi.org/10.1002/app.33570Gupta, M.K (2018). Effect of variation in frequencies on dynamic mechanical properties of jute fibre reinforcement epoxy composites. *Journal of Materials and Environmental Sciences, 9* (1), 100-106. http://doi.org/10.26872/jmes.2018.9.1.12

Ha, M.H., Shin, B.Y., and Han, D.H., (2016). Morphological, Rheological, and Mechanical Properties of Polyamide 6/Polypropylene Blends Compatibilized by Electron-Beam Irradiation in the Presence of a Reactive Agent. *Materials,* 9, 342. doi:10.3390/ma9050342 Retrieved from www.mdpi.com/journal/materials

Ishigami, A., Nishitsuji, S., Kurose, T., and Ito, H. (2019). Evaluation of toughness and failure mode of PA6 / mSEBS / PS ternary blends with an oil-extended viscoelastic controlled interface. *Polymer*, *177*, 57–64. https://doi.org/10.1016/j.

Jacob, J., Ahmed, A. S., and Yaro, S. A. (2018). *Effect Of Benzoyl Chloride Treatment On The Mechanical And Viscoelastic Properties Of Plantain Peel Powder - Reinforced Polyethylene Composites*. *13*(4), 25–29.

Jiang, Y., Wu, J., Leng, J., Cardon, L., and Zhang, J. (2019). Reinforced and toughened PP/PS composites prepared by Fused Filament Fabrication (FFF) with in-situ microfibril and shish-kebab structure. *Polymer*. https://doi.org/10.1016/j.polymer.121971

Ji-Zhao, L. (2020). Tensile properties and fire residue morphology of flame-retarded polypropylene composites. *Journal of Thermoplastic Composite Materials,* 1–19.

Jun, Y.-S. (2018). Development of Graphene-Based Electrically Conductive Polymer Nano Composites. A Ph.D thesis University of Waterloo Ontario, Canada, 124-174Jiang, Y., Wu, J., Leng, J., Cardon, L., and Zhang, J. (2019). Reinforced and toughened PP/PS composites prepared by Fused Filament Fabrication (FFF) with in-situ microfibril and shish-kebab structure. *Polymer*. https://doi.org/10.1016/j.polymer.121971

Khan, M. S. (2008). Miscibility studies of PVC / PMMA and PS / PMMA blends by dilute solution viscometry and FTIR. *African Journal of Pure and Applied Chemistry,* 2(4), 41-45 Available online at http://www.academicjournals.org/AJPAC ISSN 1996 - 0840

Korir, P.K. (2013). *Mechanical, diffusion and degradation behaviour of polypropylene and cellulose blends* (Unpolished Master of Science Thesis, Department of Physics Kenyatta University, Nairobi-Kenya, Kenya).

Kumar, A., Madhav, C. V., and Bhukya, R. (2016). *Evaluation and Characterization of Polystyrene blending with Polypropylene by using Compatibilizers*. 67–71.

Liu, C.M., Ma, F. F., Zhang, Z.X., Yang, J. H., Wang, Y., and Zhou, Z.W. (2016). Enhanced tensile creep stability of immiscible poly(L-lactide)/poly(ethylene vinyl acetate) blends achieved by adding carbon nanotubes. *Composite Part B*, 107, 174-181

Maryam, F. (2017). Application of taguchi Method for optimizing of Mechanical Properties of Polystyrene-carbon nanotube nanocomposites.*Journal of Polymers and Polymer Composites, 25,*(2)*,* 177-183.

Mamza, P. A. (2011). The physico-mechanical and morphological properties of D-cellulose-filled polystyrene (PS) and polyvinyl acetate (PVac) blends, Department of Natural Sciences, University of Jos. In Ph. D Thesis Pp. 3-10

Mamza, P.A.P., Yusuf, U., and Gimba, C.E **(**2020**).** Effect of *prosopis africana* wood fillers on the mechanical properties and creep resistance of polyvinyl chloride composites. *Nigerian Research Journal of Chemical Sciences, 8*(1), 349-357.Mgbemena, Chinedum Ogonna (2010). Evaluation of the Mechanical Properties of Polypropylene/Calcium Carbonate Nanocomposite at Various Creep Conditions. M.Sc, Thesis, Nnamdi Azikwe University Awka, Nigeria.

Martien, V. D., and Karin, M.O. (2019). Creep deflection of Wood Polymer Composite profiles at demanding conditions. https://doi.org/10.1016/j.cscm..e00224

Mascia, L., and Edward, A. (1974). The Role of Additives in Plastics, (Ed) Publishers Ltd London, 1 – 15

Mittal, V., Chaudhry, A. U., and Matsko, N.B. (2014). "True" Biocomposites with Biopolyesters and Date Seed Powder: Mechanical, Thermal, and Degradation Properties. Journal of Applied Polymer Science, 40816 (1-15) DOI: 10.1002/app.40816.

Mohan, K.R.; Achari, V.B.S., Rao, V.V.R.N and Sharma, A.K. (2011). Electrical and Optical Properties of (PEMA/PVC) Polymer Blend Electrolyte Doped with $NaClO_4$. *Polymer Testing, 30*(8), 881-886.

Mostafa, N. H., Hunain, M. B., and Khafaji, S. O.W. (2020). Mechanical and free vibration properties of clamshell particles/polyester composites. *Material Research Express,* https://doi.org/10.1088/2053-1591/ab67f8

Rana, S.S., Gupta, M. K.and Srivastava, R. K.(2017) Effect of variation in frequencies on dynamic mechanical properties of short sisal fibre reinforced epoxy composite, *Materials Today: Proceedings* (4),3387–3396

Razavi-Nouri M., Jafarzadeh-Dogouri F., Onomiehie, A. and Langroudi, A.E. (2006). Mechanical properties and water absorption behaviour of chopped rice husk filled polypropylene composites, *Iranian Polymer Journal, 15*(9), 757 – 766.

Roberts, J., Power, A., Chapman, J., Chandra, S., and Cozzolino, D. (2018). The Use of UV-Vis Spectroscopy in Bioprocess and Fermentation Monitoring. *Fermenttation, 4,* 18, (1-8). doi:10.3390/fermentation4010018

Sui, G., Jing, M., Zhao, J., Wang, K., Zhang Q., and Fu, Q. (2018). A comparison study of high shear force and compatibilizer on the phase morphologies and properties of polypropylene/polylactide (PP/PLA) blends, *Polymer* doi: 10.1016/j.polymer.09.005.

Wu, T., Yuan, D., Qiu, F., Chen, R., Zhang, G., and Qu, J. (2017). Polypropylene / polystyrene /clay blends prepared by an innovative eccentric rotor extruder based on continuous elongational fl ow : Analysis of morphology , rheology property , and crystallization behaviour. *Polymer Testing*, *63*, 73–83. https://doi.org/10.1016

Xie, J., Shuo, J., Shen, M., and Zhang, F. (2017). Recent Advances in *Momordica charantia*: Functional Components and Biological Activities [Review on *Momordica charantia*]. Retrieved from *International Journal of Molecular Sciences*. DOI:10.3390/ijms18122555